Placenta NAD^+ depletion: A Mechanism through which Gestational Obesity contributes to Placenta Dysfunction

Hannah Poisson

A thesis submitted to the University of Ottawa in partial fulfillment of the requirement of the Master's Degree of Science in Cellular and Molecular Medicine

Cellular and Molecular Medicine
Faculty of Medicine
University of Ottawa

Table of Contents

List of Tables

List of Figures

Legend

ABC: ATP-Binding Cassette
ACC: Animal Care Committee
ADP: Adenosine Diphosphate
APC: Antigen Presenting Cell
ATP: Adenosine Triphosphate
BEH: Animal Behavior and Physiology Core
BMI: Body Mass Index
BSA: Bovine Serum Albumin
CD38: Cluster of Differentiation 38
CI-NDUFB8: Complex I NADH Dehydrogenase
CII-SDHB: Complex II Succinate Ubiquinone Oxidoreductase
CIII-UQCRC2: Complex III Ubiquinol Cytochrome C Oxidoreductase
CIV-MTCO1: Complex IV Cytochrome C Oxidoreductase
COPD: Chronic Obstructive Pulmonary Disease
CRP: C-Reactive Protein
CTB: Cytotrophoblast
CV-ATP5A: Complex V ATP Synthase
CV: Chronic Villitis
CTRL: Control chow diet
DAB-HRP: 3,3'-diaminobenzidine horseradish peroxidase
DC: Detergent Compatible
DCs: Dendritic Cells
DSB: Double Strand Breaks
E: Gestational day
ETC: Electron Transport Chain
EVT: Extravillous Cytotrophoblasts
FFA: Free Fatty Acids
FGR: Fetal Growth Restriction
GDM: Gestational Diabetes Mellitus
Glut-1: Glucose Transporter Protein-1
GlyT: Glycogen Trophoblast
HFD: High-Fat Diet
HFHS: High-Fat High-Sugar diet
H&E: Hematoxylin & Eosin
IHC: Immunohistochemistry
IL: Interleukin
IRF3: Interferon Regulatory Factor 3
IWAT: Inguinal White Adipose Tissue
JNK: c-Jun N-terminal Kinase

Ki-67: Antigen Kiel 67
LGA: Large for Gestational Age
LIF: Leukemic Inhibitory Factor
LPL: Lipoprotein Lipase
LPS: Lipopolysaccharide
LZ: Labyrinth Zone
MCP-1: Monocyte Chemoattractant Protein-1
MP: Macrophages
mtDNA: Mitochondrial DNA
MVM: Microvillous Membrane
NA: Nicotinic Acid
NAAD: Nicotinic Acid Adenine Dinucleotide
NAD^+: Nicotinamide Adenine Dinucleotide
NADH: Nicotinamide Adenine Dinucleotide + Hydrogen
NADS: Nicotinamide Adenine Dinucleotide Synthetase
NADT: Total Nicotinamide Adenine Dinucleotide
NAFLD: Non-Alcoholic Fatty Liver Disease
NAM: Nicotinamide
NAMN: Nicotinic Acid Mononucleotide
NAMPT: Nicotinamide Phosphoribosyltransferase
NF-κB: Nuclear Factor Kappa B
NK: Natural Killer Cells
NMN: Nicotinamide Mononucleotide
NMNAT: Nicotinamide Mononucleotide AdenylylTransferase
NR: Nicotinamide Riboside
NRK: Nicotinamide Riboside Kinase,
OCR: Oxygen Consumption Rates
OXPHOS: Oxidative Phosphorylation
PAR: PARylation
PARP: Poly (ADP Ribose) Polymerase
PCIC: Preclinical Imaging Core
PDGF-AA: chemoattractant platelet-derived growth factor
PFA: Paraformaldehyde
PKR: Protein Kinase R
PL: Phospholipids
PPARγ: Peroxisome Proliferator-Activated Receptor Gamma
QA: Quinolinic Acid
RNS: Reactive Nitrogen Species
ROS: Reactive Oxygen Species
SD: Standard Deviation

SGA: Small for Gestational Age
SickKids: Centre for Applied Genomics at the Hospital for Sick Children
SIRTs: Sirtuins
SLC: Solute Carrier Transport Proteins
SpT: Spongiotrophoblast
SSB: Single Strand Breaks
SynT: syncytiotrophoblast cells
TCA: Tricarboxylic Acid Cycle
T2DM: Type 2 Diabetes Mellitus
TG: Triglycerides
TGC: Trophoblast Parietal Giant Cell
TGF-β: Transforming Growth Factor Beta
Th: T helper cells
Tlr9: Toll-Like Receptor 9
TNF-α: Tumor Necrosis Factor Alpha
Trp: Tryptophan
uNK: Uterine Natural Killer cells
USP: Ubiquitin Specific Proteases
WHO: World Health Organization

Abstract

English Version

Introduction: Gestational obesity is a metabolic disease on the rise in Canadian individuals of reproductive age which increases the risk of adverse pregnancy and fetal health outcomes. Although the exact mechanisms underlying these poor health consequences are currently unknown, chronic inflammation is a key contributor. Nicotinamide adenine dinucleotide (NAD^+) depletion is a hallmark of many chronic inflammatory pathophysiologies in non-pregnant individuals, leading to mitochondrial dysfunction and metabolic stress [136, 146-152, 168-169]. Considerable reduction in NAD^+ content has likewise been found to play an important role in the establishment of placental dysfunction and poor fetal growth in the context of inflammation-mediated preeclampsia [163, 170-171] – a hypertensive disorder of pregnancy. Interestingly, boosting placental NAD^+ levels via nicotinamide riboside (NR) supplementation improved placental structure/function and fetal growth profiles in a rodent model of this inflammatory disease [163]. Considering that gestational obesity is a chronic inflammatory disease of pregnancy, this thesis seeks to determine if NAD^+ depletion and mitochondrial impairment are also present, and if these factors contribute to poor placental/fetal health outcomes. This was explored using a high-fat high-sugar (HFHS) diet-induced gestational obesity murine model, with and without supplementation of NAD^+ boosting treatment.

Methods: Six-week-old C57BL/6N female mice were placed on a HFHS western diet or control (CTRL) diet for 12-15 weeks prior to pregnancy. During pregnancy, mice were maintained on the same diet and additionally received either water (H_2O; CTRL-H_2O = 11, HFHS-H_2O = 7) or the NAD^+ supplement nicotinamide riboside (NR; 400 mg/kg/day; CTRL-NR = 10, HFHS-NR = 9) daily. Dams were sacrificed at gestational day (E)18.5 and placentas and fetuses were weighed and measured, with one half of each placenta fixed for histomorphology and the other half flash-frozen for RNA and protein analysis. Samples were pooled by fetal sex per litter, and data presented as litter average.

Results: Fetuses from HFHS mothers were 0.23 g +/- 0.05 g smaller in mass and 3.37 mm +/- 0.74 mm smaller in length, and their placentas demonstrated reduced efficiencies and evidence of increased inflammation. Placental expression of PARP proteins (PARP-1, PARP-2) was elevated in placentas from obese dams. A trend towards elevated protein PARylation was observed in placentas from obese dams. NAD^+ was found to be significantly reduced in these placentas, as well as total NAD. Interestingly, placentas from obese dams also demonstrated dysregulated OXPHOS protein levels, indicative of mitochondrial impairment. Unexpectedly, the use of NR supplementation across pregnancy did not increase NAD^+ levels in the placenta, nor did it alter placental PARP/PARylation levels, mitochondrial dysfunction, and detriments to placental/fetal health.

Conclusion: This thesis provides evidence that PARP-mediated NAD^+ depletion and subsequent mitochondrial dysfunction may be components of placental pathophysiology in the context of gestational obesity - providing insight on future targets to rescue harmful effects to the placenta and fetus in pregnant populations with obesity. However, further research focused on optimizing modalities to therapeutically target placental NAD^+ signaling is warranted.

Keywords: Placenta, Gestational Obesity, Mitochondria, Chronic Inflammation, Nicotinamide Adenine Dinucleotide (NAD^+), Poly-ADP Ribose Polymerases (PARPs), Nicotinamide Riboside (NR)

French Version

Introduction : L'obésité gestationnelle est une maladie métabolique en augmentation chez les Canadiens en âge de procréer, ce qui augmente le risque d'effets indésirables sur la grossesse et la santé du fœtus. Bien que les mécanismes exacts à l'origine de ces conséquences négatives sur la santé sont actuellement inconnus, l'inflammation chronique est un contributeur clé. La déplétion en nicotinamide adénine dinucléotide (NAD^+) est une caractéristique de nombreuses physiopathologies inflammatoires chroniques chez les individus non enceintes, conduisant à un dysfonctionnement mitochondrial et à un stress métabolique [136, 146-152, 168-169]. Il a également été démontré qu'une réduction considérable de la teneur en NAD^+ joue un rôle important dans l'établissement d'un dysfonctionnement placentaire et d'une mauvaise croissance fœtale dans le contexte de la prééclampsie médiée par l'inflammation [163, 170-171] -une maladie hypertensive de la grossesse. Il est intéressant de noter que l'augmentation des niveaux de NAD^+ dans le placenta par une supplémentation en nicotinamide riboside (NR) a amélioré la structure/fonction placentaire et les profils de croissance fœtale dans un modèle de rongeur atteint de cette maladie inflammatoire [163]. Étant donné que l'obésité gestationnelle est une maladie inflammatoire chronique de la grossesse, cette thèse cherche à déterminer si une déplétion en NAD^+ et une déficience mitochondriale sont également présentes, et si ces facteurs contribuent à de mauvais résultats pour la santé du placenta et du fœtus. Ceci a été réalisée à l'aide d'un modèle murin d'obésité gestationnelle induite par un régime riche en graisses et en sucre (HFHS), avec et sans supplémentation de traitement qui augmente le NAD^+.

Méthodes: Des souris femelles C57BL/6N âgées de six semaines ont été soumises à un régime occidental HFHS ou un régime témoin (CTRL) pendant 12 à 15 semaines avant la grossesse. Pendant la grossesse, les souris ont été maintenues avec le même régime alimentaire et ont reçu en plus soit de l'eau (H_2O ; CTRL-H2O = 11, HFHS-H2O = 7), soit le supplément NAD^+, nicotinamide riboside (NR ; 400 mg/kg/jour ; CTRL-NR = 10, HFHS-NR = 9) quotidiennement. Les mères ont été sacrifiées au jour gestationnel (E 18,5) et les placentas et les fœtus ont été pesés et mesurés, une moitié de chaque

placenta a été fixée pour l'histomorphologie et l'autre moitié a été congelée pour l'analyse de l'ARN et des protéines. Les échantillons ont été regroupés selon le sexe fœtal par portée et les données sont présentées en tant que moyenne de la portée.

Résultats: Les fœtus issus de mères HFHS avaient une masse inférieure de 0,23 g +/- 0,05 g et une longueur inférieure de 3,37 mm +/- 0,74 mm, et leurs placentas présentent des efficacités réduites et des signes d'inflammation accrue. L'expression placentaire des protéines PARP (PARP-1, PARP-2) était élevée dans les placentas de mères obèses. Une tendance à l'augmentation de la PARylation des protéines a été observée dans les placentas des mères obèses. On a constaté que le NAD^+ était significativement réduit dans ces placentas, ainsi que dans le NAD total. Il est intéressant de noter que les placentas des mères obèses présentaient également des taux de protéine OXPHOS dérégulés, indiquant une déficience mitochondriale. De manière inattendue, l'utilisation d'une supplémentation en NR pendant la grossesse n'a pas augmenté les niveaux de NAD^+ dans le placenta, ni modifié les niveaux de PARP/PARylation placentaire, le dysfonctionnement mitochondrial et les effets néfastes sur la santé placentaire/fœtale.

Conclusion: Cette thèse fournit la preuve que la déplétion en NAD^+ médiée par PARP et le dysfonctionnement mitochondrial qui s'ensuit peuvent être des composants de la physiopathologie placentaire dans le contexte de l'obésité gestationnelle - fournissant un aperçu des cibles futures pour sauver les effets nocifs sur le placenta et le fœtus chez les populations enceintes souffrant d'obésité. Cependant, des recherches supplémentaires axées sur l'optimisation des modalités permettant de cibler thérapeutiquement la signalisation placentaire NAD^+ sont justifiées.

Mots-clés: Placenta, obésité gestationnelle, mitochondries, inflammation chronique, nicotinamide adénine dinucléotide (NAD^+), poly-ADP ribose polymérases (PARP), nicotinamide riboside (NR)

Acknowledgements

I would first like to thank my supervisor Dr. Shannon Bainbridge, without whom the completion of this thesis would not be possible. Dr. Bainbridge is not only beyond knowledgeable about placental and reproductive health, but she is an exceedingly compassionate and supportive mentor. I am also super grateful for my Thesis Advisory Committee (TAC): Dr. Barbara Vanderhyden and Dr. Keir Menzies, from whom I learned so much. Thank you for all of your input on my project, for attending all of my TAC meetings, and for revising all of my progress reports.

I am beyond thankful for all the members of the Placenta Lab at the University of Ottawa for their endless support. I would love to specifically thank the following members: Yusmaris Cariaco, Alexander Green, Jade Gamelin Kao, and Jasmine Tripathi for their help on my animal experiments, dissections, and RNA extraction/analysis. I would also like to thank Andrés Gerardo Bautista Orozco, Diana Isabel López Valdés, and Shannon Blake for their help on the placenta staining analysis. Without your support, this thesis couldn't have been completed -thank you so much.

I would also like to thank the following facilities for all of their assistance with experiments pertaining to my project: the Preclinical Imaging Core (PCIC) at the University of Ottawa for the completion of the mouse ultrasounds, the Louise Pelletier Imaging Core in the Department of Pathology and Laboratory Medicine at the University of Ottawa for all placental paraffinization/deparaffinization, sectioning, and staining, the Animal Behaviour and Physiology Core at the University of Ottawa for all EchoMRI testing, and the Centre for Applied Genomics at the Hospital for Sick Children (SickKids) for RNA Sequencing.

Last, I would like to thank my family, friends, and partner for putting up with me through this two-year MSc journey - thank you for loving and supporting me through all the

stress, sleepless nights, and coffee refills involved in my degree. You are all truly the best, and I appreciate you always.

Authorship Contribution

The principal investigator for the above study was Dr. Shannon Bainbridge, who was responsible for the conceptualization, funding, and oversight of the study. The Preclinical Imaging Core (PCIC) at the University of Ottawa was responsible for performing mouse ultrasounds. The Louise Pelletier Imaging Core in the Department of Pathology and Laboratory Medicine at the University of Ottawa was responsible for all placental paraffinization/
deparaffinization, sectioning, and staining. The Animal Behaviour and Physiology Core (BEH core) at the University of Ottawa was responsible for the completion of all EchoMRI testing. Jasmine Tripathi was responsible for assisting with RNA extraction and RNA-Sequencing analysis. The Centre for Applied Genomics at the Hospital for Sick Children (SickKids), affiliated with the University of Toronto, was responsible for all RNA Sequencing. Yusmaris Cariaco, Alex Green, and Jade Gamelin Kao were responsible for assistance with animal dissections. Andrés Gerardo Bautista Orozco, Diana Isabel López Valdés, and Shannon Blake were responsible for assisting with Ki67 staining analysis. Hannah Poisson was responsible for the development/carrying out of the animal model, all dissections pertaining to the animal model, and all other experiments/analysis pertaining to the animal model. The manuscript was prepared by Hannah Poisson, and revised by Dr. Shannon Bainbridge.

Ethics, Animal Care Committee, and Protocol Review:

No human recruitment, samples, or data were used, thus ethics approval was not required for the current study. An animal care committee (ACC) protocol (#3937) was approved for this study, with a copy of the ACC protocol included in the Appendix.

Chapter 1 - Introduction

1. Introduction

1.1 Obesity

Obesity is a pressing health concern, identified as a leading risk factor for the development of non-communicable diseases and premature death. The World Health Organization defines obesity as “excessive fat accumulation that might impair health”, diagnosed at a body mass index (BMI) of > 30 kg/m^2 [(1)]. There has been a dramatic increase in the prevalence of this condition over the past 50 years, with estimates that approximately 20% of the global adult population are currently obese. North America is disproportionately represented within the obesity epidemic, with estimated rates of obesity ranging from 25-35% of the adult population [(2)]. These statistics are alarming, indicative of a large and steadily growing population of individuals at high risk for the development of obesity-mediated cardiometabolic diseases, cognitive and psychological disorders, and some types of cancers.

1.2 Gestational Obesity

Gestational obesity refers to a population of individuals who enter pregnancy with a BMI of > 30 kg/m^2. Like other cases of obesity, gestational obesity is also on the rise, with 13.3% of Canadian pregnant individuals having obesity prior to pregnancy, and 48.8% gaining above the recommended weight in pregnancy [(3).].This is of concern as obesity in pregnancy is associated with numerous adverse gestational health outcomes, such as gestational diabetes, pre-term birth, still birth, and preeclampsia [(4-9)]. Additionally, gestational obesity has been linked to increased morbidity and premature mortality, as well as poor fetal health outcomes via in-utero fetal programming [(9-13)], referring to permanent alterations in the development of fetal organ systems during critical windows of development in response to adverse in-utero exposures [(10-14)]. Interestingly, gestational obesity has been linked to extremes in abnormal fetal growth profiles, associated with both large for gestational age (LGA) infants, defined as neonates whose birthweight is ³ 90th percentile for gestational age [(15)], and small for gestational age

(SGA) infants, defined as neonates whose birthweight is £ 10th percentile for their gestational age [16-18].

While both fetal growth extremes have been associated with obesity, they vary in the obesity-associated morbidities they present. LGA infants may display catch-down growth, a term used to describe a period in which children grow at a slower pace in early life (first 2 years) following a period of increased in-utero growth [19]. This catch-down growth in early childhood has been identified as a positive outcome for LGA children, as it can help regulate a healthy normal weight [20-21]. Indeed, LGA children who do not display catch-down growth are at a higher risk of becoming overweight or obese in childhood, and of developing cardiometabolic health disturbances in young adulthood [22]. Conversely, SGA infants typically exhibit catch-up growth, a term which describes children that grow at a rapid pace in early life following a period of reduced in-utero growth, specifically jumping up by "one-percentile band or more on standard infant growth charts" [23-24]. This catch-up growth can lead to increased weight gain and visceral adiposity in SGA infants [25-26], increasing their risk of developing obesity in childhood, adolescence, and adulthood [27-28]. Moreover, this increased adiposity puts SGA infants at a higher risk of developing other components of metabolic disease, such as insulin resistance, glucose intolerance, cardiovascular disease, and dyslipidemia in adulthood [29].

1.3 Inflammatory profile in gestational obesity

While specific mechanisms through which gestational obesity is associated with these poor pregnancy and fetal health outcomes remain unclear, a ***chronic state of low-level, systemic inflammation*** and establishment of ***placental dysfunction*** appear to be central. This systemic inflammation chiefly arises from the presence of large adipocyte beds in different anatomical compartments in the body. The mechanism underlying the development of these large adipocyte beds can be explained by the following: Obesity is established due to an imbalance between energy intake and energy expenditure, in which the former supersedes the latter [30]. This excess energy

intake of macronutrients over a long period of time overstimulates white adipose tissue, leading to hyperplasia, an increase in the number of adipocytes, and hypertrophy, an increase in the size of adipocytes [31]. Adipose tissue is very metabolically and hormonally heterogenous, meaning that its accumulation in different anatomical components in the body leads to diverse clinical outcomes [32]. That being said, as the number and size of adipocytes increase, their blood supply decreases, initiating a state of hypoxia – a period of oxygen deficiency [33].

This state of oxidative stress subsequently triggers recruitment of pro-inflammatory macrophages (MPs) to the hypoxic sites. Most produce proinflammatory mediators, including tumor necrosis factor-alpha (TNF-α), interleukin (IL)-6 and adiponectin [34-38]. In turn, IL-6 stimulates hepatocytes to produce c-reactive protein (CRP) which likewise contributes to the inflammatory state [39]. Also contributing to systemic inflammation are pro-inflammatory serine kinase cascades which are activated by increased amounts of free fatty acids in obesity. Some of these kinases implicated include c-Jun N-terminal kinase (JNK), which balances cell survival and death in response to stress [40], protein kinase R (PKR), which activates signalling cascades such as JNK and nuclear factor kappa B (NF-κB) [41], and IκB kinase, which is a part of the NF-κB cascade and upon whose phosphorylation leads to transcription of inflammatory and immune response genes [42]. Overall, activation of these cascades leads to stimulation of adipose tissue to release IL-6, further promoting CRP production from the liver [43].

1.4 Pregnancy induced changes to the immune system

While obesity itself contributes drastically to a state of chronic inflammation in gestational obesity, it is also important to note that pregnancy itself is also characterized by its own inflammatory profile. While inflammation in obesity is majorly driven by adipocytes, inflammation in pregnancy is driven by alterations in hormone levels, including changes to progesterone, estradiol, leukemic inhibitory factor (LIF), and prostaglandins [44-45]. Further, inflammation in pregnancy differs at different stages of pregnancy, namely at embryo implantation, trophoblast invasion leading to formation of

the placenta, fetal growth, and delivery.This occurs via tight inflammatory control by adaptive T-helper (Th) cells - proinflammatory Th-1 cells and anti-inflammatory Th-2 cells [46]- which alternate their prevalence based on the stage of pregnancy. During the first trimester of pregnancy, the processes of implantation and placentation are dominated by proinflammatory Th-1 cells, however this switches in the second trimester where anti-inflammatory Th-2 cells become more prominent to allow for fetal growth [47]. Finally, the proinflammatory Th-1 state returns during the third trimester to help facilitate labour and delivery [47]. Interestingly while normal weight pregnancies follow these Th-mediated inflammatory switches, pregnancies coupled with gestational obesity fail to enter the Th-2 anti-inflammatory phase in the second trimester, and instead maintain a high level of inflammation dominated by Th-1 cells [48]. This is further explained in *1.6*.

Returning to normal weight pregnancies, the changes in inflammatory profile across pregnancy stages can be explained by the following: Prior to implantation the increase in progesterone levels during the secretory phase of the menstrual cycle, leads to decidual differentiation in the endometrium [49]. This decidual differentiation triggers a recruitment of uterine natural killer (uNK) cells into the uterine decidua - derived from hematopoietic stem cells. Indeed, both the uterus and placenta contain a high composition of hematopoietic stem cells, which can differentiate into natural killer (NK) cells or antigen-presenting cells (APC), including MPs and dendritic cells (DCs) [50-53]. Following implantation, the attachment of the embryo itself triggers recruitment of immune cells such as proinflammatory Th-1 cells, mast cells, DCs, monocytes, and MPs to the site of implantation. Pro-inflammatory cytokines such as IL-6, IL-8, and TNF-α are then secreted by these recruited immune cells as well as from uNKs [54-55]. One of the most dominating inflammatory cell types during this period are pro-inflammatory M1-decidual MPs, which promote inflammation via release of TNF-α, IL-6, and IL-1b [47, 56-57]. Following implantation is the process of placentation, a period in which extravillous cytotrophoblasts (CTBs) proliferate and invade the decidualized endometrium and myometrium [58]. Unlike the implantation phase dominated by M1-MPs, the placentation phase is chiefly headed by M2-MPs which promote anti-inflammatory factors such as IL-10 and transforming growth factor beta (TGF-β) [59-60]. This dominance of anti-

inflammatory M2-MPs continues into the second and third trimester of pregnancy [59]. At the time of delivery, the gestational parent's body returns to a pro-inflammatory state. This is again dominated by M1-MPs which promote successful labor by releasing pro-inflammatory cytokines that assist in increasing uterine contractions to deliver the baby and placenta, and also allow the uterus to be returned to its pre-pregnancy state [61-62]. There is also an increase in pro-inflammatory cytokines that migrate to the cervix to assist with cervical ripening [63-65].

All this considered, it is evident that both obesity and pregnancy have varying factors that lead to their unique inflammatory states. Again, obesity's inflammatory state is driven by adipocytes, whereas pregnancy's inflammatory state is driven by alterations in hormone levels and Th cells. However when combined, their inflammatory profiles propagate more serious effects on the gestational parent and their baby, than either cases of inflammation would do alone. For instance, this altered inflammatory state has been shown to dysregulate the development of the fetus by altering placental function, which will be further discussed in *1.6*. Further research is required to characterize this unique chronic inflammatory state, and how inflammation from obesity and pregnancy inform one another.

1.5 The Placenta

The placenta is the vital organ of pregnancy required to support fetal growth and development [66]. The placenta originates from the outer trophectoderm shell that encapsulates the early embryo at the time of implantation, quickly differentiating into the villous cytotrophoblast cells (CTBs) and the overlying multinucleated mass referred to as the syncytiotrophoblast cells (SynTs). The SynTs immediately send out projections into the uterine wall, forming lacunae that serve as the original source of nutrition for the embryo [49]. The underlying CTBs then begin to proliferate and send projections through the SynT mass, becoming coated in an SynT layer – generating a primary chorionic villous structure [67]. Mesenchymal cells begin to form in the core of these tree-like structures, followed by the establishment of fetal vasculature within this villous core,

developmental milestones that mark the formation of the secondary and tertiary chorionic villi, respectively. At the same time, extravillous cytotrophoblast cells (EVTs) terminally differentiate at the distal end of the CTB columns, rendering them highly invasive and allowing them to invade deeper into the uterine wall, where they take part in the active remodelling of the uterine spiral arteries [49, 68]. Namely, EVTs replace the vascular endothelium of the uterine vessels, and promote the breakdown of the vascular smooth muscle cells – ultimately increasing the diameter and reducing the resistance in these vessels to permit optimal blood flow into the placenta [68]. This uterine remodelling is complete by the end of the first trimester, when gestational parent blood then freely flows into the intervillous space, bathing the highly branched chorionic villous structures in nutrient and oxygen rich blood. On the opposing side, the umbilical vasculature connects the fetus to capillary beds within the chorionic villous trees [69]. These trees become bathed with the gestational parent blood within the intervillous space and serve as the site of all nutrient and gas exchange.

The placenta is described as a selective barrier, permitting the passage of many substances the fetus needs to survive, while at the same time preventing the passage of some potentially harmful substances. This selective barrier is not only structural in nature, with any substances entering the fetal circulation required to pass through the SynT, CTB, and fetal vascular endothelial layers (**Fig 1.1**), but also consists of a number of passive and active transport systems established on the apical and basal membranes of each of these cell types [70]. Passage across the placental barrier can occur via simple diffusion, which is utilized for oxygen exchange, or protein-mediated transport including facilitated diffusion and active transport [71-72]. Most substances including biological small molecules, antibodies, hormones, and drugs use active transport, and are therefore limited in entry to the fetal circulation as they need a membrane protein to do so [73-74]. The apical and basal sides of the placental barrier are also unique in their structural and biochemical properties. The apical component is the side containing microvilli in contact with the maternal blood, and contains an abundance of transport proteins including influx transporters, to increase transport of nutrients into the cell, and efflux transporters, to increase the transport of xenobiotics, environmental

pollutants, and stress hormones out of the cell [75]. The basal component is the side without microvilli facing the fetal capillaries, but still contains transporters including ATP-Binding Cassette (ABC) and Solute Carrier (SLC) transport proteins [72].

Due to clear ethical constraints and sampling limitations, animal models, and most commonly mouse models, are widely used to study the development and function of the placenta across pregnancy. Human and mouse placentas are quite similar in their overall structure (**Fig 1.1**) and share similar placental development mechanisms, however there are a few important differences to note. The human placenta can be considered as having two distinct functional compartments: 1) the extravillous compartment – comprised of EVTs that serve to anchor the placenta to the uterine wall, invade into the uterine decidua and take part in active remodelling of the uterine spiral arterioles; 2) The villous compartment – comprised of highly branched chorionic villous tree structures that encase fetal blood vessels and which are bathed in the gestational parent's blood within the intervillous space, permitting all gestational parent-fetal exchange [76]. Conversely, in the mouse model the 'extravillous compartment' is composed of parietal giant cells and glycogen trophoblasts (referred to as the junctional zone cells) [77]. These mouse trophoblasts are not as invasive as human trophoblasts, leading to shallower invasion of placental cells in the uterine wall [78]. However, the actual process of remodelling of the uterine arteries is fairly similar between both species, driven in large part by trophoblast-uNK cell interactions [79]. Regarding the villous compartment, both human and mouse placentas are hemochorial, meaning that the gestational parent blood comes in direct contact with the fetal trophoblast cells [77], but never mixes with the fetal blood directly. However, while humans have a single syncytiotrophoblast layer in their villous compartment, mice have two (SynT-1 and SynT-2) in their exchange region – referred to as the labyrinth zone [80] . Additionally, while humans have an incomplete villous CTB layer underneath their single SynT layer, mice have an incomplete trophoblast giant cell layer on the outside of their two SynT layers (**Fig. 1.1**) [81].

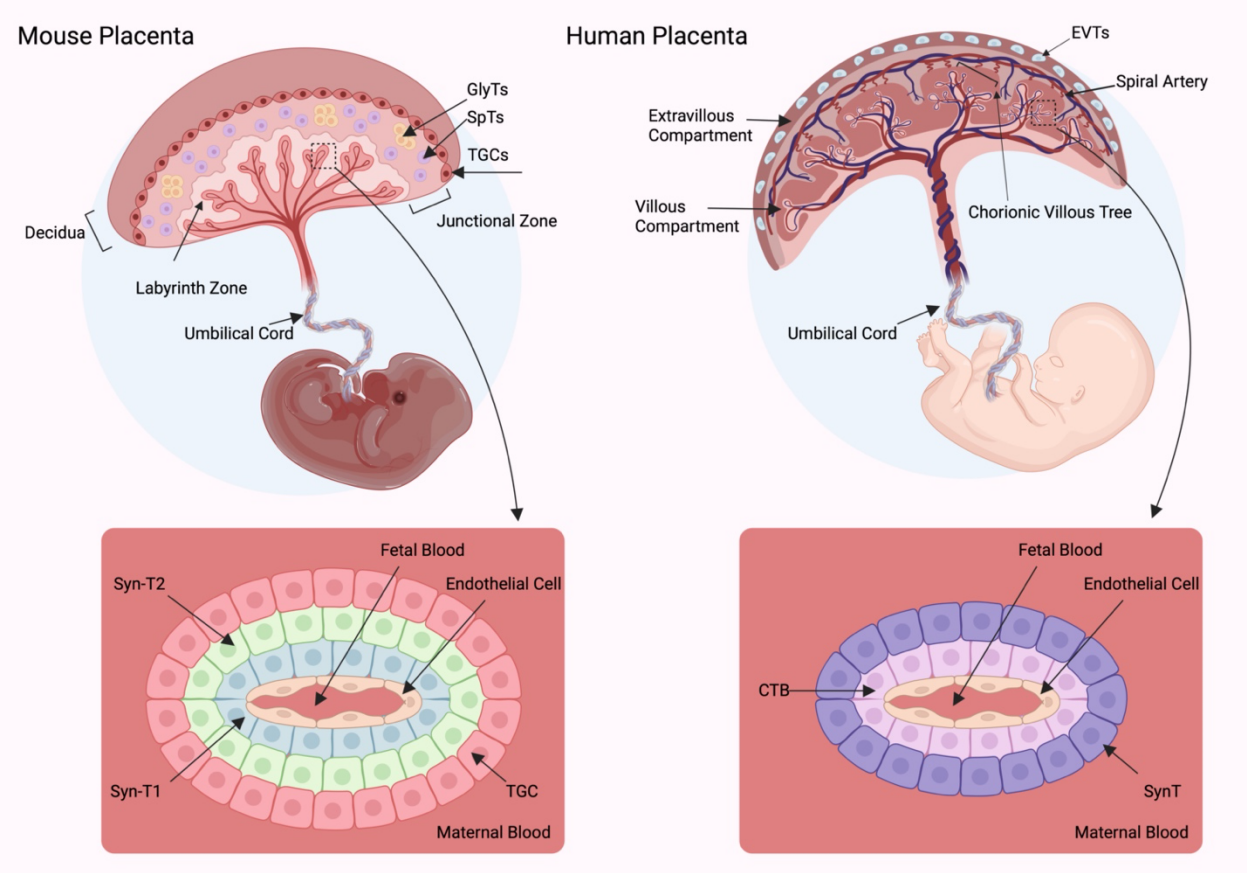

Figure 1.1. Mouse versus human placenta comparison.

The mouse placenta can be split into three zones: the decidua (extravillous compartment containing uterine arteries), the junctional zone (containing glycogen trophoblasts, spongiotrophoblasts, and trophoblast parietal giant cells which carry out uterine artery remodelling) and the labyrinth zone (the villous compartment containing fetal trophoblasts). Fetal trophoblasts in the mouse placenta have two layers of syncytiotrophoblast: syncytiotrophoblast layer I and syncytiotrophoblast layer II. The human placenta contains an extravillous compartment (decidua, complete with extravillous trophoblasts that carry out uterine artery remodelling) and a villous compartment (contains chorionic villous trees made up of fetal trophoblasts). Fetal trophoblasts in the human placenta have a single syncytiotrophoblast layer. GlyT = glycogen trophoblast/glycogen cell, SpT = spongiotrophoblast, TGC = trophoblast parietal giant cell, SynT1= syncytiotrophoblast layer I, SynT2 = syncytiotrophoblast layer II, EVT = extravillous cytotrophoblast, CTB = cytotrophoblast, SynT = syncytiotrophoblast. This figure was created using BioRender.com.

1.6 Gestational Obesity and the Placenta

As previously stated, obesity in pregnancy leads to a state of low-level, chronic, systemic inflammation which has profound impacts on the health of the pregnancy, in large part through adverse effects on placental development and function. In generally healthy pregnancies, the process of placentation puts the gestational parent into an anti-inflammatory state, through dominance of CD4+ Th-2 cells which secrete cytokines

that recruit M2-MPs, promoting anti-inflammatory factors such as IL-10 and TGF-β [48, 59-60]. However in obesity, the gestational parent will remain in that inflammatory state due to multiplication and enlargement of adipocytes around different tissues that cause the body to enter a hypoxic state [33]. This oxidative stress triggers recruitment of pro-inflammatory molecules to these hypoxic sites [34-38]. As a result, the gestational parent will instead contain a surplus of CD4+ Th-1 cells which are capable of entering the placenta [82-83]. These CD4+ Th1s secrete cytokines that recruit M1-MPs which in turn release inflammatory markers such as TNF-α, IL-6, and IL-1b [47, 56-57]into the placenta, shifting it to a pro-inflammatory state [84].

The placenta itself also attracts pro-inflammatory cells. For instance, trophoblast signals (i.e. chemoattractant platelet-derived growth factor (PDGF-AA)) are known to stimulate migration of endometrial stromal cells towards the implantation site [85], who then control the activation, proliferation, and differentiation of CD4+ T cells [86]. In addition, the maternal side of the placenta contains a surplus of immune cells, being composed of 70% decidual stromal cells and 30% decidual immune cells, which include NK cells (70%), MPs (15%), and T cells (15%) [87]. In an obesogenic environment, these maternal immune cells will continue to carry out their respective functions, however there will be a surplus of pro-inflammatory signalling at the maternal-fetal interface due to the fact that the placenta does not switch to the Th-2 anti-inflammatory phenotype (and remains in the Th-1 proinflammatory phenotype). Evidently, the placenta is placed into a more elevated state of inflammatory stress than it would under healthy conditions.

Placentas collected from patients with gestational obesity demonstrate increased levels of pro-inflammatory cytokines and chemokines, such as IL-6, IL-8, IL-1b, TNF-α, and monocyte chemoattractant protein-1 (MCP-1) [88-91] ,as well as an upregulation of reactive oxygen species (ROS) [92] and oxidized lipids [93]. ROS and oxidized lipids further contribute to activation of stress and pro-inflammatory signalling pathways. These include the placental p38-MAPK pathway, which leads to an upregulation of c-fos, c-jun, and ATF – modulators of pro-inflammatory gene expression [94], and the STAT3 pathway, that can encode inflammatory genes, including IL-6 [88, 95-98].

Interestingly, while a high BMI characteristic of obesity is associated with these pro-inflammatory pathways in the placenta, the same observations have not been made when examining the fetal systemic inflammatory profile [88]. This would suggest that obesity-mediated inflammation likely indirectly impacts fetal development, through its direct effects on placenta structure and function, rather than exposing the fetus to a surplus of pro-inflammatory cytokines [88, 99].

Indeed, obesity-mediated inflammation is strongly associated with structural and functional placenta deficits. Human placentas exposed to an obesogenic environment demonstrate a number of pathological findings at the time of delivery, including evidence of maternal and fetal vascular malperfusion, reduced chorionic villi maturation, reduced nutrient/gas exchange surface area, increased inflammatory lesions, and villitis [100-102]. Measurements of placental efficiency, calculated as a ratio of fetal to placental weight, demonstrate a BMI dependent decrease in the ability of the placenta to properly exchange nutrients and gases to the fetus [103]. These obesity-mediated structural and function changes to the placenta are accompanied by detrimental impacts to the fetus, such as increased mortality and abnormal fetal growth trajectories [104]. Likewise, placentas collected from rodent models of gestational obesity demonstrate decreased weight, surface area, maternal blood spaces, and downregulation of genes involved in vascular development coupled to a reduced size in the labyrinth exchange area [105]. These obesity-mediated changes to the placentas were also associated with poor fetal health outcomes, such as fetal growth restriction[105-106].

Apart from inflammation, gestational obesity also impacts placental function via alterations in nutrient availability. In the context of gestational obesity, an overconsumption of macronutrients can be transported across the placenta and mirrored in the fetal circulation. For instance, placental and fetal glucose concentrations are often higher in cases of gestational obesity. As one of the primary molecules used by both the placenta and fetus for energy metabolism, the placenta demonstrates a high expression of the primary glucose transporter protein-1 (Glut-1) on both the apical microvillous membrane (MVM) and basement membrane of the SynT cells. In

gestational obesity the placental expression of Glut-1 is increased, resulting in an excess of placental and fetal glucose uptake consumption [107-111]. In addition to glucose, individuals with gestational obesity also have elevated levels of circulating free fatty acids (FFA), phospholipids (PL), and triglycerides (TG). Elevations in these lipids contribute to elevated insulin resistance in gestational parent adipose tissue, leading to increased lipid breakdown (lipolysis) and FFA release – increasing lipid delivery to the placenta and the fetus [112]. Further, placental lipoprotein lipase (LPL) activity, which is required to hydrolyze TGs into FFAs in order to permit placental uptake and transfer [112-113], is found to be higher in placentas from gestational obesity, permitting more FFA to reach the fetus [114-115]. Collectively, altered placental nutrient transfer and subsequent fetal macronutrient profile can directly contribute to the adverse fetal organ programming – predisposing these offspring to obesity and cardiometabolic disorders in later life [10-14].

As mentioned previously, gestational obesity also impacts placental function via oxidative stress, which arise from an elevation in the production of ROS or reactive nitrogen species (RNS), or from a downregulation of antioxidant enzymes, or both [116]. Many ROS and RNS are formed through cellular metabolic pathways in the mitochondria, such as the electron transport chain (ETC) [117], and their levels are controlled by antioxidants. Placentas are rich in mitochondria, and thus a primary source of pro-oxidants and antioxidants [118]. However, placentas exposed to an obesogenic environment exhibit elevated ROS production [119-121] and reduced anti-oxidant production [120-121] –tightly linked to the elevated inflammation in the gestational obesity placenta [47, 56-57], dually contributing to a state of oxidative stress [122]. This imbalance in ROS levels and antioxidant levels leads to metabolically stressed mitochondria with dysregulated metabolic rates and mitochondrial activity [117]. Indeed, mitochondria isolated from gestational obesity placentas demonstrate a downregulation of genes related to oxidative phosphorylation and mitochondrial fusion/fission dynamics [123-124], suffer impairments to their respiratory complex function [125-126], and contain lower levels of mitochondrial DNA (mtDNA) content [126]. Further, these placentas demonstrate a collective reduction in mitochondrial density, reductions in b-oxidation

activity, elevations in lipid storage, and decreased ATP generation [125, 127]. Unsurprisingly, these placental mitochondrial deficits observed in gestational obesity are associated with poor fetoplacental outcomes including altered exchange efficiencies, and fetal growth extremes including both fetal overgrowth (large for gestational age, LGA) and fetal undergrowth (small for gestational age, SGA, fetal growth restriction (FGR)) [17-18] [122, 128-129]. Although the literature suggests evident placental mitochondrial dysfunction in light of gestational obesity, the specific mechanisms that link the inflammatory obesogenic environment to the ensuing placental mitochondrial dysfunction remain unclear.

1.7 NAD^+ Depletion and Mitochondrial Dysfunction in Chronic Inflammatory Disease

Outside of pregnancy, pathological states of chronic inflammation are known to be intimately associated with metabolic dysregulation in a number of tissue beds such as the colon, liver, kidney, muscle, brain, and heart - primarily the result of intracellular nicotinamide adenine dinucleotide (NAD^+) depletion and ensuing dysregulated NAD^+ signalling [130]. NAD^+, a form of vitamin B3, is a critical intracellular cofactor largely responsible for supporting energy metabolism processes within a cell [132-134]. NAD^+ content is typically tightly controlled through a homeostatic balance between biosynthesis/salvage and consumption pathways [135-136]. Specifically, NAD^+ is used as a hydride acceptor to carry out redox reactions, which makes it an essential molecule in catabolic pathways, including glycolysis, glutaminolysis, and fatty acid oxidation [131-134]. The electrons that are accepted by NADH through these redox reactions are then donated to the ETC to produce adenosine triphosphate (ATP), the primary source of energy for the cell [131]. NAD^+ also plays a role in anabolic pathways such as fatty acid synthesis; this occurs when NAD^+ is phosphorylated to $NADP^+$ so that it may act as a hydride acceptor to become NADPH [131-134]. Besides redox reactions, NAD^+ is a critical cofactor for non-redox related enzymes, such as poly-ADP ribose polymerases (PARPs) and sirtuins (SIRTs) [131-134] . In fact, intracellular NAD^+ availability is largely determined by the activity levels of these consuming enzymes which compete for these NAD^+ stores [36-37].

The PARP family of enzymes, composed of 17 members, carry out a number of cellular functions, including DNA repair, chromatin remodelling, cell cycle arrest, and immune modulation [131-136]. Many of these enzymatic actions involve a reversible post-transcriptional reaction known as PARylation, in which the PARP enzyme hydrolyzes NAD^+ to nicotinamide (NAM) so that a polymer of ADP-ribose can be added to a target protein (**Fig 1.2**) [130]. PARP-1 and PARP-2 are two of the primary PARylating enzymes, and are major cellular consumers of NAD^+, with estimates that PARP-1 consumes ~ 90% of all NAD^+ utilized by PARPs [134]. In a study that used an isotope-tracing approach to assess NAD^+ consumption fluxes by NAD^+ consumers across multiple human and mouse cell lines (i.e. T47D, MCF7, C2C12), they illustrated that PARPs consume about 33% of all NAD^+ under basal conditions, but become the primary consumer in stressed environments with DNA damage [137]. On the other hand, SIRTs are a family of enzymes whose activity promotes mitochondrial biogenesis and function, regulate metabolic and stress responses, and are considered to be highly important for increased lifespan [131-132]. Like PARPs, SIRTs use NAD^+ as a co-factor for their protein acetylation enzymatic activity, also breaking down NAD^+ to NAM in the process (**Fig 1.2**) [130]. All 7 members of the SIRT family share a highly conserved NAD^+ binding domain [138], however SIRT-1 and SIRT-3 are the most dependent on NAD^+ bioavailability to perform their cellular functions [130]. Like PARPs, SIRTs consume about 33% of all NAD^+ under basal conditions [137]. The last third of NAD^+ consumption includes NAD^+ Kinase, which consumes 10% of all NAD^+, cluster of differentiation 38 (CD38), and other NAD^+ consuming enzymes [137]. Being that both PARPs and SIRTs require NAD^+ for their respective cellular functions, they are in a constant tug-of-war with one another, fighting for limited NAD^+ resources (**Fig 1.2**).

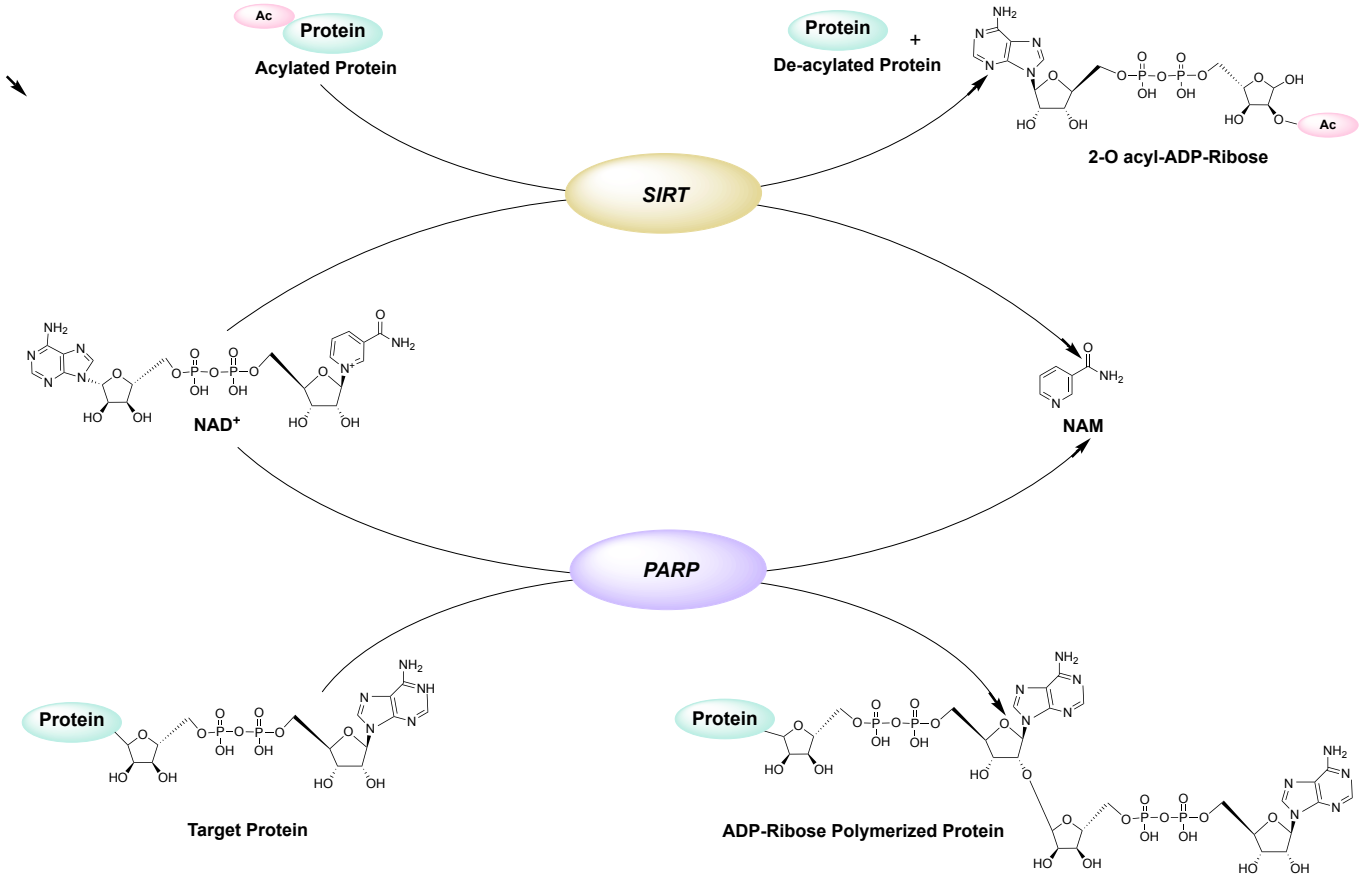

Figure 1.2. NAD$^+$ as a co-factor in reactions mediated by SIRTs and PARPs.

SIRTs use NAD+ as a cofactor to remove an acyl-group from their own substrate, forming deacylated substrate 2-O-acyl-ADP-ribose and NAM as their final products. When PARP locates DNA strand breaks, it attaches to them, and uses NAD+ to produce ADP-ribose, which then gets polymerized to nuclear acceptor proteins such as histones, transcription factors, topoisomerases, DNA helicases, and PARP itself. SIRT= sirtuin, PARP = poly-ADP ribose polymerase, NAM = nicotinamide, NAD+ = nicotinamide adenine dinucleotide. This figure was created using ChemDraw 23.1.1.

In response to DNA damage and several proinflammatory signals (i.e. NF-κB, p53) [174-177], PARPs are catalytically activated by both double-strand (DSB) and single-strand (SSB) DNA breaks [139]. When PARPs locate DSBs and/or SSBs, they attach to them and carry out their previously described functions using NAD$^+$ to produce ADP-ribose, which then gets polymerized to nuclear acceptor proteins such as histones, transcription factors, topoisomerases, DNA helicases, and PARP itself [140-141], allowing for DNA repair. However in cases of chronic cellular stress, such as extensive DNA damage which could occur via processes of aging or chronic inflammation, PARPs become overactivated, rapidly depleting cellular stores of NAD$^+$ [142]. In turn, this reduces the amount of bioavailable NAD$^+$, thus restricting the ability of SIRTs to carry out their

respective functions [137, 143-145].This overconsumption of NAD^+ also greatly impairs mitochondrial function, as it limits levels of NAD^+ for use in catabolic pathways such as the Krebs Cycle, dysregulating mitochondrial respiration [142]. In turn, this limits synthesis of ATP [142]. In the non-pregnant population, disorders characterized by chronic inflammation (i.e. inflammatory bowel disease [39], Parkinson's disease [146-147], and chronic obstructive pulmonary disease (COPD) [148-149] , to name a few), demonstrate systemic PARP hyperactivation and subsequent NAD^+ depletion. In parallel, these conditions are also known to demonstrate mitochondrial impairment and metabolic dysfunction. As a result, investigations into the potential for therapeutically targeting NAD^+ signalling pathways have been explored in these non-pregnant populations, with significant improvements in disease outcomes [150-152]. For instance, strategies that use treatment of NAD^+ precursors to boost physiological levels of NAD^+ have demonstrated considerable potential, effectively elevating systemic NAD^+ levels and improving energy metabolism. The most commonly described NAD^+ precursors and their derivatives tested include nicotinamide (NAM), nicotinamide mononucleotide (NMN), nicotinic acid (NA), and nicotinamide riboside (NR) (**Fig 1.3**).

Of these aforementioned molecules, NR has become a more favorable precursor as it has been shown to have positive NAD^+ boosting impacts with no detrimental side effects [153-154]. For instance, administration of a single dose of 1000 mg of NR to clinical populations did not cause any flushing, a reaction that was demonstrated by patients treated with a single dose of 500 mg of NA [155]. Moreover, in a study using the maximum reported dosage of NR in patient populations at 2000 mg/day for 12 weeks, they did not observe any adverse health outcomes – demonstrating that treatment with NR might be safer in humans than other NAD^+ boosters [156]. Other than being identified as a safe therapeutic, NR administration has demonstrated positive outcomes in non-pregnant populations with obesity. For instance, in a human obesity study, NR treatment of 1000 mg/kg/day for 6 weeks increased NAAD and methyl nicotinamide concentrations in skeletal muscle of individuals with obesity [156-158]. This was associated with increased lean/skeletal muscle mass, sleeping metabolic rate, and concentrations of acetylcarnitine – a molecule that assists the body in turning fat into energy [159].

Another human obesity study that administered an escalating dose of NR (250 to 1000 mg/day) for 5 months to adult BMI-discordant (within-pair difference of < 2.5 kg/m^2 in BMI) monozygotic twins, discovered that NR increased systemic NAD$^+$ levels, muscle/white adipose tissue NAD$^+$ biosynthesis, and muscle mitochondrial number, as well as improved myoblast differentiation and gut microbiota composition [160]. In this light, the success of NR treatment in mitigating effects of obesity in non-pregnant human populations prompts interest into its effects on pregnant populations with obesity.

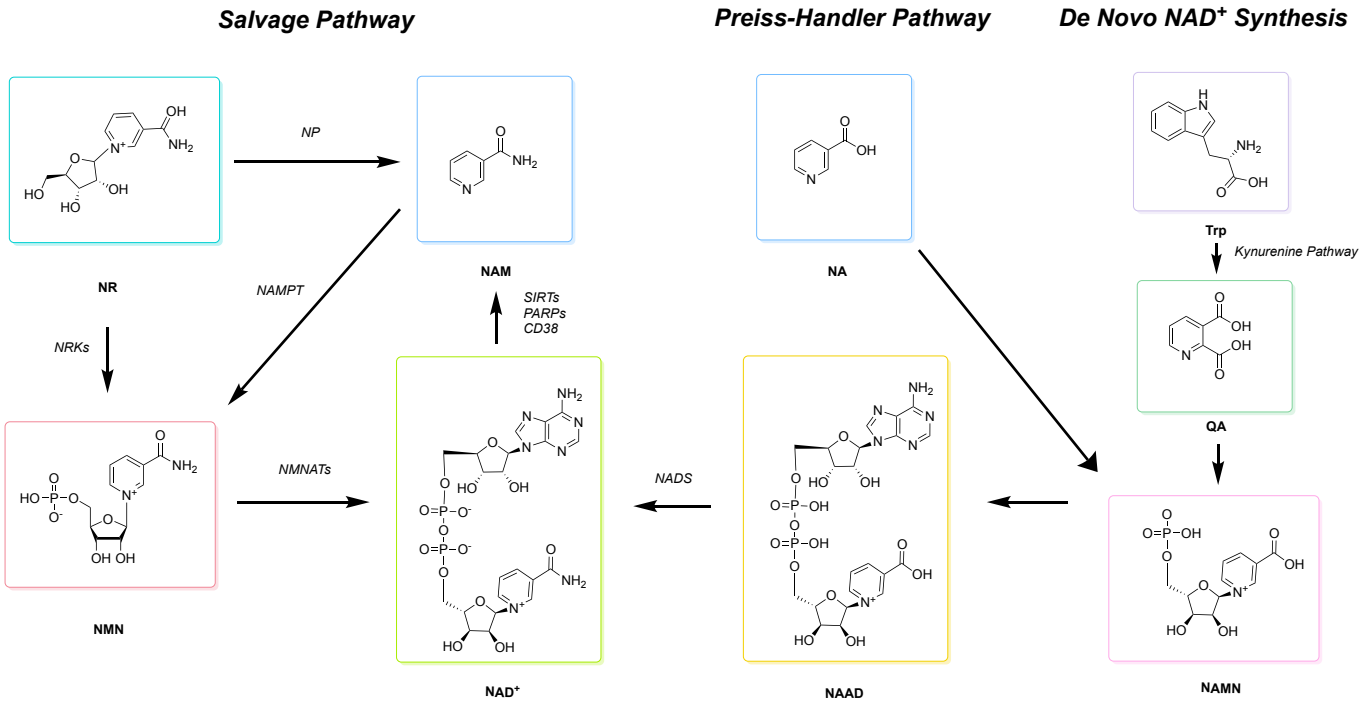

Figure 1.3. NAD$^+$ pre-cursors and their derivatives.

NAD$^+$ can be produced via the salvage pathway by converting NR to NMN (via NRKs) and then to NAD$^+$ via NMNATs, or by converting NMN directly to NAD$^+$ via NMNATs. NAD$^+$ can likewise be produced via the Preiss-Handler pathway, in which NA is converted to NAMN, then to NAAD, and then to NAD$^+$ via NADS. NAD$^+$ may be converted to NAM by SIRTs, PARPs, and CD38 in consumption reactions. NAD$^+$ can also be formed through de novo synthesis, in which Trp is converted into QA through the kynurenine pathway, and then converted to NAMN, to NAAD, and to NAD$^+$. SIRT= sirtuin, PARP = poly-ADP ribose polymerase, CD38 = cluster of differentiation 38, NAM = nicotinamide, NAD$^+$ = nicotinamide adenine dinucleotide, NR = nicotinamide riboside, NMN = nicotinamide mononucleotide, NA = nicotinic acid, NAAD = nicotinic acid adenine dinucleotide, NAMN = nicotinic acid mononucleotide, NAMPT = nicotinamide phosphoribosyltransferase, NRK = nicotinamide riboside kinase, NMNAT = Nicotinamide mononucleotide adenylyl transferases, NADS = NAD synthetase, Trp = Tryptophan, QA = Quinolinic Acid. This figure was created using ChemDraw 23.1.1.

While NAD$^+$ depletion and the impacts of NAD$^+$ boosters have not been tested in human pregnancy, some results in animal models of pregnancy show promise. In a mouse

model of obesity, NAD^+ has been found to be depleted in oocytes via a SIRT-3 dependent pathway [161]. Interestingly, boosting NAD^+ levels with NR treatment in this model rescued obesity-mediated detriments to the oocyte by improving its overall quality and early embryonic competence [161]. In a similar mouse model, levels of nicotinamide phosphoribosyltransferase (NAMPT) and NAD^+ were found to be depleted in obesity-exposed oocytes, with evidence of dysregulated oocyte metabolism [162]. Again replenishment of NAD^+, this time using nicotinic acid (NA), significantly ameliorated oxidative stress and metabolic function in these oocytes [162]. However no research currently exists on the impacts of NAD^+ boosters on placental health in the context of gestational obesity.

1.8 Placental NAD^+ depletion and Mitochondrial Dysfunction in Gestational Obesity

A clear understanding that inflammation-driven NAD^+ depletion can underlie the establishment of systemic metabolic dysfunction in non-pregnant individuals has led our research group to explore whether this same pathophysiology may be involved in the establishment of placental dysfunction in the context of chronic inflammatory disorders of pregnancy. Our group first sought to test this hypothesis in patients with an inflammation-driven form of preeclampsia – a hypertensive disorder of pregnancy. Placentas collected from this unique patient population not only demonstrated heightened immune cell infiltration and expression of pro-inflammatory cytokines, but also demonstrated increased total protein PARylation (a marker of PARP activation) and decreased stores of NAD^+ [163]. Likewise, in a rodent model established to mimic this inflammation-mediated preeclampsia phenotype, PARP-mediated NAD^+ depletion was noted in the placentas coupled to evidence of mitochondrial dysfunction, decreased placental efficiency, and fetal growth restriction [163]. Importantly, in this model, replenishment of placental NAD^+ content using NR rescued this adverse pregnancy phenotype [163] – the first evidence to suggest that therapeutically targeting NAD^+ signalling may improve placental function and pregnancy outcomes in conditions of chronic inflammation.

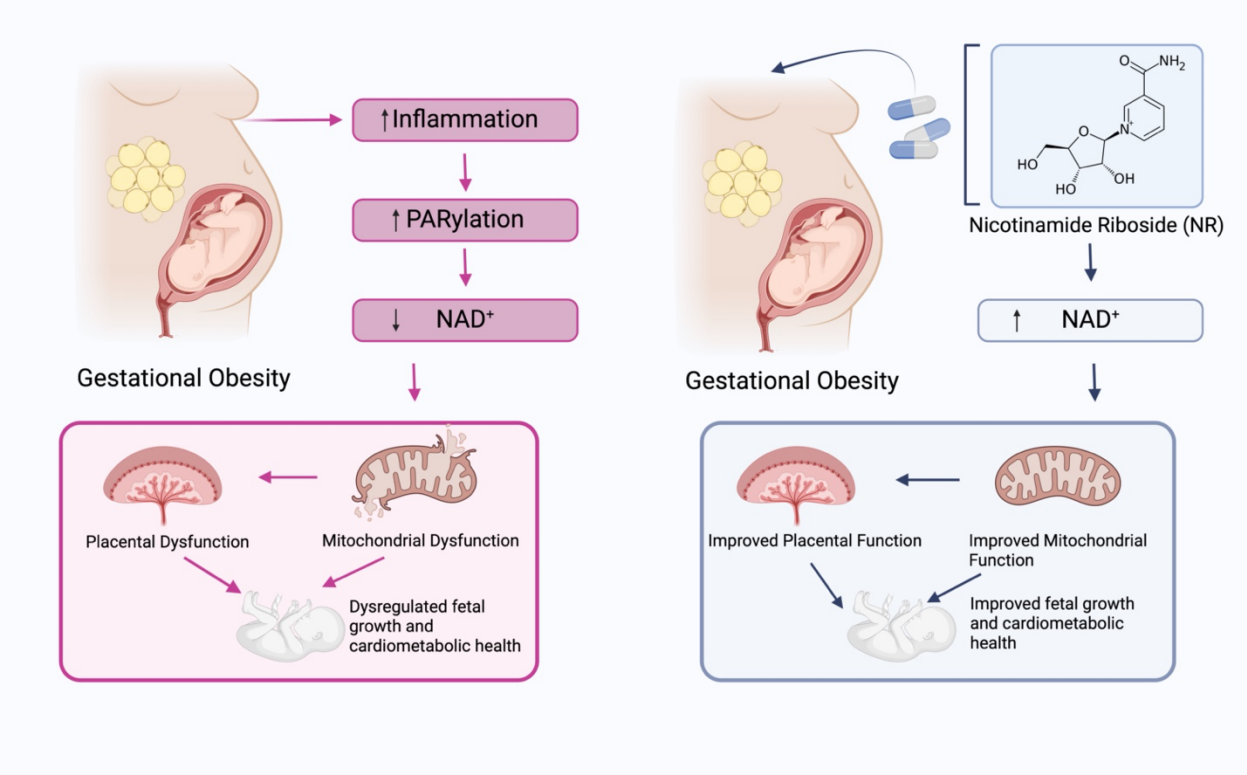

Figure 1.4. Chronic inflammatory mechanism imparted by gestational obesity.

Chronic inflammation from gestational obesity leads to increased PARylation activity, depleting NAD^+ stores, and rendering mitochondria impaired - leading to poor placental function and fetal growth dysregulation (A). Nicotinamide Riboside (NR) supplement increases NAD^+ levels, restoring healthy placental and mitochondrial function (B). This figure was created using BioRender.com.

As detailed, obesity-mediated inflammation in non-pregnant models is known to illicit NAD^+ depletion and mitochondrial dysfunction in a number of tissue beds including muscle, liver, kidney, adipose tissue, and intestine [130] – findings that have been successfully reversed through NAD^+ boosting strategies [164-167]. Whether this same pathophysiology holds true in the establishment of placental dysfunction in the context of gestational obesity has yet to be explored. Using a mouse model of 'western' diet-induced gestational obesity, the current study will build upon this novel body of work, elucidating whether PARP-mediated NAD^+ depletion likewise accompanies mitochondrial dysfunction and placental disease observed in gestational obesity. Furthermore, we will determine if boosting NAD^+ is able to rescue these poor placental and fetal phenotypes (**Fig 1.4**).

Chapter 2 – Hypothesis & Research Aims

2.1 Hypothesis

The overarching hypothesis of the current study is that ***obesity-mediated inflammation depletes placental NAD^+, impairing mitochondrial health, and can be rescued via gestational NAD^+ supplementation***. More specifically, we hypothesize that chronic administration of a high-fat high-sugar 'western' diet to a pregnant mouse model will lead to increased placental inflammation, triggering poly-ADP ribose polymerase (PARP) overactivation, NAD^+ depletion, and subsequent mitochondrial impairment in these placentas, ultimately leading to poor fetal growth profiles. We further propose that therapeutically boosting placental NAD^+ content using an NAD^+ supplement throughout pregnancy will improve the metabolic health of the placenta, and ultimately improve fetal growth and health outcomes.

2.2 Specific Research Aims

In the current MSc thesis, the previously stated hypothesis was tested through the completion of the following research aims:

Aim 1. Evaluate the effects of gestational obesity on placental development and fetal growth using a HFHS diet obesity mouse model with and without NR treatment.

Aim 2. Determine the effects of gestational obesity on placental PARP signaling, NAD^+ content, and mitochondrial function in a HFHS mouse model of gestational obesity with and without NR treatment.

Chapter 3 - Methods

3. Methods

3.1 Mouse model of gestational obesity

All animal experiments were performed in accordance with the University of Ottawa Animal Care Committee and Protocol Review (protocol #HS3937). C57BL/6N mice (Charles River Laboratories International, Inc.) were housed at 23℃ and kept on a 12:12-hr light-dark cycle. Beginning at 6 weeks of age, female mice were maintained on either control (CTRL) diet (Chow) or high-fat high-sugar (HFHS) diet (42% kcal fat, 34% sucrose by weight, TD.88137 Harlan-Tekklad) for 12-15 weeks (dependent on time to pregnancy from first mating) and weighed weekly. Immediately prior to breeding (after 12 weeks of diet administration), pre-pregnancy fat mass percentage was assessed by Echo-MRI and a 6-hour fasted glucose test was performed to assess baseline glucose handling.

Beginning at 18 weeks of age (12 weeks after diet administration), female mice were mated with 10-week-old C57BL/6N male mice maintained on a control chow diet. Vaginal plugs were checked daily to confirm pregnancy, with the presence of the plug denoted as gestational day(E) 0.5. Maternal body weights were recorded daily to track gestational weight gain, with ultrasound (Preclinical Imaging Core (PCIC)) performed at E12.5 to confirm the presence of pregnancy.

Pregnant dams were maintained on their assigned pre-pregnancy diet (CTRL or HFHS) and beginning at E0.5 dams from both diet exposures received either 400 mg/kg/day nicotinamide riboside (NR) or water (H_2O) as a control, via oral gavage daily for the duration of gestation. As such, four experimental groups were established (**Fig. 3.1**):

1) **CTRL-H_2O** (n=11): Dams were maintained on CTRL chow diet and received sterile water via oral gavage from gestational day 0.5-18.5.
2) **HFHS-H_2O** (n=7): Dams were maintained on HFHS diet and received sterile water via oral gavage from gestational day 0.5-18.5.

3) **CTRL-NR** (n=10): Dams were maintained on CTRL chow diet and received NR via oral gavage from gestational day 0.5-18.5.

4) **HFHS-NR** (n=9): Dams were maintained on HFHS diet and received NR via oral gavage from gestational day 0.5-18.5.

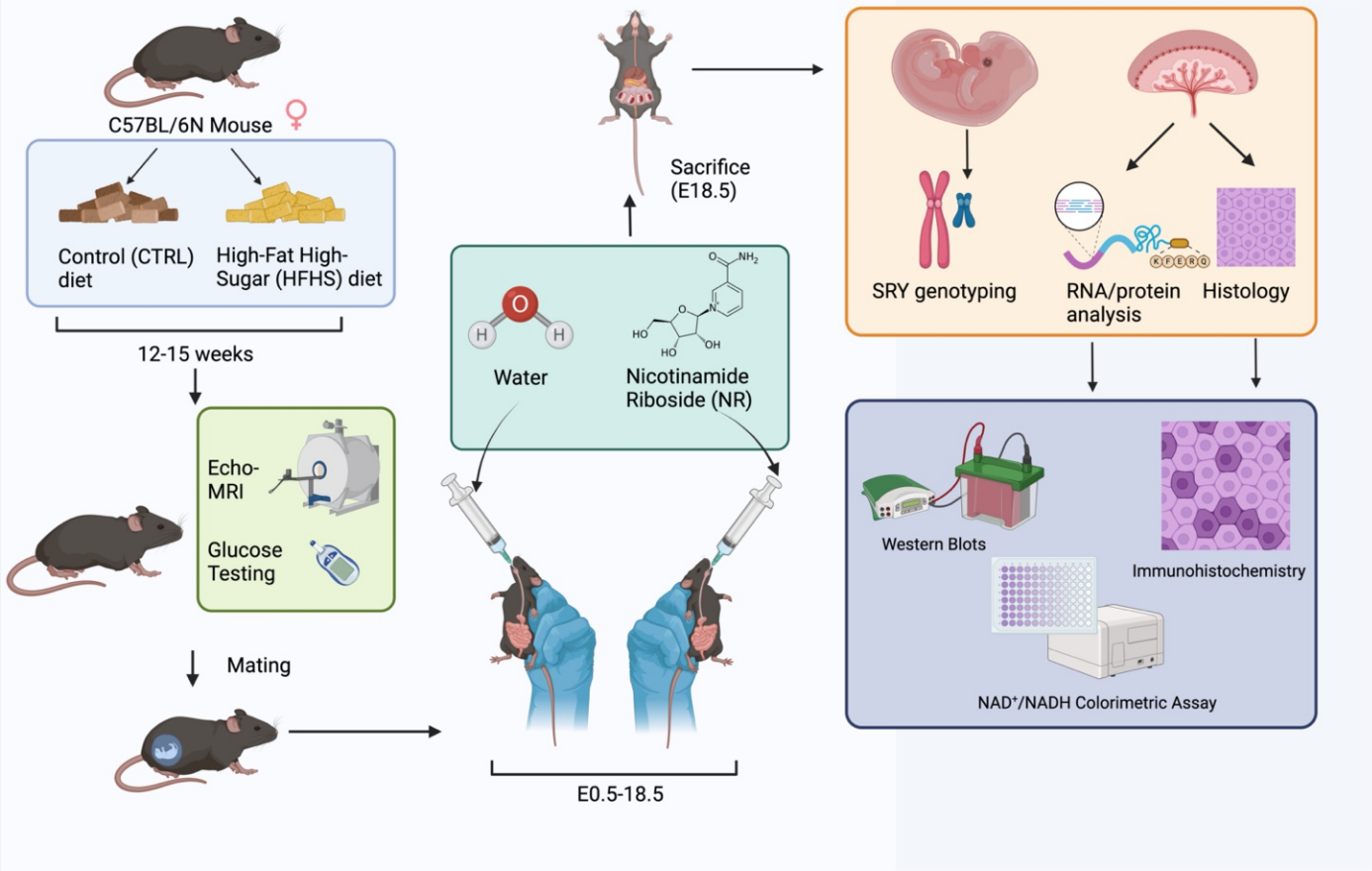

Figure 3.1. Mouse model experimental plan detailing diet administration and NR treatment.

Mice were sacrificed at E18.5. Fetuses were weighed, images taken for crown-rump length measurements, and tails were collected for SRY genotyping. Placentas were halved, with half flash frozen for RNA/protein analysis, and half fixed for histology measurements. CTRL=control; HFHS= High-Fat High-Sugar; H_2O=Water; NR=Nicotinamide Riboside.

All dams were sacrificed at E18.5, with maternal serum and liver collected and flash frozen in liquid N_2 for RNA/protein analysis. Maternal spleen and inguinal white adipose tissue (IWAT) were weighed. Fetuses were weighed, images taken for crown-rump length measurements, and tails collected for SRY genotyping. Placentas were weighed then halved at the umbilical insertion site, with half fixed in 4% paraformaldehyde (PFA) for histological analysis and half flash frozen in liquid N_2 for RNA/protein analysis.

3.2 Echo-MRI

Echo-MRI was performed on all female mice pre-pregnancy following 12 weeks of diet as an indicator of fat mass and lean mass percentage. Briefly, non-anesthetized mice were placed in the freestanding EchoMRI LLC machine in the open-end of a size 40 plastic tube (used for mice between 20-60 g), and gently pushed to the end of the tube. Sufficient space was ensured for mouse body length (not including tail). For obese mice that were > 40 g in weight, an additional 1.5 cm of length was left for breathing room. The tube was placed in the machine, and mice scanned for 40 seconds. Mice were in the tube for a maximum of 3 minutes to minimize stress (including initial placement and scan). Results were exported and analyzed in Microsoft Excel.

3.3 Fasted Glucose Testing

A fasted glucose test (6 hour fast) was also performed on all female mice pre-pregnancy after 12 weeks of diet to confirm glucose handling at baseline. Mice were fasted at 7 am for 6 hours, prior to measurement collection at 1 pm, obtained via the tail nick method.

3.4 SRY Genotyping

Crude DNA was extracted using 3 mm fetal tails (stored at -20℃ following sacrifice) mixed in 75 µL of 50 mM NaOH at 98℃ for 30 minutes. This solution was neutralized using 300 µL of 100 mM NaOAc. Following this, a 1X reaction composition was prepared (2 µL DNA, 4 µL sterile H_2O, 10 µL 2X Phire tissue direct PCR master mix (ThermoFisher #F170S), 1 µL 10 µM HMGR F, 1 µL 10 µM HMGR R, 1 µL 10 µM SRY F, and 1 µL 10 µM SRY R) and then loaded in the PCR thermocycler for 1 hour and 30 minutes using the following cycling conditions:

- 98℃ (3 min)
- These conditions x 40:
    - 98℃ (10 sec)

    - 65℃ (10 sec)
    - 72℃ (30 sec)
- 72℃ (5 min)

8 µL of each sample was loaded into a 2% agarose gel (2 g agarose, 98 mL 1X TAE, SYBR safe DNA gel stain) and electrophoresis was run for 1 h 30 minutes at 120 V. Gels were imaged using the ChemiDoc imager.

3.5 Placenta Histomorphology

Placentas fixed in PFA were paraffinized, sectioned, and put on glass slides. Sections were stained with hematoxylin and eosin (H&E) using standard protocols. Serial sections of each sample also underwent immunohistochemistry (IHC) staining for Ki-67 (marker of proliferation; Abcam, ab16667; 1:200). IHC staining was performed using the Leica Bond™ system. Antigen retrieval was performed using sodium citrate buffer (pH6, 20 minutes), followed by primary antibody incubation for 30 minutes at room temperature, and visualization using the 3,3'-diaminobenzidine horseradish peroxidase (DAB-HRP) conjugated compact polymer system. Images of all the slides were captured using Axio Scan.Z1 microscope at 20X magnification. From the midline H&E-stained placenta sections, measurements of total placenta depth were captured, along with those for each placental region (decidua, junctional zone, labyrinth zone) using ZEN 3.1 blue edition. To assess cellular proliferation, Ki-67 positive cells were counted across the entire placenta using QuPath [180]. Results were normalized based on total tissue area.

3.6 Placenta Gene Expression

Flash frozen placenta tissue was pooled per litter (n= 5-8 samples/experimental group), with 10 mg pulverized and lysed in Trizol (Tri-Reagent) using a bead mill. RNA was quantified in a NanoDrop® ND-1000 UV-Vis Spectrophotometer and sent to the Centre for Applied Genomics, at the Hospital for Sick Children (SickKids) affiliated with the University of Toronto, for Bulk RNA sequencing. DNA libraries were prepared using the

NEBNext® Ultra™ II Directional RNA Library Prep Kit coupled with NEBNext poly(A) mRNA Isolation. Paired end 2x150-bases untrimmed reads were obtained from pooled DNA libraries using NovaSeq S4 flowcell on an Illumina NovaSeq 6000 Sequencer. These untrimmed reads were generated in the FastQ format, generated using bcl2fastq2 v2.20. Sequencing results were separated by library barcoding, and barcodes removed using the TCAG platform. Subsequently, data was imported into the Galaxy Platform maintained by GenAP (http://www.genap.ca) and hosted by the Digital Research Alliance of Canada. Quality of sequencing was assessed using the FastQC function. Sequences were aligned to the mouse genome and read quantification and assignment was performed using the HISAT2 and feature counts functions, respectively. Count normalization and differential gene expression between diet and treatment groups was performed using DESeq2 and an FDR of 10%. Genes were ranked according to their p-values, and subsequent Gene Set Enrichment Analysis was conducted in RStudio, utilizing Gene Ontology's biological process as the source database. Z-scores were calculated from normalized counts of leading genes within enriched GO terms and heat maps generated in R studio.

3.7 Placenta PARP Protein Expression and Activity

Flash frozen placenta tissue was pooled by sex per litter (n= 3-6 samples/experimental group), crushed in liquid N_2, and 10-35 mg of tissue was homogenized in RIPA buffer (5 µL RIPA buffer/mg placenta tissue). The homogenate was then centrifuged twice at 16,000 relative centrifugal force (rcf) for 10 minutes at 4ºC. Protein concentration of the supernatant was determined using a detergent compatible (DC) protein assay (Bio-Rad Laboratories, Hercules, California, USA, Cat. #5000113) using Bovine Serum Albumin (BSA) standards that were mixed in RIPA buffer. Samples were diluted in 4x Laemmli Buffer (Bio-Rad Laboratories, Hercules, California, USA, Cat. #1610747) to a stock concentration of 2 mg protein/mL. Samples were stored at -80ºC until use for western blot analyses.

Western blots were performed using 12% SDS-PAGE gels and the TGX Stain-free FastCast Acrylamide Kit (Bio-Rad Laboratories, Hercules, California, USA, Cat.

#1610183). Briefly, equivalent protein amounts (20 mg) were loaded into gels for SDS-PAGE and transferred to LF PVDF membrane (Bio-Rad Laboratories, Hercules, California, USA, Cat. #10026934) using the Trans-Blot TurboTransfer system (Bio-Rad Laboratories, Hercules, California, USA, Cat. #1704150EDU). Equivalent total protein loading between samples was detected on the ChemiDoc system (Bio-Rad Laboratories, Hercules, California, USA, Cat. #12003153) using stain-free blot settings. Membranes were incubated with antibodies against PARP 1 (1:1000; Santa-Cruz Biotechnology, sc-8007), PARP 2 (1:50; Enzo Life Sciences, O8855) and Poly/Mono ADP-Ribose (1:1000; Cell Signaling Technology, #83732), followed by incubation with (H+L)-HRP conjugated secondary antibody (1:10,000; Bio-Rad Laboratories, Hercules, California, USA, Cat. #1706515). Bands were detected using Clarity Western ECL substrate (Bio-Rad Laboratories, Hercules, California, USA, Cat. #1705061) under chemiluminescence settings on the ChemiDoc imager. Blots were quantified using ImageJ FIJI software.

3.8 Placenta NAD^+ Content

Crushed frozen placenta tissue (pooled by sex per litter; 20-30 mg) and maternal liver tissue (20-40 mg) were homogenized in 300 µL of NAD^+/NADH extraction buffer (AB65348). Maternal serum was diluted in NAD^+/NADH extraction buffer by a factor of 8. NAD^+/NADH/Total NAD quantification was carried out using the abcam NAD^+/NADH kit (AB65348) as per the manufacturer's instructions.

3.9 Placenta Mitochondrial Protein Content

Using placental protein isolates and western blot protocols described in section 3.2.4, expression of mitochondrial oxidative phosphorylation (OXPHOS) proteins was assessed using the OXPHOS rodent primary antibody cocktail (Abcam, ab110413) and a Goat Anti-Mouse IgG (H+L)-HRP conjugated secondary antibody (Bio-Rad Laboratories, Hercules, California, USA, Cat. #170-6516).

3.10 Data Analysis

All statistical analysis – except for RNA data– was performed using Graphpad Prism software (version 10.2.2). Data are presented as mean ± standard deviation (SD). Depending on the dataset, an unpaired t-test or two-way ANOVA with a Bonferroni post-hoc multiple comparisons test was performed to assess differences in diet and treatment. Any values ± 2 SD from the mean were excluded from the analysis as outliers. A p-value of £ 0.05 was used to indicate significance. For RNA data, count normalization and differential gene expression between diet and treatment groups was performed using DESeq2 and an FDR of 10%. Genes were ranked according to their p-values, and subsequent Gene Set Enrichment Analysis was conducted in RStudio, utilizing Gene Ontology's biological process as the source database. Z-scores were calculated from normalized counts of leading genes within enriched GO terms and heat maps generated in R studio.

Chapter 4 - Results

4. Results

4.1 C57BL/6N female mice fed a HFHS diet are obese prior to pregnancy

The current study sought to develop a murine model of gestational obesity using a 'westernized' HFHS diet, to determine the effects of obesity-mediated inflammation on placental NAD^+ signaling pathways. To generate this model, young female mice were placed on a HFHS diet for 12-15 weeks prior to pregnancy. At the end of this pre-pregnancy exposure the HFHS females were 9.98 g +/- 1.13 g heavier than CTRL females (**Fig. 4.1A**), with 9.48% +/- 1.03% greater fat mass (**Fig. 4.1B**), and higher fasting blood glucose levels (**Fig. 4.1C**). Beginning at 12 weeks of diet exposure, mice mating was initiated. Mice on the HFHS diet did not demonstrate any differences in fertility compared to mice on CTRL diet, demonstrated by similar length of time taken to achieve pregnancy (**Fig. 4.1D**), rate of successful pregnancy after first vaginal plug (**Fig. 4.1E**), and necessity for re-mating (**Fig. 4.1F**). At E0.5 the daily water or NR experimental treatments were commenced (**Fig. 4.1G**). Initially 10-11 dams were included in each experimental group, however 3 dams in HFHS-H_2O were lost due to end-point ulcerative dermatitis and 1 dam in the HFHS-NR group was lost due to preterm birth at E17.5.

During pregnancy, HFHS females gained less gestational weight than CTRL females (**Fig. 4.1H**), a potential indicator of reduced litter size and/or fetal growth restriction (FGR). This reduced gestational weight gain was observed in both the HFHS-H_2O and HFHS-NR experimental groups. At the time of sacrifice (E18.5), HFHS female mice demonstrated greater inguinal white adipose tissue (IWAT) mass and spleen mass (**Supplemental Fig. 4.5.1**), another indicator of obesity, as similarly seen in other studies [181]. These greater masses were observed in both untreated and NR treated HFHS maternal organs.

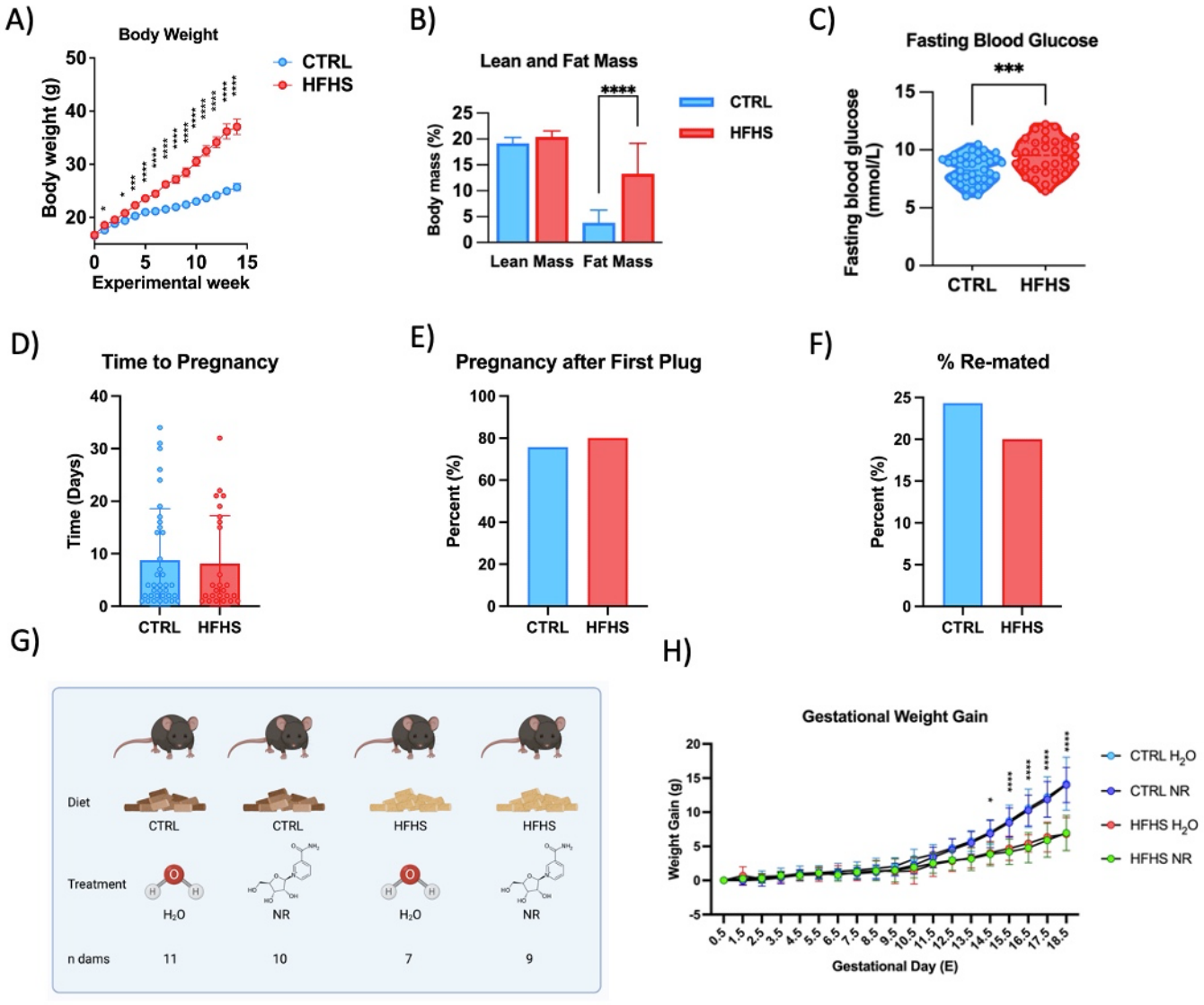

Figure 4.1 Dam measurements in a HFHS diet-induced model of obesity.

Pre-gestational body-weight over 12-15 weeks of diet exposure (A), fat mass percentage measured via Echo-MRI after 12 weeks of diet (B), and fasting blood glucose after 12 weeks of diet (C). Time (days) taken to become pregnant following first paired mating (D), percentage of mice pregnant after observation of first vaginal plug (E), and percentage of mice that were re-paired following failure to achieve pregnancy in first pairing (F). Total mice sacrificed per experimental group (G) and gestational weight gain from embryonic day 0.5-18.5 (H). Differences in diet exposure assessed via unpaired t-test with Bonferroni post-hoc test (*p<0.05). Two-way ANOVA with Bonferroni post-hoc test assessed differences by diet and treatment (*p<0.05). CTRL= control chow diet, HFHS = high-fat high-sugar diet, NR=nicotinamide riboside, E = gestational day.

4.2 Gestational obesity leads to placental inflammation, abnormal placental development, and fetal growth restriction

No differences in litter size were noted across experimental groups (**Fig. 4.2A**). Fetuses from HFHS mothers were 0.23 g +/- 0.05 g lighter (**Fig. 4.2B**) and 3.37 mm +/- 0.74 mm shorter (**Fig. 4.2C**) than fetuses from CTRL mothers. These differences were more pronounced in female fetuses compared to male fetuses (**Supplemental Fig. 4.5.2**). No difference in total placental weight was observed across groups (**Fig. 4.2D**), however, placental efficiency, measured as the ratio of fetal mass to placental mass, was markedly reduced in offspring from HFHS mothers (**Fig. 4.2E**). This effect was more pronounced in female fetuses (**Supplemental Fig. 4.5.2**). Unfortunately, no protective effects of NR on fetal growth or placental efficiency were observed (**Fig. 4.2A-E**).

Detailed histomorphology analysis of collected placentas demonstrated no differences in total or region-specific depths collectively (**Fig. 4.2G-K**), however when examined individually by fetal sex, male placentas from HFHS mothers did demonstrate a trend towards a smaller labyrinth zone (LZ) (**Fig. 4.2L-M**). The total number of proliferating cells (Ki-67 positive) in placental cross sections did not differ according to maternal diet (**Fig. 4.2N**) or according to fetal sex (**Supplement Fig. 4.5.2**). NR treatment demonstrated no effect on histomorphometry measurements of the placenta, nor on number of proliferating cells (**Fig. 4.2N**).

Placental gene expression profiles demonstrated evidence of increased expression in genes pertaining to a positive immune response including genes belonging to the complement system (i.e., C1qb, C2, C4a, C9, Cfi, Itgam, Masp2, Plscr1), genes leading to activation of pro-inflammatory cytokines (i.e., Elf1) and proinflammatory pathways such as PI3K/Akt and NF-κβ/MAPK (ie., Appl2, Malt1, Tbk1, Tlr9) (**Fig. 4.2O; Supplemental Fig. 4.5.4**) in HFHS placentas compared to controls. Slight changes in expression of some of these genes were observed with NR treatment (i.e., Itgam, Malt1, Masp2) (**Fig. 4.2P**).

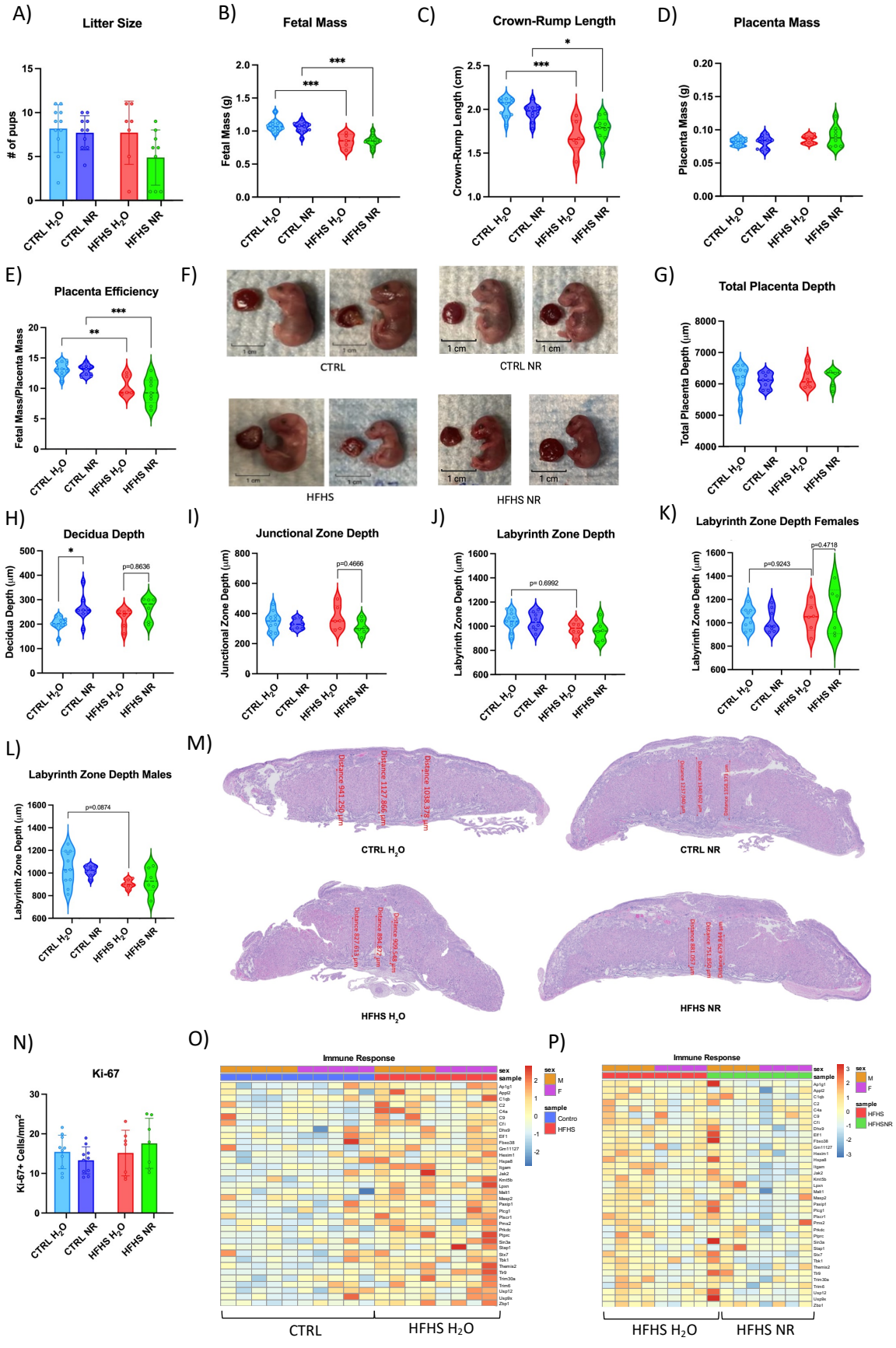
A)
Litter Size
# of pups
CTRL H2O
CTRL NR
HFHS H2O
HFHS NR
B)
Fetal Mass
Fetal Mass (g)
C)
Crown-Rump Length
Crown-Rump Length (cm)
D)
Placenta Mass
Placenta Mass (g)
E)
Placenta Efficiency
Fetal Mass/Placenta Mass
F)
CTRL
CTRL NR
HFHS
HFHS NR
G)
Total Placenta Depth
Total Placenta Depth (μm)
H)
Decidua Depth
Decidua Depth (μm)
p=0.8636
I)
Junctional Zone Depth
Junctional Zone Depth (μm)
p=0.4666
J)
Labyrinth Zone Depth
Labyrinth Zone Depth (μm)
p= 0.6992
K)
Labyrinth Zone Depth Females
Labyrinth Zone Depth (μm)
p=0.9243
p=0.4718
L)
Labyrinth Zone Depth Males
Labyrinth Zone Depth (μm)
p=0.0874
M)
CTRL H2O
CTRL NR
HFHS H2O
HFHS NR
N)
Ki-67
Ki-67+ Cells/mm2
O)
Immune Response
sex
sample
M
F
Contro
HFHS
CTRL
HFHS H2O
P)
Immune Response
HFHSNR
HFHS H2O
HFHS NR

Figure 4.2. Fetal and placental phenotype measurements in a HFHS diet-induced model of obesity. Litter size from dams sacrificed at E18.5 (A). Fetal mass (B) and crown-rump length (C) from pups extracted from dams sacrificed at E18.5. Placenta mass (D) and placenta efficiency (E) measured by dividing the fetal mass by the placental mass. Representative images of fetuses from CTRL, HFHS, CTRL-NR, and HFHS-NR dams taken on E18.5 (F). Total placenta depth (G), decidua depth (H), junctional zone depth (I), overall labyrinth zone depth (J), female labyrinth zone depth (K), and male labyrinth zone depth (L). Representative images of labyrinth zone depth in male placentas (M). Overall Ki-67 positive cells (N) in IHC placentas, counted using QuPath. Two-way ANOVA with Bonferroni post-hoc test assessed differences by diet and treatment (*p<0.05). Gene set enrichment analysis revealed enrichment in genes related to positive immune regulation (O-P). Z-scores were calculated for the leading genes in the indicated biological processes, and normalized gene expression was represented as heatmaps (*p<0.05). CTRL= control chow diet, HFHS = high-fat high-sugar diet, NR=nicotinamide riboside, Ki-67 = Antigen Kiel 67.

4.3 Gestational obesity leads to increased placental PARP expression and activity and reduced NAD^+ content

To examine whether obesity-mediated inflammation activated placental PARP enzymes, the protein expression of two key PARP enzymes was assessed by western blot, along with total protein PARylation as a measurement of PARP activity. Placentas from the HFHS exposed pregnancies demonstrated increased expression of both PARP-1 (**Fig. 4.3A-C**) and PARP-2 (**Fig. 4.3D-E**) – both key NAD^+ consuming PARP enzymes whose activation has been previously linked to inflammatory signaling [182]. Likewise, PARP activity, measured by total protein PARylation, trended towards an increased expression in placentas from the HFHS group (**Fig. 4.3F-G**). NR treatment did not change PARP-1 or PARP-2 protein expression, nor protein PARylation (**Fig. 4.3A-G**).

We next directly assessed NAD^+ and NADH content using a colorimetric assay. Importantly NAD^+ and total NAD (NADT) were significantly downregulated in HFHS placentas compared to control placentas (**Fig. 4.3J-M**). Additionally, analysis of our placenta gene expression dataset demonstrated decreased expression of genes involved in NADH regeneration, including genes implicated in glycolysis (i.e., Aldoa, Eno1, Gapdh, Gpi1, Hk1), those involved in gluconeogenesis (i.e., Gapdh), and those involved in complex I of the ETC (i.e., Ndufa1, Ndufa10, Ndufa11, Ndufa2, Ndufa5, Ndufb10, Ndufb11, Ndufb2, Ndufb5, Ndufb7, Ndufb8, Ndufc1, Ndufs5, Ndufs6, Ndufs7) (**Fig. 4.3H; Supplemental Fig. 4.5.4**), which may indicate increased difficulty of HFHS

placentas to maintain healthy NAD^+/NADH homeostasis required for appropriate metabolic regulation. Interestingly, some of these NADH regenerative genes were upregulated in HFHS-NR treated placentas (i.e., Aldoa, Gapdh, Gpi1, Ndufa1, Ndufa10, Ndufa11, Ndufa2, Ndufa5, Ndufb10, Ndufb5, Ndufb7, Ndufb8, Ndufc1, Ndufs5, Ndufs6, Ndufs7) (**Fig. 4.3**), however NR supplementation did not increase placental NAD^+ protein content. Likewise, no NR-mediated increase in NAD^+ content was observed in the maternal liver or serum either (**Supplemental Fig. 4.5.3**) – indicating that the NR intervention was not working as anticipated.

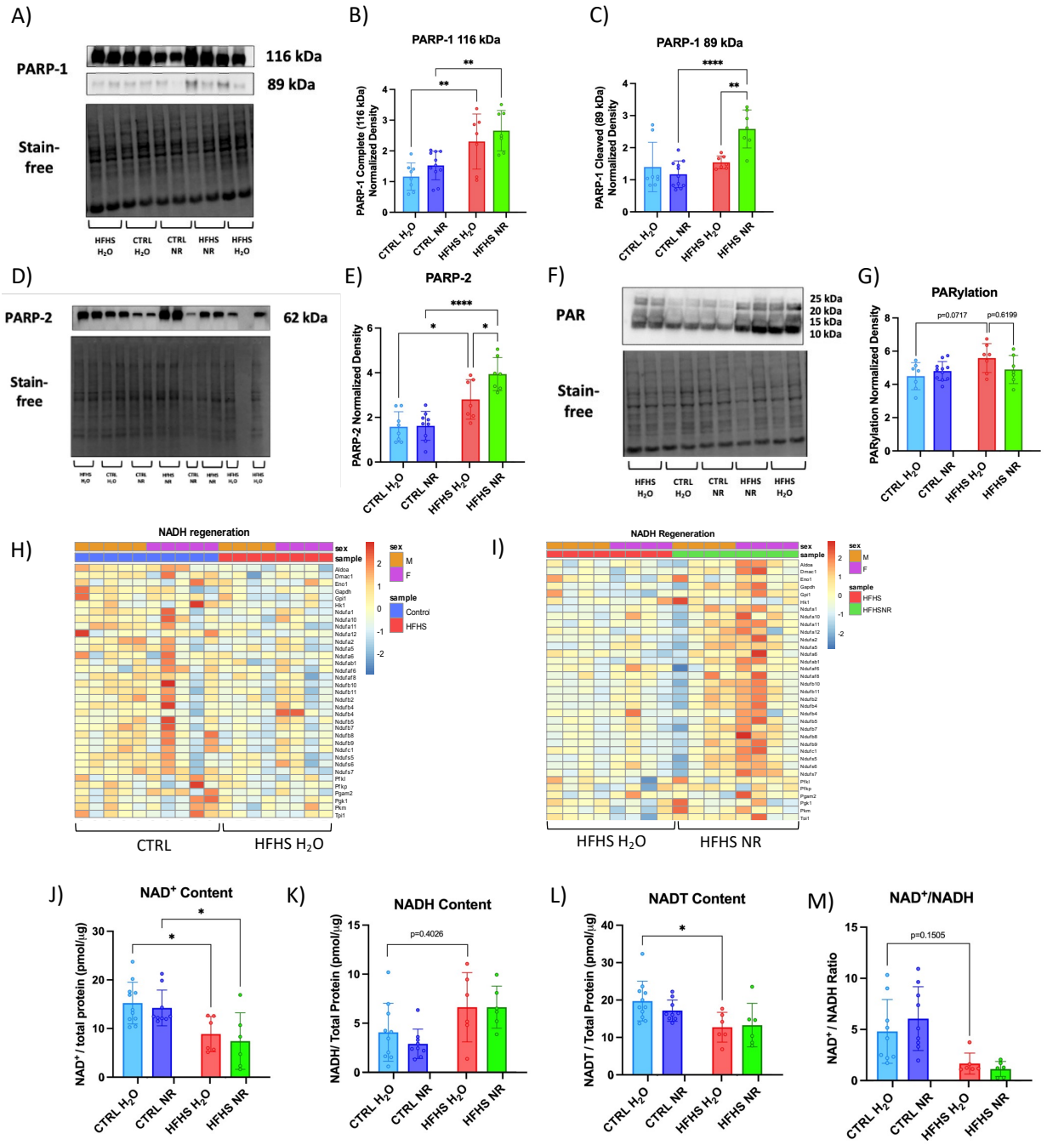

Figure 4.3. Effect of HFHS diet-induced obesity on placental PARP protein expression, activity and NAD⁺ content.

PARP-1 protein expression (A-C), PARP-2 protein expression (D-E), and total protein PARylation (F-G) measured using western blot. Two-way ANOVA with Bonferroni post-hoc test assessed differences by diet and treatment (*p<0.05). Gene set enrichment analysis revealed enrichment in genes related to NADH regeneration (H-I). Z-scores were calculated for the leading genes in the indicated biological processes, and normalized gene expression was represented as heatmaps (*p<0.05). NAD⁺ (J), NADH (K), and total NAD content (L), as well as NAD⁺/NADH ratio (M) calculated from a colorimetric NAD⁺ assay. Two-way ANOVA with Bonferroni post-hoc test assessed differences by diet and treatment (*p<0.05). CTRL = control chow diet, HFHS = high-fat high-sugar diet, NR=nicotinamide riboside, NADH = nicotinamide adenine dinucleotide + hydrogen, NAD⁺ = nicotinamide adenine dinucleotide, NADT = total

nicotinamide adenine dinucleotide, PARP-1 = Poly (ADP Ribose) Polymerase-1, PARP-2 = Poly (ADP Ribose) Polymerase-2, PAR = PARylation.

4.4 Gestational obesity leads to increased dysregulated mitochondrial protein expression

The impact of placental PARP-mediated NAD^+ depletion on mitochondrial health was examined by measuring the expression of key mitochondrial proteins involved in oxidative phosphorylation (OXPHOS proteins). In placentas from HFHS exposures, an overexpression of Complex V: ATP synthase (CV-ATP5A) and Complex II: Succinate Ubiquinone Oxidoreductase (CII-SDHB), and a trend towards an under expression of Complex IV: Cytochrome C Oxidoreductase (CIV-MTCO1) was observed compared to control placentas (**Fig. 4.4A-F**). There were no sex-related alterations to OXPHOS protein content (**Supplementary Fig. 4.5.4**). Unexpectedly, no improvements in mitochondrial proteins were observed with NR supplementation (**Fig. 4.4A-F).**

Likewise, expression of mitochondrial genes involved in electron ETC assembly (**Fig. 4.4G-H**) such as those involved in ETC complex I (i.e., Ndufa1, Ndufa10, Ndufa11, Ndufa2, Ndufa5, Ndufb10, Ndufb11, Ndufb2, Ndufb5, Ndufb7, Ndufb8, Ndufc1, Ndufs5, Ndufs6, Ndufs7), complex II (i.e, Sdhaf2, Sdhaf3), complex III (i.e., Uqcc2, Uqcc3) and complex IV (i.e., Chchd7, Coa3, Coa4, Cox14, Cox16, Cox17) were found to be downregulated in HFHS placentas demonstrating potential dysfunction in placental mitochondria to carry out respiration (**Supplemental Fig. 4.5.4**). Interestingly, expression of some of these genes were unregulated in HFHS placentas treated with NR (i.e, Ndufa1, Ndufa10, Ndufa11, Ndufa2, Ndufa5, Ndufb10, Ndufb5, Ndufb7, Ndufb8, Ndufc1, Ndufs5, Ndufs6, Ndufs7, Sdhaf2, Sdhaf3, Uqcc2, Uqcc3, Chchd7, Coa3, Coa4, Cox14, Cox16, Cox17). Additionally, expression of genes involved in ATP synthesis (**Fig. 4.4I-J**) including those involved in ETC complex I (i.e., Ndufa10, Ndufa7, Ndufb8, Ndufb9, Ndufs6, Ndufs7, Ndufs8, Ndufv2), complex II (i.e., Sdhaf2, Sdhb, Sdhc), complex III (i.e., Uqcrb, Uqcrh, Uqcrq), and complex IV (i.e., Coa6, Cox4i1, Cox7c) were found to be downregulated in HFHS placentas, demonstrating potential dysfunction in placental mitochondria to produce ATP (**Supplemental Fig. 4.5.4**).

Interestingly, expression of some of these ATP synthesis genes was upregulated in HFHS placentas treated with NR (i.e., Ndufa10, Ndufa7, Ndufb8, Ndufb9, Ndufs6, Ndufs7, Ndufs8, Ndufv2, Sdhaf2, Sdhb, Sdhc, Uqcrb, Uqcrh, Uqcrq, Coa6, Cox4i1, Cox7c). There were no sex-related differences in mitochondrial gene expression (**Fig. 4.4G-J**).

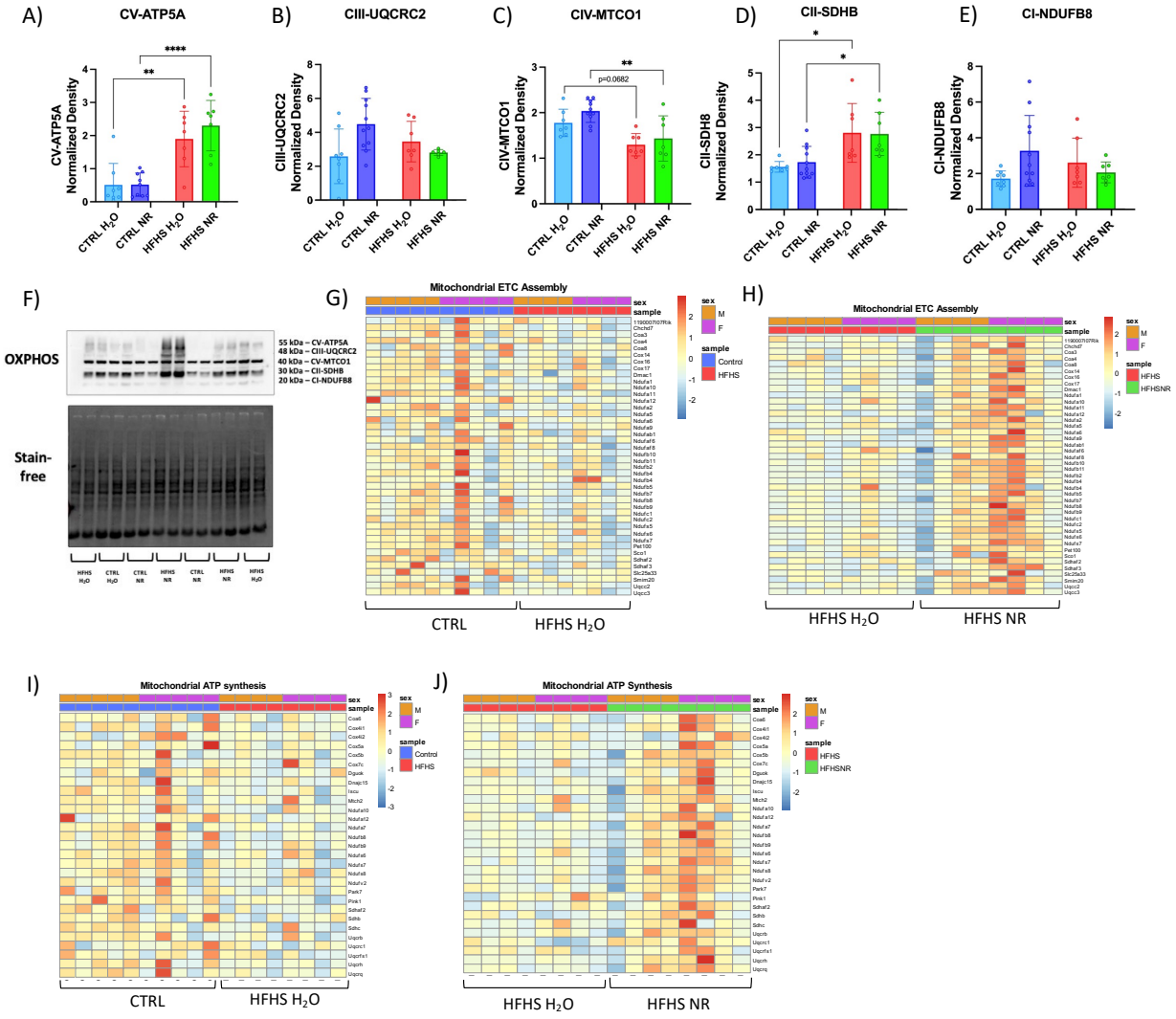

Figure 4.4. Effect of HFHS diet-induced obesity on mitochondrial health.
Mitochondrial OXPHOS protein expression (A-F) measured using western blot. Two-way ANOVA with Bonferroni post-hoc test assessed differences by diet and treatment (*p<0.05). Gene set enrichment analysis revealed enrichment in genes related to mitochondrial electron transport chain (ETC) assembly (G-H) and mitochondrial ATP synthesis genes (I-J). Z-scores were calculated for the leading genes in the indicated biological processes, and normalized gene expression was represented as heatmaps (*p<0.05). CTRL = control chow diet, HFHS = high-fat high-sugar diet, NR=nicotinamide riboside, ETC = electron transport chain, ATP = adenosine triphosphate, OXPHOS = oxidative phosphorylation, CV-ATP5A = Complex V ATP Synthase, CIII-UQCRC2 = Complex III Ubiquinol Cytochrome C Oxidoreductase, CIV-MTCO1 = Complex IV Cytochrome C Oxidoreductase, CII-SDHB = Complex II Succinate Ubiquinone Oxidoreductase, CI-NDUFB8 = Complex I NADH Dehydrogenase.

4.5 Supplemental Data

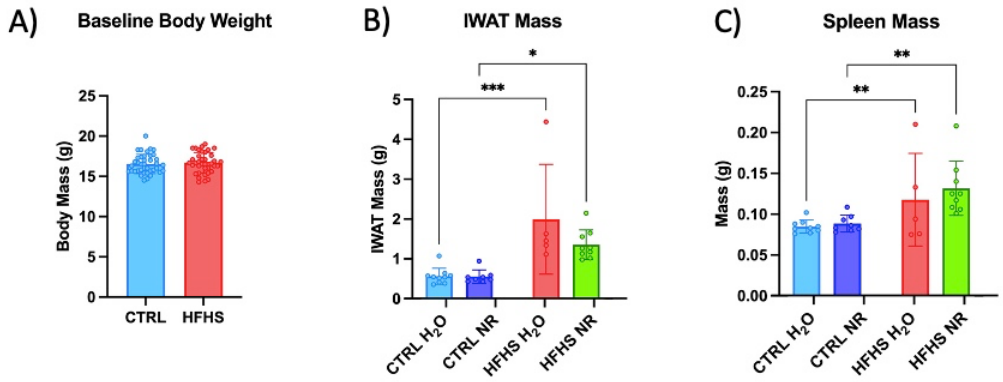

Supplemental Figure 4.5.1 Dam measurements in a HFHS diet-induced model of obesity. Baseline body mass of 6-week-old female mice prior to diet administration (A). IWAT (B) and spleen (C) mass of female mice following sacrifice. Differences in diet exposure assessed via unpaired t-test with Bonferroni post-hoc test (*p<0.05). Two-way ANOVA with Bonferroni post-hoc test assessed differences by diet and treatment (*p<0.05). CTRL= control chow diet, HFHS = high-fat high-sugar diet, NR=nicotinamide riboside, IWAT =inguinal white adipose tissue.

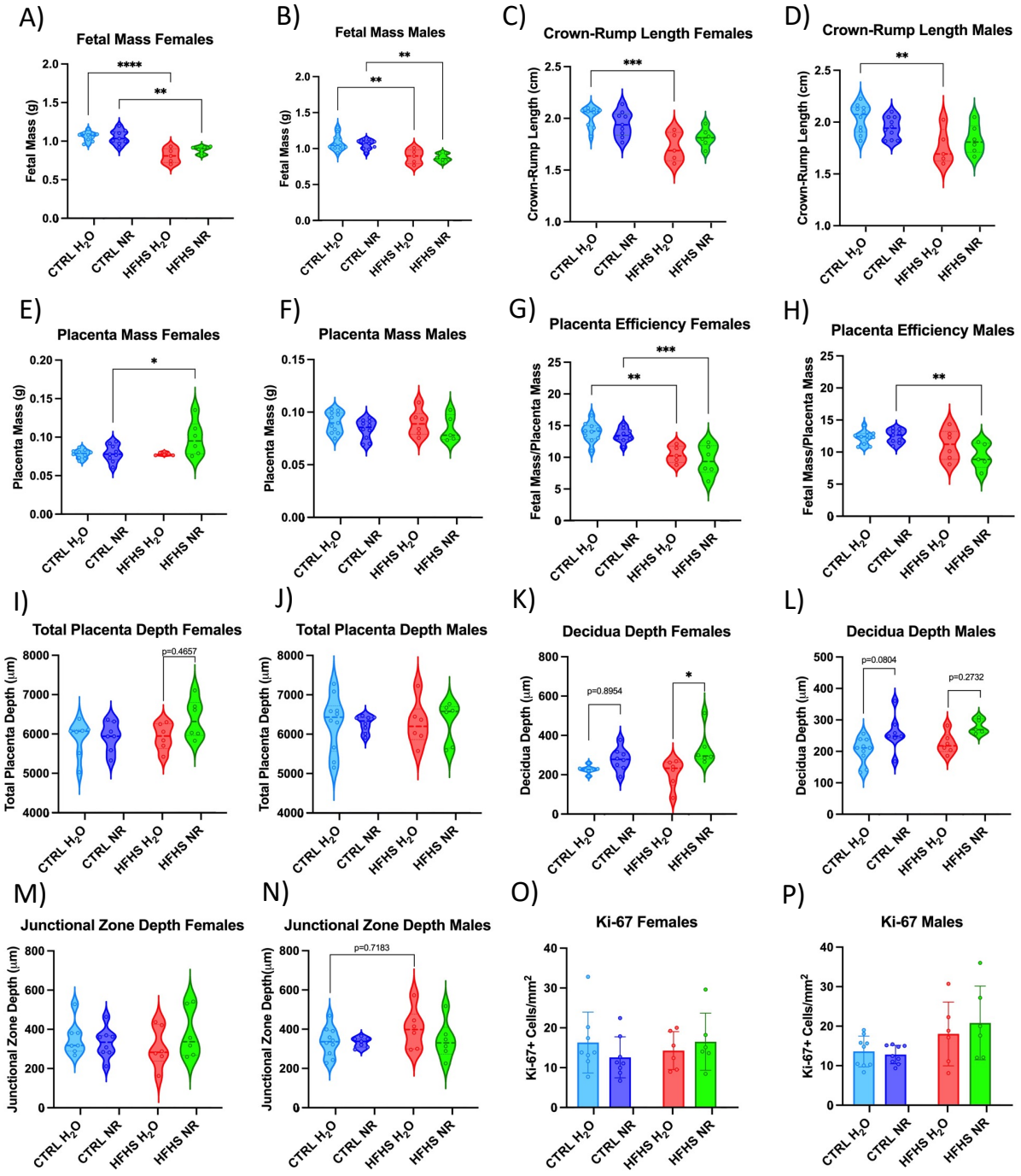

Supplemental Figure 4.5.2 Fetal and placental phenotype measurements in a HFHS diet-induced model of obesity.

Fetal mass (A-B) and crown-rump length (C-D) from female and male pups extracted from dams sacrificed at E18.5. Placenta mass (E-F) and placenta efficiency (G-H), measured by dividing the fetal mass by the placental mass, from female and male placentas. Total placenta depth (I-J), decidua depth (K-L), and junctional zone depth (M-N) in female and male placentas. Ki-67 positive cells (O-P) in female and male placentas, counted using QuPath. Two-way ANOVA with Bonferroni post-hoc test assessed differences by diet and treatment (*p<0.05). CTRL= control chow diet, HFHS = high-fat high-sugar diet, NR=nicotinamide riboside, Ki-67 = Antigen Kiel 67.

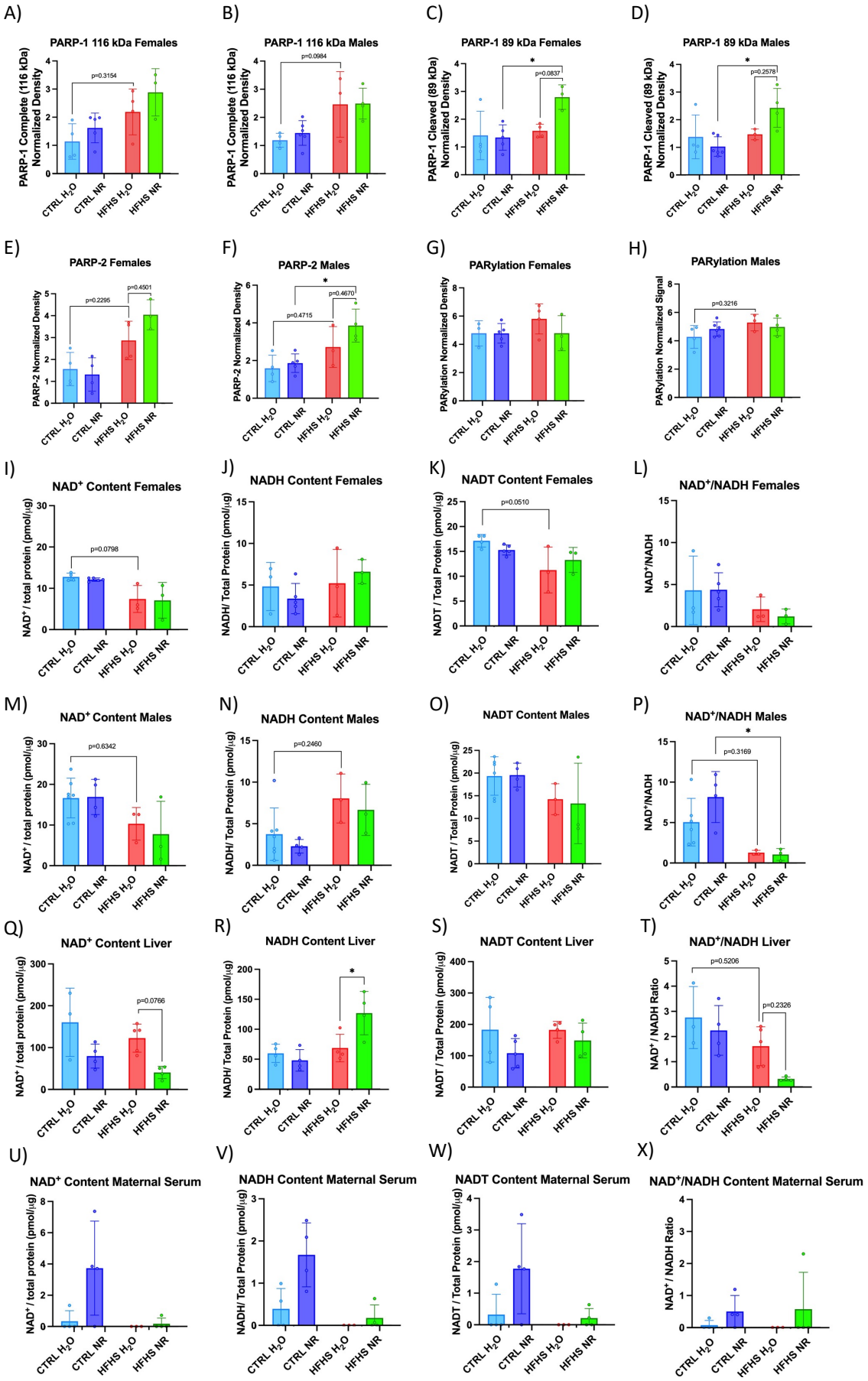
A)
PARP-1 116 kDa Females
PARP-1 Complete (116 kDa) Normalized Density
p=0.3154
B)
PARP-1 116 kDa Males
PARP-1 Complete (116 kDa) Normalized Density
p=0.0984
C)
PARP-1 89 kDa Females
PARP-1 Cleaved (89 kDa) Normalized Density
*
p=0.0837
D)
PARP-1 89 kDa Males
PARP-1 Cleaved (89 kDa) Normalized Density
*
p=0.2578
E)
PARP-2 Females
PARP-2 Normalized Density
p=0.2295
p=0.4501
F)
PARP-2 Males
PARP-2 Normalized Density
*
p=0.4670
p=0.4715
G)
PARylation Females
PARylation Normalized Density
H)
PARylation Males
PARylation Normalized Signal
p=0.3216
I)
NAD+ Content Females
NAD+ / total protein (pmol/µg)
p=0.0798
J)
NADH Content Females
NADH/ Total Protein (pmol/µg)
K)
NADT Content Females
NADT / Total Protein (pmol/µg)
p=0.0510
L)
NAD+/NADH Females
NAD+/NADH
M)
NAD+ Content Males
NAD+ / total protein (pmol/µg)
p=0.6342
N)
NADH Content Males
NADH/ Total Protein (pmol/µg)
p=0.2460
O)
NADT Content Males
NADT / Total Protein (pmol/µg)
P)
NAD+/NADH Males
NAD+/NADH
*
p=0.3169
Q)
NAD+ Content Liver
NAD+ / total protein (pmol/µg)
p=0.0766
R)
NADH Content Liver
NADH/ Total Protein (pmol/µg)
*
S)
NADT Content Liver
NADT / Total Protein (pmol/µg)
T)
NAD+/NADH Liver
NAD+ / NADH Ratio
p=0.5206
p=0.2326
U)
NAD+ Content Maternal Serum
NAD+ / total protein (pmol/µg)
V)
NADH Content Maternal Serum
NADH/ Total Protein (pmol/µg)
W)
NADT Content Maternal Serum
NADT / Total Protein (pmol/µg)
X)
NAD+/NADH Content Maternal Serum
NAD+ / NADH Ratio
CTRL H2O
CTRL NR
HFHS H2O
HFHS NR

Supplemental Figure 4.5.3 Effect of HFHS diet-induced obesity on placental PARP protein expression, activity, and NAD^+ content.
PARP-1 protein expression (A-D), PARP-2 protein expression (E-F), and total protein PARylation (G-H) measured using western blot in female and male placentas. NAD^+, NADH, and total NAD content, as well as NAD^+/NADH ratio in female and male placentas (I-P). NAD^+, NADH, and total NAD content, as well as NAD^+/NADH ratio in liver and serum from female parent mice (Q-X). Two-way ANOVA with Bonferroni post-hoc test assessed differences by diet and treatment (*$p<0.05$). CTRL = control chow diet, HFHS = high-fat high-sugar diet, NR=nicotinamide riboside, NADH = nicotinamide adenine dinucleotide + hydrogen, NAD^+ = nicotinamide adenine dinucleotide, NADT = total nicotinamide adenine dinucleotide, PARP-1 = Poly (ADP Ribose) Polymerase-1, PARP-2 = Poly (ADP Ribose) Polymerase-2, PAR = PARylation.

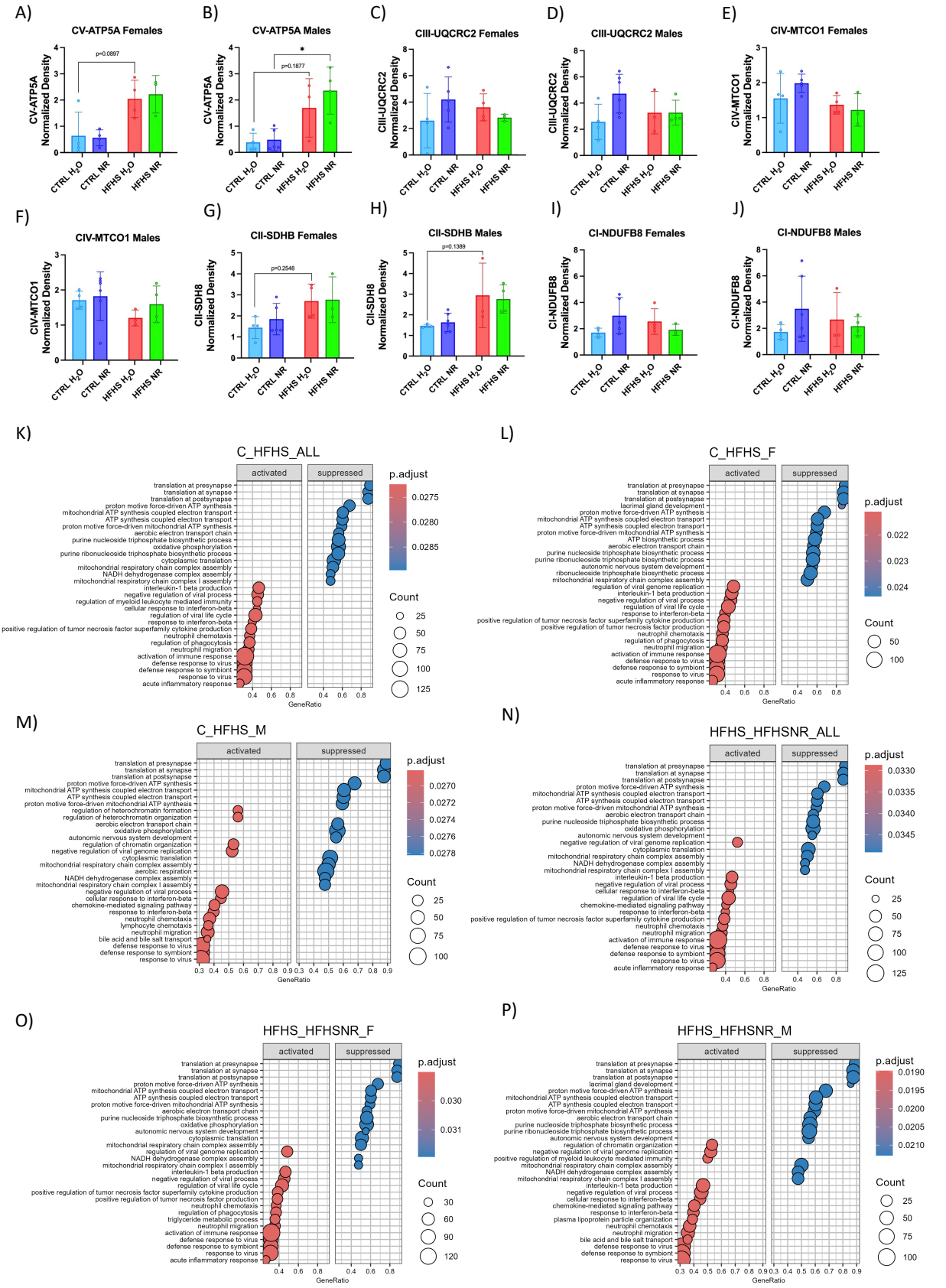
A)
CV-ATP5A Females
CV-ATP5A Normalized Density
p=0.0897
B)
CV-ATP5A Males
CV-ATP5A Normalized Density
*
p=0.1877
C)
CIII-UQCRC2 Females
CIII-UQCRC2 Normalized Density
D)
CIII-UQCRC2 Males
CIII-UQCRC2 Normalized Density
E)
CIV-MTCO1 Females
CIV-MTCO1 Normalized Density
F)
CIV-MTCO1 Males
CIV-MTCO1 Normalized Density
G)
CII-SDHB Females
CII-SDHB Normalized Density
p=0.2548
H)
CII-SDHB Males
CII-SDHB Normalized Density
p=0.1389
I)
CI-NDUFB8 Females
CI-NDUFB8 Normalized Density
J)
CI-NDUFB8 Males
CI-NDUFB8 Normalized Density
CTRL H2O
CTRL NR
HFHS H2O
HFHS NR
K)
C_HFHS_ALL
L)
C_HFHS_F
M)
C_HFHS_M
N)
HFHS_HFHSNR_ALL
O)
HFHS_HFHSNR_F
P)
HFHS_HFHSNR_M
activated
suppressed
p.adjust
Count
GeneRatio

Supplemental Figure 4.5.4 Effect of HFHS diet-induced obesity on mitochondrial health.
Mitochondrial OXPHOS protein expression (A-J) measured using western blot in female and male placentas. Two-way ANOVA with Bonferroni post-hoc test assessed differences by diet and treatment (*p<0.05). Pathway enrichment analysis revealed pathways activated and suppressed in overall (female + male), female, or male HFHS H_2O placentas compared to overall (female + male), female, or male CTRL H_2O placentas (K-M), and overall (female + male), female, or male HFHS-NR placentas compared to overall (female + male), female, or male HFHS-H_2O placentas (N-P). CTRL = control chow diet, HFHS = high-fat high-sugar diet, NR=nicotinamide riboside, ETC = electron transport chain, ATP = adenosine triphosphate, OXPHOS = oxidative phosphorylation, CV-ATP5A = Complex V ATP Synthase, CIII-UQCRC2 = Complex III Ubiquinol Cytochrome C Oxidoreductase, CIV-MTCO1 = Complex IV Cytochrome C Oxidoreductase, CII-SDHB = Complex II Succinate Ubiquinone Oxidoreductase, CI-NDUFB8 = Complex I NADH Dehydrogenase.

Supplemental Table 4.5.1 List of primary and secondary antibodies used for western blot experiments.

Primary Antibody	Company	Product Number	Size (kDa)	Dilution	Function
anti-Poly/ Mono ADP-Ribose	Cell Signaling Technology	#83732	No specific band (total protein measurement)	1:1000	ADP-ribosylation is involved many cellular processes: • Recruiting of DNA repair proteins that contain PAR-binding modules to sites of DNA damage • Mitotic spindle formation • Chromatin decondensation • Cell stress response • Retroviral silencing • RNA biology, and transcription
anti-PARP-1	Santa-Cruz Biotechnology	#sc-8007	116 kDa (total protein) 89 kDa (cleaved)	1:1000	PARP-1 is a DNA-binding enzyme that is involved in: • DNA repair • Inflammatory gene modulation • Stress response • Chromatin remodulation • Transcriptional regulation • Apoptosis In times of cellular stress, PARP-1 catalyzes the transfer of ADP-ribose units from NAD^+ to acceptor molecules (i.e., chromatin)
anti-PARP-2	Enzo Life Sciences	#O8855	62 kDa	1:50	PARP-2 is a DNA-binding enzyme that is involved in: • DNA Repair • Inflammatory gene modulation

					• Stress Response In times of cellular stress, PARP-2 catalyzes the transfer of ADP-ribose units from NAD^+ to acceptor molecules (i.e., chromatin)
anti-OXPHOS cocktail	Abcam	#ab110413	CV-ATP5A: 55 kDa CIII-UQCRC2: 48 kDa CIV-MTCO1: 40 kDa CII-SDHB: 30 kDa CI-NDUFB8: 20 kDa	1:1000	This OXPHOS cocktail contains a mixture of 5 mouse monoclonal antibodies, one each against the 5 different mitochondrial subunits that are involved in oxidative phosphorylation: • CI-NDUFB8 subunit • CII-SDHB subunit • CIII-Core protein 2 (UQCRC2) subunit • CIV-MTCO1 subunit • CV-ATP5-alpha subunit Altered levels of assembly of these subunits can occur due to: • Mutations in the subunits themselves • Mutations in assembly factors for the complexes • mtDNA depletion • Physiological and or pathological changes (hormone treatment, exercise, diet or oxidative stress)
Secondary Antibody	**Company**	**Product Number**	**Size (kDa)**	**Dilution**	**Function**
Goat Anti-Mouse IgG (H+L)-HRP conjugate	Bio-Rad Laboratories	#170-6516	n/a	1:10,000	Secondary antibody used for anti-PARP-1, anti-PARP-2, and anti-OXPHOS
Goat Anti-Rabbit IgG (H+L)-HRP Conjugate	Bio-Rad Laboratories	#170-6515	n/a	1:10,000	Secondary antibody used for anti-PAR/MAR

Chapter 5 - Discussion

5.1 Discussion

This study is the first to discover a potential contributing role for depleted intracellular NAD^+ content in establishing placental dysfunction and poor pregnancy outcomes in gestational obesity. Specifically, using a diet-induced, HFHS 'westernized' mouse model of gestational obesity, a link between obesity-mediated inflammation and PARP overexpression/over-activation in the placenta was identified, which was further associated with placental NAD^+ depletion. This model also demonstrated that dysregulated placental NAD^+ signaling was associated with mitochondrial dysregulation, altered placental structure/efficiency, and reduced fetal growth - characterizing a novel pathway that could be therapeutically targeted in hopes of improving poor pregnancy and fetal health outcomes in gestational obesity. Likewise, the current study tested the therapeutic potential of NR supplementation throughout pregnancy – a safe NAD^+ booster that has shown promise in improving systemic metabolic health in non-pregnant populations. Unexpectedly, NR treatment was unsuccessful at boosting placental NAD^+ levels, and was unable to protect the placental/fetal health profiles in our model. While surprising, these results have led to in-depth considerations of how-to best target NAD^+signaling pathways in this unique patient population, including considerations of appropriate supplement selection, dose, and timing of treatments.

5.1.1 Characteristics and relevance of the HFHS mouse model to study gestational obesity

The typical North American diet includes ~ 33-40% fat by energy (% kcal fat) [183-184], whereas individuals with obesity may over consume an *additional* 27% kcal fat (up to 67% kcal fat) [184]. Comparatively, rodents maintained on a standard chow diet consume ~ 10% kcal fat [184]. The fat content utilized in our HFHS gestational model (42% kcal fat) likewise represented an increase of ~ 30% kcal fat - mimicking fat over-consumption observed in humans with obesity. Previous rodent models of gestational obesity have often opted for a higher 60% kcal high-fat diet (HFD), as it induces a more dramatic obesity phenotype at a more rapid pace. However, this is not as representative of

human obesity, which is typically established over a longer period of time. Although the rate at which an individual becomes obese depends on multiple factors including their genetics, metabolism, caloric intake, activity level, age, sex, and hormone levels– a human at a healthy weight would typically take years to become obese. For instance, a 25-year-old adult male with a BMI of 25 kg/m^2 would need to consume excess energy or reduce physical activity or both by 680 kcal/day to reach a BMI >30 kg/m^2 by age 50-59 [185-186]. Comparatively, mice placed on a 60% kcal HFD become obese in as little as 5-6 weeks [187-189] – translating to ~ 4-5 years in humans [190].

Our model further replicated the human 'western diet', by pairing a moderately HF content to a moderately high-sugar content (34% sucrose by weight). Healthy Canadians typically consume ~19% of daily calories from sugars, with ~9% being added sugars (i.e., sucrose, high fructose corn syrup) [191-192]. Individuals consuming a more unhealthy 'western diet', often coupled with obesity, demonstrate an increase in dietary added sugars (~ 13-50%) [193-195] which contribute to obesity through elevations in inflammation, blood pressure, visceral adiposity, and dyslipidemia [196]. These alarming statistics have prompted the World Health Organization (WHO) to recommend that added sugars should contribute to less than 5-10% of total energy intake [191]. Given that high levels of added sugar play a significant role in establishing obesity, models that neglect high-sugar content may not accurately represent obesity in clinical populations.

Overall, our HFHS model was successful at establishing gestational obesity. Indeed, HFHS dams demonstrated increased pre-pregnancy body weight, body fat percentage, and fasting glucose levels compared to CTRL dams. These higher fasting blood glucose levels in HFHS dams are indicative of a pre-diabetic state commonly observed in humans with obesity. While entering pregnancy at a much higher weight, HFHS dams gained ~ 50% *less* weight across pregnancy compared to the CTRL dams, indicative of potentially SGA fetuses, which aligns with similar murine models [105, 197-198]. Comparatively, humans with obesity demonstrate both increased and decreased weight gain during gestation. While gestational parents with obesity that gained more weight

throughout gestation were more likely to deliver LGA infants, those who gained less gestational weight were more likely to deliver SGA infants [199-200]. Indeed, the likelihood of a gestational parent with obesity delivering an SGA infant increases with each 1 kg lost during pregnancy [201].

Interestingly, we did not observe any differences in reproductive health metrics in HFHS dams compared to CTRL dams, with similar lengths of time taken to achieve pregnancy, percentage (%) of successful pregnancies following the first vaginal plug, and % of dams that required re-mating. These findings were somewhat surprising given previous reports of reduced reproductive capacity in similar rodent gestational obesity models [202-203] and human obese populations [204-205]. However, these discrepancies may be due to the environment in which HFHS and CTRL dams were housed. Indeed, some of our CTRL dams demonstrated higher than anticipated reproductive challenges (i.e. 8.78 days to first vaginal plug vs. 6.25 in historical cohorts) (unpublished data, Bainbridge Lab 2024). Thus, perhaps animal housing conditions increased mouse stress, through increased room traffic or handling by animal care staff- leading to a longer time to achieve pregnancy in both HFHS *and* CTRL dams. As elevated maternal stress is known to have adverse fetal programming effects, this is an important consideration. However, despite being housed side-by-side under similar conditions, observed effects on placental/fetal health were limited to HFHS dams.

5.1.2 Consequences of gestational obesity on fetal growth profiles

Fetuses from HFHS dams had lower weights and crown-rump lengths at E18.5 compared to fetuses from CTRL dams, indicative of obesity-mediated FGR. This aligns with similar rodent gestational obesity models, which have identified FGR as characteristic of this phenotype [106, 163, 181, 206-207]. Moreover, the identified FGR in our model was more pronounced in female fetuses than male fetuses – attesting to the "males live dangerously in the womb" hypothesis in which male fetuses prioritize their own growth over placental adaptability, whereas female fetuses prioritize placental adaptability over their own growth [265-266]. Unexpectedly, these harmful effects to fetal

growth were unable to be rescued with NR treatment. In human populations, gestational obesity is linked to both LGA fetuses and SGA fetuses [3, 208], although the LGA phenotype is more common. Indeed, in Canadian populations with gestational obesity, 8.6% of fetuses are born SGA, and 14.1% of fetuses are born LGA [3]. Evidently, gestational obesity has multidirectional effects on fetal growth trajectories, which highlights the importance of investigating varying mechanisms of gestational obesity/placental dysfunction.

An important factor contributing to these fetal growth dichotomies in gestational obesity could be gestational parent predisposition to insulin resistance and/or the development of gestational diabetes mellitus (GDM). In these situations, the gestational parent tissues are highly resistant to insulin signaling and subsequent glucose uptake, leading to a state of profound hyperglycemia. This excess circulating glucose is then shuttled to the fetal circulation, resulting in fetal hyperglycemia [209], which stimulates the fetal pancreas to release an excess of fetal insulin, increasing fat and protein storage in the fetus – promoting fetal overgrowth [209-211]. Indeed, 15-45% of infants born to gestational parents with GDM are LGA [211], and historical clinical management has focused on managing glycemic control to prevent this associated fetal growth [212]. Interestingly, GDM patients who undergo aggressive glucose management are at a higher risk of having SGA infants [213] – demonstrating the delicate balance required to appropriately regulate fetal glucose exposure and fetal growth profiles.

Comparatively, restricted fetal growth and subsequent low birth weight infants may indicate a more profound degree of obesity-mediated placental dysfunction. Indeed, cases of SGA in gestational obesity are commonly observed in association with placental insufficiency, placental tumors, placental abruption, and placenta previa [214]. Moreover, it is well established that inflammation has profound impacts on placental structure, leading to inhibition of spiral artery remodelling [215], vascular malperfusion, reduced villi maturation, increased inflammatory lesions, and villitis [100]. These observations align with the current study and similar gestational obesity models, in which reduced fetal growth was observed in HFHS exposed dams coupled to

decreased placental efficiency [105]. It is possible that in these rodent models and human cases of gestational obesity leading to SGA infants, there may be a more profound inflammatory disturbance or a higher degree of placental sensitivity to the obesity-mediated inflammatory insults. In fact, SGA infants demonstrate elevated cord serum levels of tumor necrosis factor alpha (TNF-α), c-reactive protein (CRP), and interleukin (IL)-8 – proinflammatory cytokines that are known to stimulate nuclear factor kappa B (NF-κB) and interferon regulatory factor 3 (IRF3) signalling [216-217].

5.1.3 Consequences of gestational obesity on placental structure and function

Placental dysfunction in gestational obesity is well described in both human populations and rodent models [108]. While no overall differences in placental weight or depth were noted in the current study, placental efficiency- the ratio of fetal weight to placental weight which indirectly measures the placenta's efficiency in fetal nutrient/oxygen exchange [218-219]- was decreased in HFHS dams. This effect was more pronounced in female fetuses - again supporting the "males live dangerously in the womb" hypothesis as female fetuses illustrate a lower priority to support their own growth. Additionally, the depth of the placental labyrinth zone (LZ)– the site of maternal-fetal exchange – trended towards being smaller in male fetuses exposed to HFHS diet compared to those exposed to CTRL diet. Once more, this aligns with the previously mentioned hypothesis – in that male fetuses will suffer more detriments to their placental adaptability in exchange for self-growth, such as failing to adapt the structure of their LZ to an obesogenic environment. Unexpectedly, these harmful effects to placental and fetal health were unable to be rescued with NR treatment – leading our group to consider alternative solutions for NAD^+ boosting.

Similar gestational obesity rodent models have also demonstrated evidence of smaller LZ with reduced vascular density, oxygen diffusion capacity, and maternal blood space volume [105, 220] – parameters worth exploring in the future in our model. Human placentas exposed to obesity likewise demonstrate immature villous exchange unit development and lower vascular density – findings that also indicate poor exchange

capacity [102, 221-223]. Our HFHS dams also demonstrated evidence of low-grade systemic inflammation – evidenced through altered placental gene expression of inflammatory regulation. Genes implicated in the complement system (i.e., C1qb, C2, C4a, C9) [224] – an immune response positively correlated with BMI and adiposity [225] - were upregulated in HFHS placentas. Interestingly, activation of the complement system has been identified as a link between excess adipose tissue and preeclampsia [225]. Indeed, gestational parents with obesity that also had increased serum concentrations of complement fragments Bb and C3a were more likely to develop preeclampsia [269-270]. Additionally, gene expression of toll-like receptor 9 (Tlr9) – a pattern recognition receptor that binds CpG oligonucleotides to initiate Th-1 immune responses (i.e., NF-κB pathway) [226] and ubiquitin specific proteases (USP; i.e., USP12, USP9X) - genes likewise linked to the activation of Th-1 proinflammatory pathways (i.e., NF-κB) [226, 271] were elevated in HFHS placentas compared to CTRL placentas. TLR-9 activation leads to upregulation of pro-inflammatory cytokines such as IL-6 and IL-12 [226]. This finding aligns well with other rodent and human studies that have demonstrated elevated expression of TLRs as well as increased protein/gene expression of pro-inflammatory markers IL-6, IL-12, and TNF-α in serum/placenta impacted by gestational obesity [82, 206, 227-235]. Activation of USP-12 has also been associated with induction of angiotensin type II cardiac hypertrophy [272]. Unfortunately, this inflammation was not significantly alleviated in HFHS placentas treated with NR.

In regard to human sex-specific histological findings in gestational obesity, chronic villitis (CV) – an inflammatory response characterized by immune cell invasion into chorionic villi leading to placental dysfunction [236] - is increased in female placentas [237-238]. CV has been linked to FGR and pregnancy loss [239-241], which may explain why female fetuses in our study suffered more severe detriments to their weight. Comparatively, male placentas in gestational obesity demonstrate a higher prevalence of patchy villous edema – a lesion characterized by fluid accumulation in the stroma of chorionic villi associated with fetal vascular malperfusion [237-238], indicating blood flow dysregulation between the gestational parent and fetus. Interestingly, an increased prevalence of

these lesions is linked to fetal congenital heart disease [242] and pre-term birth [243], conditions that are more prevalent among male fetuses [244-245].

5.1.4 Impact of gestational obesity on placental NAD^+ signalling

In this study, increased protein expression of both PARP-1 and PARP-2 was observed in placentas of HFHS dams compared to CTRLs. PARP-1 and PARP-2 are PARylating enzymes, meaning they transfer ADP-ribose chains onto amino acid residues to modulate protein function [130, 246-247]. Protein PARylation is required for many cellular functions, including appropriate DNA damage response, transcription, cellular metabolism, and cell death processes [182, 247-250]. PARP-1 and PARP-2 are also the primary PARPs that become highly activated under pro-inflammatory conditions and further increase local expression of chemokines and pro-inflammatory mediators [182, 251-253] - contributing to the establishment of a vicious pro-inflammatory positive feedback loop. Additionally, this study identified a trend in heightened PARP 1/2 activation (i.e., protein PARylation), which may be due to the pro-inflammatory obesogenic environment.

Interestingly, both PARP-1 and PARP-2 have been identified as critical targets to treat metabolic disorders, such as obesity, in non-pregnant populations. Inhibition of PARP-1 has been found to be effective at reducing body weight gain, white adipose tissue content, and cell size in mice that were fed a HFD [273]. In non-obese C57BL/6J mice, PARP-1 knockout increased energy expenditure, but reduced weight gain [135]. Other studies have identified that PARP-1 inhibition reduces inflammation, by leading to a reduction in downstream inflammatory markers characteristic of the NF-κB pathway [274-275]. On the other hand, PARP-2 is capable of positively regulating peroxisome proliferator-activated receptor gamma (PPARγ), a key protein that initiates white adipose tissue differentiation, thus a major regulator of energy, lipid, and glucose homeostasis [60-61]. Indeed, non-pregnant obese PARP-2 -/- mouse models appear protected from the diet-induced obesity phenotype [62].

While PARP-1 and PARP-2 are the two major PARylating enzymes that consume NAD^+ [134], with PARP-1 consuming 90% of all PARP-consumed NAD^+ [276], there are 15 other PARPs that make up the PARP superfamily. This superfamily includes those involved in antiviral response (PARPs 4, 5, 7, 9, 10, 11, 12, 13, 14, 15), those implicated in stress response (PARPs 2, 5, 10, 12, 13, 16), those implicated in DNA repair (PARPs 2, 3, 5), and those likewise involved in inflammation (PARPs 2, 5, 6, 7, 9, 10, 12, 13, 14) [182]. Further research is required to elucidate the roles of these PARPs in processes related to gestational obesity, especially for those PARPs previously implicated in pathophysiology of inflammation.

Inflammation-mediated PARP overactivation and subsequent NAD^+ depletion has been identified as a key mechanism underlying metabolic stress in numerous chronic inflammatory disorders in *non-pregnant* populations (i.e. non-alcoholic fatty liver disease (NAFLD), Crohn's disease, and type 2 diabetes mellitus (T2DM)) [152, 254-256]. The central finding of the current study was that PARP-mediated NAD^+ depletion may be likewise involved in the establishment of placental dysfunction and poor pregnancy outcomes in HFHS diet-exposed pregnancies. The presence of sufficient intracellular NAD^+ is critical to cell health, as NAD^+ is a major player in over 488 different human bodily reactions, including 371 redox reactions, 26 biosynthesis/metabolism reactions, and 29 reactions where NAD^+ is a substrate [257]. Interestingly, loss-of-function variants in NAD^+ synthesis genes are associated with an increased risk of congenital defects and miscarriage in human populations - termed congenital NAD^+ deficiency disorder [170]. Likewise, C57BL/6J wild-type mice demonstrated these same types of congenital malformations and embryo loss when NAD^+ precursors tryptophan and vitamin B3 are removed from their diet during pregnancy [171]. In both human and animal models described, offspring demonstrated defects in the development of their heart, kidney, limbs/digits and palates [170-171]. Intriguingly, many of these same congenital defects and increased rates of miscarriage are also associated with gestational obesity [258-259]. In the current study, no obvious congenital malformations were observed in our HFHS fetuses – however, placental NAD^+ depletion was associated with impairments to fetal

growth and placental dysfunction – which was reflected in dysregulation of placental mitochondria.

Placental mitochondrial health was assessed through protein expression of key oxidative phosphorylation (OXPHOS) proteins. HFHS-exposed placentas demonstrated increased expression of both Complex V ATP Synthase (CV-ATP5A) and Complex II Succinate Ubiquinone Oxidoreductase (CII-SDHB). CV-ATP5A is a protein that makes up Complex V in the mitochondria's ETC, whose role is to form ATP from adenosine diphosphate (ADP) in the presence of a proton gradient [260-263]. This is essential to produce sufficient energy (ATP) for healthy cellular function. CII-SDHB is a protein that forms one of the subunits of complex II of the ETC. This complex is chiefly responsible for linking two important mechanisms: the tricarboxylic acid cycle (TCA) and OXPHOS pathway [125, 264]. Further, the SDHB subunit in particular is employed in aerobic energy metabolism [125, 264]. A previous clinical study assessing placental OXPHOS protein levels in individuals with obesity found CV-ATP5A and CII-SDHB levels to be markedly decreased, which aligned with diminished levels of ATP [125]. However, a HFHS murine model of gestational obesity identified elevated levels of placental CV-ATP5A and CII-SDHB in HFHS dams [105] - which aligned with the current study. It was proposed that these elevated OXPHOS protein levels are a compensatory mechanism for depleted ATP synthesis in these mitochondria [105]. Namely, systemic inflammation established by simultaneous states of obesity and pregnancy impairs oxidative phosphorylation and ATP formation, putting cells into metabolic and energetic distress. In turn, mitochondria will upregulate formation of OXPHOS proteins to allow for the continuation of oxidative phosphorylation and ATP generation.

Placental mitochondrial health was likewise evaluated via gene expression of key genes involved in ETC formation and ATP synthesis. Interestingly, placentas in an obesogenic environment demonstrated a downregulation in expression of genes related to ATP synthesis and ETC activity. These findings align with other studies investigating impacts of gestational obesity on placental mitochondria in both rodent and human models. Namely, murine HFD models have identified downregulation of key mitochondrial

transcription factors involved in mitochondrial biogenesis, respiratory function, and fusion/fission (ERR-a, Nrf1, Fis1, Mfn2), as well as alterations to OXPHOS protein content (complexes I-V), and respiratory capacity [105, 124]. In humans, placentas impacted by gestational obesity have likewise been found to contain lower levels of mitochondrial DNA (mtDNA), ETC activity, ATP generation, citrate synthase activity, and higher ROS (i.e., hydrogen peroxide) levels [123-126, 172]. To the best of our knowledge, our study is the first that has found an association between mitochondrial dysfunction in gestational obesity to placental PARP-mediated NAD^+ depletion - providing a potential underlying explanation as to why these poor mitochondrial outcomes occur.

5.1.5 Therapeutically targeting placental NAD^+ depletion in gestational obesity

The conceptualization of this thesis was inspired by a previous study from our group that discovered placental PARP-mediated NAD^+ depletion in a rat model of lipopolysaccharide (LPS)-induced inflammatory preeclampsia [163]. This NAD^+ depletion was rescued by treatment with NR which prevented the development of preeclamptic features. Thus, the goal of the current study was to observe if this PARP-mediated NAD^+ depletion was likewise involved in gestational obesity, another chronic inflammatory disease of pregnancy, and furthermore, whether NR could prevent the development of adverse gestational obesity outcomes. Like our HFHS model, fetuses from LPS treated dams showed evidence of FGR, and placentas demonstrated alterations to their LZ size, as well as increased inflammation - evidenced by upregulation of TNF-α levels. LPS-treated placentas also demonstrated upregulated PARP activity (PARylation) – which was coupled to a downregulation of NAD^+ content and mitochondrial dysregulation (via decreased oxygen consumption rates (OCR) in ETC complexes I and II) [163] . Interestingly, NR treatment in the LPS-treated dams was capable of reversing detrimental effects to placental and fetal health [163]. More specifically, NR treatment reversed FGR in fetuses from LPS-treated dams, as well as increased LZ area, decreased PARylation, increased NAD^+ levels, and improved mitochondrial OCR in LPS-treated placentas [163] . Unexpectedly, NR was incapable of

exerting these same effects in the HFHS model – no ameliorations to fetal mass, placental structure, PARylation, NAD^+ content, or mitochondrial content was observed.

It is important to note that the same calculated dose of NR was used in both the LPS-induced rodent model and the current HFHS diet-induced rodent model. However, it is possible that the chronicity of the inflammatory insults and the widespread/systemic metabolic dysregulation imparted by gestational obesity leads to a more severe phenotype that could not be as easily rescued by NR at this same dose. For reference, the HFHS diet was administered for 12-15 weeks in the female mice prior to and throughout pregnancy, in comparison to the LPS-induced inflammatory model in which LPS was injected peritoneally only from gestational days 13-18 [(163)]. Hence, the length of the inflammatory insult was much longer in the HFHS model compared to the LPS model - and as a result, may have needed a higher dose of NR in order to observe beneficial effects. However, in the HFHS gestational obesity model, a dose response to determine optimal NR concentration was not performed, instead simply relying on the proven effective dose in our previous model. Going forward, our group will perform a dose response to determine the optimal concentration of NR needed to boost NAD^+ in our obese mice.

Another factor contributing to NR's inability to rescue obesity-mediated insults, could be the timing of the NR administration with respect to the inflammatory insult. In the LPS model, NR administration (from gestational days 1-19) was initiated prior to the inflammatory LPS insult (gestational days 13-18) [(163)]. Comparatively, in the HFHS model, NR was administered to HFHS mice after the inflammatory insult of a 12–15-week HFHS diet exposure – only after the obesity had been established. Hence, NR in the LPS model was designed as a more preventative intervention, whereas NR in the HFHS model was employed instead as a therapeutic intervention. Perhaps by the time NR is administered, the inflammatory HFHS phenotype is too severe to be changed by an acute treatment of NR over the course of pregnancy. Indeed, studies in the oocyte have demonstrated that a longer 3-month administration of NR, beginning at the same time as HFD administration, was able to successfully boost oocyte NAD^+ levels, as well

as improve oocyte structure and metabolism [161]. Unfortunately, in a real-life context, it is unlikely that an individual would begin NR treatment *before* becoming obese and prior to pregnancy - it is far more likely that an individual with obesity would attempt NR treatment in hopes of alleviating potential impacts of obesity once they become pregnant. Hence, in terms of model design, it may not be clinically relevant to begin NR treatment prior to obesity onset. However, it would be worth further investigation to test if a longer combined pregestational and gestational administration of NR in obese mice could be more effective at boosting NAD^+, and thus protect against obesity-mediated adverse pregnancy and fetal health outcomes.

In addition to performing a NR dose response and attempting a more prolonged NR administration in this model, a future direction could involve exploring alternative NAD^+ boosters. Nicotinamide mononucleotide (NMN), the phosphorylated form of NR, for instance, has been shown to have positive impacts on sperm quality, adiposity, and metabolism when administered to murine offspring born to dams with obesity [277-278]. Moreover, NMN treatment in HFD-fed dams was capable of boosting hepatic and muscle NAD^+ levels, improving glucose tolerance, and upregulating hepatic citrate synthase activity [279]. It would likewise be interesting to observe if NMN supplementation to dams with obesity could improve placental dysfunction and impacts to fetal offspring via in-utero programming. Furthermore, given that NMN has been established as safe and well-tolerated in healthy adult men and women [280], it be of interest to see what impact it might have in human cases of gestational obesity.

To expand upon why NMN might be a more favorable NAD^+ booster than NR, we can turn to the differences between how NR and NMN are converted into NAD^+ in the NAD^+ salvage pathway. In NAD^+ biosynthesis, NMN is directly converted into NAD^+, whereas NR must first be phosphorylated to NMN, which is then converted into NAD^+[153, 281-284]. While no studies have investigated whether this “extra step” to convert NR to NAD^+ significantly slows down its ability to increase bioavailable NAD^+ levels in comparison to NMN, it is well-established that much of NR is actually broken down in the gut into nicotinamide (NAM) before it reaches tissues [137, 153, 285], the first being the liver. The

small fraction of NR that remains in the bloodstream and not taken up by the gut is quickly metabolized into NAM [285]. NAM is primarily metabolized in the liver, leading to production of NAD^+ [286-289]. Unexpectedly in the current study, we did not observe boosted NAD^+ levels in livers from HFHS dams treated with NR. This leads us to believe that our dose was either too low or too acute – so that most NR was directed to the gut, making it undetectable in surrounding tissues. Also, perhaps the extra step of having to convert NR into NAM in the gut prior to producing NAD^+, increases the chance that most of these molecules will only be capable of reaching the gut. Therefore, by the time it reaches the uterine sac, there is little NAD^+ leftover to reach the placenta and exert beneficial effects.

In this vein, other molecules worth future investigation include nicotinamide mononucleotide adenyltransferase (NMNAT), an enzyme that converts NMN to NAD^+ in the NAD^+ salvage pathway [290-291], and nicotinamide phosphoribosyl transferase (NAMPT), the rate-limiting enzyme in the NAD^+ salvage pathway that converts NAM into NMN. Mammals contain three main NMNAT isoenzymes that are encoded by different genes, so named NMNAT-1, NMNAT-2, and NMNAT-3, with NMNAT-3 being the isotype primarily associated with NAD^+ biosynthesis in the mitochondria [290-292]. Interestingly, boosting NMNAT-3 levels in human-cultured cells has been found to be associated with increased mitochondrial NAD^+ synthesis [291]. A transgenic mouse model with overexpressed NMNAT-3 likewise demonstrated elevations in NAD^+ in various tissues in accordance to ameliorated insulin resistance, TCA activity, fatty acid oxidation, and reduced ROS [293]. NAMPT, on the other hand, is an enzyme that co-localizes with the mitochondria and is chiefly used by tissues to synthesize NAD^+ through salvage of NAM [294-295]. Interestingly, in a HFD mouse model of gestational obesity, NAMPT signalling and NAD^+ content was downregulated in oocytes exposed to an obesogenic environment, while meiotic defects and ROS activity was upregulated [162]. However, an overexpression of NAMPT, via NAMPT-cRNA injections into oocytes affected by gestational obesity, successfully boosted NAD^+ content while reducing meiotic defects and ROS levels [162]. As such, it would be of interest to discover if an

overexpression of NMNAT-3 or NAMPT enzymes would successfully boost NAD^+ levels in our HFHS model of gestational obesity.

Another factor contributing to the ineffectiveness of NR in the placenta could be due to the presence of a fatty maternal liver, a condition in which fat content agglomerates in the liver and which is highly associated with obesity. It is well established that obesity can lead to NAFLD, which can be rescued via NAD^+ supplementation [296-298]. Given that the liver is the main tissue that utilizes NAD^+, the fatty liver may be even more prone to take up NAM from the gut to improve its function. Indeed, in a study that treated obese HFHS mice with NR, they found that NR boosted NAD^+ levels in the liver so much so that it reversed NAFLD and HFHS-induced mitochondrial dysfunction [299]. This may in part explain why the same dose of NR was capable of exerting beneficial impacts on preeclamptic placentas in the LPS-model [163], because a fatty liver is not a component of this preeclampsia model, and thus the liver did not require the NAD^+ supplementation to regulate its metabolic function - allowing more NAM (and thus NAD^+) to reach the placenta.

5.2 Limitations

Although the current study has illustrated novel findings, there are some limitations to be considered in the interpretation of the results. Primarily, within our HFHS diet-induced gestational obesity model, there were some mice that were more obesity prone, and thus gained more weight than others. In this sense, it would be important to elucidate whether there are metabolic differences between placentas of obesity prone dams (that were on the higher end of gaining weight) in comparison to placentas of more obesity resistant dams (who were on the lower end of gaining weight). Moreover, it would be important to differentiate whether placentas from obesity prone dams respond differently to NR treatment than placentas from obesity resistant dams.

In addition, our model was also limited by only using 1 dose of NR (400 mg/kg/day). Although this dose was proven to be effective at rescuing impacts of inflammation on

placenta dysfunction in our LPS preeclamptic rat model [163], it is possible given the chronicity of the HFHS inflammatory phenotype and presence of a fatty liver, that this dose was not sufficient to exert rescuing effects on placentas impacted by gestational obesity. Additionally, it has been well established that gestational obesity can lead to adverse in-utero programming, propagating poor fetal growth profiles and cardiometabolic disease later in life [10-14]. Although our model has elucidated the implications of obesity-mediated inflammation on the placenta, it has not outlined what the impacts of this specific HFHS model have on the offspring, and how the offspring are impacted by NR treatment. Indeed, research has been conducted on NAD^+ depletion in offspring impacted by gestational obesity. Namely, it was discovered that adult obese offspring that were supplemented with NAD^+ boosting treatment experienced improvements in fat deposition, glucose tolerance, and metabolism, via increased hepatic genes involved in fatty acid oxidation and reduced hepatic genes involved in fat synthesis/uptake [277]. Thus, it would be worth further investigation to observe if different NR doses could exert rescuing effects on placental dysfunction and on adverse fetal programming in this model.

Last, although this murine model has allowed us to investigate a novel mechanism implicated in gestational obesity, it is still limited by the fact that we have not explored this mechanism in pregnant human populations with obesity. It is well-established that obesity leads to decreased NAD^+ levels in adipose tissue [167, 300], however it remains unclear the status of NAD^+ levels in human placentas in an obesogenic environment. We also know that NR, a form of vitamin B3, is orally bioavailable and a safe therapeutic to use in humans [301-304]. Therefore, if NAD^+ levels were found to be depleted in a clinical model of maternal obesity, NR supplementation via prenatal vitamins may prove to be a novel therapeutic option to avoid poor placental/fetal health outcomes.

5.3 Future Directions

This body of work importantly identifies NAD^+ depletion as a contributor to mitochondrial dysfunction and metabolic disturbance in the placenta in gestational obesity. However, our method of NAD^+ boosting with NR was ineffective to reverse these detrimental effects. Within the scope of using NR as a treatment, future work will need to test varying doses of NR, as well as different timings of NR administration to observe if it can exert beneficial effects on the placenta. Additionally, the effects of different NAD^+ boosters (NMN, nicotinic acid (NA)) and NAD^+ salvage pathway enzymes (NMNAT, NAMPT) in the context of gestational obesity would be worth investigating to observe if they are capable of boosting placental NAD^+ content and rescuing placental dysfunction.

Future work will also explore the impacts of our HFHS model on in-utero programming, by following offspring from HFHS mothers into adulthood to observe impacts on their cardiometabolic health. Moreover, we will observe if NAD^+ boosting therapies administered to HFHS dams can rescue dangerous cardiometabolic disease phenotypes in HFHS offspring. In addition, the discovery of the involvement of PARPs in NAD^+ depletion in this model prompts the exploration of various PARP knockout models to observe the effects of PARP inhibition on rescuing obesity-mediated inflammatory placental dysfunction. Finally, we plan to assess clinical models of gestational obesity to characterize placental NAD^+ depletion in the human placenta, and to determine if NAD^+ boosting vitamins would serve as effective therapeutics.

5.4 Conclusion

In conclusion, we have discovered that PARP-mediated NAD^+ depletion in the placenta may be a component of gestational obesity, which triggers mitochondrial and metabolic disarray, compromising the structure and function of the placenta and fetal growth profiles. While we were unable to upregulate NAD^+ content with NR, we suspect that if we are able to identify an adequate dose of NR, treat HFHS mice with NR for a longer period of time, or use an alternative NAD^+ booster, we could potentially alleviate damaging effects propagated by this lack of NAD^+. The current project did not assess

the impacts of NAD^+ depletion on in-utero programming of HFHS offspring. However, we know that the chronic inflammation imparted by gestational obesity has detrimental impacts on the health of the growing fetus, so it would be important to explore this aspect in our model.

References

1. FAO, IFAD, UNICEF, WFP, and WHO. (2019). The State of Food Security and Nutrition in the World 2019. Safeguarding against economic slowdowns and downturns. Rome, FAO. License: CC BY-NC-SA 3.0 IGO.
2. Blüher, M. (2019). Obesity: Global epidemiology and pathogenesis. *Nature Reviews Endocrinology*, *15*(5), 288–298.
3. Dzakpasu, S., et al. (2015). Contribution of prepregnancy body mass index and gestational weight gain to adverse neonatal outcomes: population attributable fractions for Canada. *BMC pregnancy and childbirth*, *15*, 21.
4. Chu, S. Y., et al. (2007). Maternal obesity and risk of stillbirth: a meta-analysis. *American journal of obstetrics and gynecology*, *197*(3), 223–228.
5. O'Brien, T. E., et al. (2003). Maternal body mass index and the risk of preeclampsia: a systematic overview. *Epidemiology (Cambridge, Mass.)*, *14*(3), 368–374.
6. Ehrenberg, H. M., et al. (2002). Prevalence of maternal obesity in an urban center. *American journal of obstetrics and gynecology*, *187*(5), 1189–1193.
7. Watkins, M. L., et al. (2003). Maternal obesity and risk for birth defects. *Pediatrics*, *111*(5), 1152–1158.
8. Chu, S. Y., et al. (2007). Maternal obesity and risk of gestational diabetes mellitus. *Diabetes care*, *30*(8), 2070–2076.
9. McDonald, S. D., et al. (2010). Overweight and obesity in mothers and risk of preterm birth and low birth weight infants: systematic review and meta-analyses. *BMJ (Clinical research ed.)*, *341*, c3428.
10. Pantham, P., Aye, I. L., & Powell, T. L. (2015). Inflammation in maternal obesity and gestational diabetes mellitus. *Placenta*, *36*(7), 709–715.
11. Catalano, P. M., et al. (2006). Adiponectin in human pregnancy: implications for regulation of glucose and lipid metabolism. *Diabetologia*, 49, 1677-1685.
12. Waller, D.K. (2007). Pre pregnancy obesity as a risk factor for structural birth defects. *Arch. Pediatric Adolescent Med.*, *161*, 745.
13. Yogev, Y. & Catalano, P.M. (2009). Pregnancy and obesity. *Obstet. Gynecol. Clin. North. Am. 36*, 285-300.

14. Ismail-Beigi, F., Catalano, P.M., & Hanson, R.W. (2006). Metabolic programming: fetal origins of obesity and metabolic syndrome in the adult. *Am. J. Physiol. Metab.*, *291*, E439-E440.
15. Bocca-Tjeertes, I.F., et al. (2014). Growth patterns of large for gestational age children up to age 4 years. *Pediatrics, 133*, e643–9.
16. Schlaudecker, E. P., et al. (2017). Small for gestational age: Case definition & guidelines for data collection, analysis, and presentation of maternal immunisation safety data. *Vaccine*, *35*(48), 6518–6528.
17. Hong, Y. H., & Chung, S. (2018). Small for gestational age and obesity related comorbidities. *Annals of pediatric endocrinology & metabolism*, *23*(1), 4–8.
18. Hong, Y. H., & Lee, J. E. (2021). Large for Gestational Age and Obesity-Related Comorbidities. *Journal of obesity & metabolic syndrome*, *30*(2), 124–131.
19. Nordman, H., Jääskeläinen, J., & Voutilainen, R. (2020). Birth size as a determinant of cardiometabolic risk factors in children. *Hormone Research in Paediatrics*, *93*(3), 144–153.
20. Lei, X., et al. (2018). Childhood health outcomes in term, large-for-gestational-age babies with different postnatal growth patterns. *Am. J. Epidemiol.*, *187*(3), 507–14.
21. Lei, X., et al. (2017). Childhood health outcomes in term, large-for-gestational-age babies with different postnatal growth patterns. *American Journal of Epidemiology*, *187*(3), 507–514.
22. Renom Espineira, A., et al. (2011). Postnatal growth and cardiometabolic profile in young adults born large for gestational age. *Clin. Endocrinol., 75*(3), 33541.
23. Ong, K.K., et al. (2000). Association between postnatal catch-up growth and obesity in childhood: prospective cohort study. *BMJ, 320*, 967–71.
24. Wilmott, R. W. (2013). “catching-up” on catch-up growth. *The Journal of Pediatrics*, *162*(2), 220.
25. Eriksson, J.G., et al. (2001). Early growth and coronary heart disease in later life: longitudinal study. *BMJ, 322*, 949–53.
26. Woo Baidal, J.A., et al. (2016). Risk factors for childhood obesity in the first 1,000 days: a systematic review. *Am J Prev Med., 50*, 761–79.

27. Li, P., et al. (2022). Early-life weight gain patterns of term small-for-gestational-age infants and the predictive ability for later childhood overweight/obesity: A prospective cohort study. *Frontiers in Endocrinology*, *13*.
28. Nordman, H., et al. (2020). Birth size as a determinant of cardiometabolic risk factors in children. *Karger Publishers*.
29. Varvarigou, A.A. (2010). Intrauterine growth restriction as a potential risk factor for disease onset in adulthood. *J Pediatr. Endocrinol. Metab. 23*, 215–24.
30. Krzysztoszek, J., Wierzejska, E., & Zielińska, A. (2015). Obesity. An analysis of epidemiological and prognostic research. *Arch. Med. Sci., 11*, 24–33.
31. Ellulu, M.S., et al. (2017). Obesity and inflammation: the linking mechanism and the complications. *Arch. Med. Sci., 13*(4), 851-863.
32. Kwok, K., Lam, K., & Xu, A. (2016). Heterogeneity of white adipose tissue: molecular basis and clinical implications. *Exp. Mol. Med., 48*, e215.
33. Cinti, S., et al. (2005). Adipocyte death defines macrophage localization and function in adipose tissue of obese mice and humans. *J. Lipid. Res., 46*, 2347–55.
34. Karastergiou, K., & Mohamed-Ali, V. (2010). The autocrine and paracrine roles of adipokines. *Mol. Cell. Endocrinol., 318*, 69–78.
35. Walsh, S.W. (2007). Obesity: a risk factor for preeclampsia. *Trends Endocrinol. Metab*., *18*(10), 365–370.
36. Madan, J.C., et al. (2009). Maternal obesity and markers of inflammation and pregnancy. *Cytokine, 47*(1), 61–64.
37. Rentnakaran, R., et al. (2003). C-reactive protein and gestational diabetes: the central role of maternal obesity. *J. Clin Endocrinol. Metab*., *88* (8), 3507–3512.
38. Wolf, M., et al. (2001). Obesity and preeclampsia: the potential role of inflammation. *Obstet. Gynecol., 98* (1), 757–762.
39. Zhang, S., et al. (2009). Suppression of interleukin-6-induced C-reactive protein expression by FXR agonists. *Biochem. Biophys. Res. Commun., 379*, 476–9.
40. Wagner, E.F., & Nebreda, A.R. (2009). Signal integration by JNK and p38 MAPK pathways in cancer development. *Nat. Rev. Cancer., 9*, 537–549.

41. García, M.A., et al. (2006). Impact of protein kinase PKR in cell biology: from antiviral to antiproliferative action. *Microbiol. Mol. Biol. Rev., 70*(4), 1032-60.
42. Israël A. (2010). The IKK complex, a central regulator of NF-kappaB activation. *Cold Spring Harb. Perspect. Biol*., *2*(3).
43. Rocha, V.Z., & Libby, P. (2009). Obesity, inflammation, and atherosclerosis. *Nat. Rev. Cardiol., 6*, 399–409.
44. Mjosberg, J., et al. (2010). FOXP3+ regulatory T cells and T helper 1, T helper 2, and T helper 17 cells in human early pregnancy decidua. *Biol Reprod., 82*, 698–705.
45. Sykes, L., et al. (2012). The Th1:th2 dichotomy of pregnancy and preterm labour. *Mediators Inflamm*., 967629.
46. Zhu, J. (2018). T Helper Cell Differentiation, Heterogeneity, and Plasticity. *Cold Spring Harb. Perspect. Biol., 10*(10), 1–17.
47. Mor, G., Aldo, P., & Alvero, A. B. (2017). The unique immunological and microbial aspects of pregnancy. *Nat. Rev. Immunol., 17*(8), 469–482.
48. Abelius, M.S., et al. (2015). The placental immune milieu is characterized by a Th2- and anti-inflammatory transcription profile, regardless of maternal allergy, and associates with neonatal immunity. *Am. J. Reprod. Immunol., 73*, 445–59.
49. Moffett, A., & Shreeve, N. (2023). Local immune recognition of trophoblast in early human pregnancy: controversies and questions. *Nat. Rev. Immunol., 23*, 222–235.
50. Hanna, J.G., et al. (2006). Decidual NK cells regulate key developmental processes at the human fetal-maternal interface. *Nat. Med., 12*, 1065–1074.
51. Kammerer, U., et al. (2006). *Characterization of Human Dendritic Cells at the Materno-fetal Interface. Landes Bioscience/Springer Science.*
52. Abrahams, V.M., et al. (2004). Macrophages and apoptotic cell clearance during pregnancy. *Am. J. Reprod. Immunol., 51*, 275–282.
53. Roussev, R.G., et al. (2008). Duration of intralipid's suppressive effect on NK cell's functional activity. *Am. J. Reprod. Immunol., 60*, 258–263.
54. Koga, K., & Mor, G. (2008). Expression and function of toll-like receptors at the maternal-fetal interface. *Reprod. Sci., 15*, 231–242.

55. Yoshinaga, K. (2008). Review of factors essential for blastocyst implantation for their modulating effects on the maternal immune system. *Semin Cell Dev Biol.,19*, 161–169.
56. Svensson, J. et al. (2011). Macrophages at the fetal-maternal interface express markers of alternative activation and are induced by M-CSF and IL-10. *J. Immunol., 187*, 3671–3682.
57. Mills, C. D., et al. (2000). M-1/M-2 macrophages and the Th1/Th2 paradigm. *J Immunol., 164*, 6166–6173.
58. Pijnenborg, R., et al. (1983). Uteroplacental arterial changes related to interstitial trophoblast migration in early human pregnancy. *Placenta*, *4*, 397-414.
59. Brown, M. B., et al. (2014). M1/M2 macrophage polarity in normal and complicated pregnancy. *Front. Immunol., 5*, 606.
60. Mantovani, A., et al. (2013). Macrophage plasticity and polarization in tissue repair and remodelling. *The Journal of pathology, 229*, 176–185.
61. Zhang, Y. H., et al. (2017). Modulators of the Balance between M1 and M2 Macrophages during Pregnancy. *Front. Immunol., 8*, 120.
62. Hamilton, S. et al. (2012). Macrophages infiltrate the human and rat decidua during term and preterm labor: evidence that decidual inflammation precedes labor. *Biol. Reprod., 86*, 39.
63. Smith, R. (2007). Parturition. *N. Engl. J. Med., 356*, 271–283.
64. Yellon, S.M. (2020). Immunobiology of Cervix Ripening. *Front. Immunol., 10*, 3156.
65. Barclay, C.G., et al. (1993). Interleukin-8 production by the human cervix. *Am. J. Obstet. Gynecol., 169*, 625–32.
66. Burton, G. J., & Fowden, A. L. (2015). The placenta: a multifaceted, transient organ. *Philosophical transactions of the Royal Society of London. Series B, Biological sciences*, *370*(1663), 20140066.
67. Kim, S.M., & Kim, J.S. (2017). A review of mechanisms of implantation. *Dev. Reprod., 21*, 351.

68. Sato, Y., Fujiwara, H., & Konishi, I. (2011). Mechanism of maternal vascular remodeling during human pregnancy. *Reproductive medicine and biology*, *11*(1), 27–36.
69. Wang, Y., & Zhao, S. (2010). Vascular Biology of the Placenta. *Morgan & Claypool Life Sciences*. *Chapter 2, Placental Blood Circulation*.
70. Gupta, R. C. (2022). Reproductive and Developmental Toxicology. *Academic Press, an imprint of Elsevier.*
71. Watson, E.D., & Cross, J.C. (2005). Development of structures and transport functions in the mouse placenta, *Physiology (Bethesda), 20*, 180–193.
72. Arumugasaamy, N., et al. (2020). Microphysiological systems of the placental barrier. *Adv, Drug, Deliv, Rev*., *161-162*, 161-175.
73. Al-Enazy, S., et al. (2017). Placental control of drug delivery, *Adv. Drug Deliv. Rev*., *116*, 63–72.
74. Palmeira, P., et al. (2012). IgG placental transfer in healthy and pathological pregnancies, *Clin. Dev. Immunol*.
75. Klaassen, C.D., & Lu, H. (2008). Xenobiotic transporters: ascribing function from gene knockout and mutation studies, *Toxicol. Sci*., *101*, 186–196.
76. Holder, B., et al. (2021). 'Fetal side' of the placenta: anatomical mis-annotation of carbon particle 'transfer' across the human placenta. *Nat. Commun., 12*, 7049.
77. Soncin, F., Natale, D., & Parast, M.M. (2015). Signaling pathways in mouse and human trophoblast differentiation: a comparative review. *Cell Mol. Life Sci., 72*(7), 1291-302.
78. Benirschke, K., & Kaufmann, P. (2000). Pathology of the Human Placenta. *Springer.*
79. Kieckbusch, J., Gaynor, L.M., & Colucci, F. (2015). Assessment of Maternal Vascular Remodeling During Pregnancy in the Mouse Uterus. *J. Vis. Exp., 106*, e53534.
80. Simmons, D.G., et al. (2008). Early patterning of the chorion leads to the trilaminar trophoblast cell structure in the placental labyrinth. *Development., 135*, 2083–2091.

81. Shibata, S., et al. (2020). Unique features and emerging in vitro models of human placental development. *Reprod. Med. Biol., 19*(4), 301-313.
82. Challier, J.C., et al. (2008). Obesity in pregnancy stimulates macrophage accumulation and inflammation in the placenta. *Placenta, 29*(3), 274–281.
83. Laskewitz, A., et al. (2019). The influence of maternal obesity on macrophage subsets in the human decidua. *Cell Immunol., 336*, 75–82.
84. Monaco-Brown, M., & Lawrence, D. A. (2022). Obesity and maternal-placental-fetal immunology and health. *Frontiers in Pediatrics*, *10*.
85. Schwenke, M., et al. (2013). Control of human endometrial stromal cell motility by PDGF-BB, HB-EGF and trophoblast-secreted factors. *PLoS One*. *8*(1), e54336.
86. Queckbörner, S., et al. (2020). Endometrial stromal cells exhibit a distinct phenotypic and immunomodulatory profile. *Stem Cell Res. Ther., 11*, 15.
87. Du, M.R., Wang, S.C., & Li, D.J. (2014). The integrative roles of chemokines at the maternal-fetal interface in early pregnancy. *Cell Mol. Immunol., 11*(5), 438-48.
88. Aye, I.L., et al. (2014). Increasing maternal body mass index is associated with systemic inflammation in the mother and the activation of distinct placental inflammatory pathways. *Biol. Reprod., 90*(6), 129.
89. Basu, S., et al. (2011). Pregravid obesity associates with increased maternal endotoxemia and metabolic inflammation. *Obesity (Silver Spring)., 19*, 476–482.
90. Pantham, P., Aye, I.L., & Powell, T.L. (2015). Inflammation in maternal obesity and gestational diabetes mellitus. *Placenta, 36*(7), 709–715.
91. Roberts, K.A., et al. (2011). Placental structure and inflammation in pregnancies associated with obesity. *Placenta, 32*(3), 247–254.
92. Roberts, V.H., et al. (2009). Effect of increasing maternal body mass index on oxidative and nitrative stress in the human placenta. *Placenta, 30*(2), 169–175.
93. Aye, I.L., et al. (2012). Oxysterols exert proinflammatory effects in placental trophoblasts via TLR4-dependent, cholesterol-sensitive activation of NF-kappaB. *Mol. Hum. Reprod., 18*(7), 341–353.
94. Whitmarsh, A.J. (2010). A central role for p38 MAPK in the early transcriptional response to stress. *BMC Biol., 8*, 47.

95. Saben, J., et al. (2013). Early growth response protein-1 mediates lipotoxicity-associated placental inflammation: role in maternal obesity. *Am. J. Physiol. Endocrinol. Metab., 305*, E1–E14.
96. Catlett-Falcone, R., et al. (1999). Constitutive activation of Stat3 signaling confers resistance to apoptosis in human U266 myeloma cells. *Immunity, 10*, 105–115.
97. Zhong, Z., Wen, Z., & Darnell, J.E. Jr. (1994). Stat3: a STAT family member activated by tyrosine phosphorylation in response to epidermal growth factor and interleukin-6. *Science, 264*, 95–98.
98. Heinrich, P.C., et al. (2003). Principles of interleukin (IL)-6-type cytokine signalling and its regulation. *Biochem. J., 374*, 1–20.
99. Radaelli, T., et al. (2006). Maternal interleukin-6: marker of fetal growth and adiposity. *J. Soc. Gynecol. Investig., 13*, 53–57.
100. Beneventi, F., et al. (2023). Placental pathologic features in obesity. *Placenta, 144*, 1–7.
101. Calderon, I. M. P., et al. (2007). Morphometric study of placental villi and vessels in women with mild hyperglycemia or gestational or overt diabetes. *Diabetes Research and Clinical Practice*, *78*(1), 65–71.
102. Musa, E., et al. (2023). Obesity and gestational diabetes independently and collectively induce specific effects on placental structure, inflammation and endocrine function in a cohort of South African women. *The Journal of Physiology*, *601*(7), 1287–1306.
103. Scott, H., et al. (2022). Maternal Underweight and Obesity Are Associated with Placental Pathologies in Human Pregnancy. *Reprod. Sci., 29*, 3425–3448.
104. Aune, D., et al. (2014). Maternal body mass index and the risk of fetal death, stillbirth, and infant death: A systematic review and meta-analysis. *JAMA - Journal of the American Medical Association*, *311*(15), 1536–1546.
105. Napso, T., et al. (2022). Diet-induced maternal obesity impacts feto-placental growth and induces sex-specific alterations in placental morphology, mitochondrial bioenergetics, dynamics, lipid metabolism and oxidative stress in mice. *Acta. Physiol. (Oxf), 234*(4), e13795.

106. de Barros Mucci, D., et al. (2020). Impact of maternal obesity on placental transcriptome and morphology associated with fetal growth restriction in mice. *Int. J. Obes., 44*, 1087–1096.

107. Michelsen, T.M., et al. (2019). Uteroplacental Glucose Uptake and Fetal Glucose Consumption: A Quantitative Study in Human Pregnancies. *J. Clin. Endocrinol. Metab*., *104*(3), 873–82.

108. Kelly, A.C., Powell, T.L., & Jansson, T. (2020). Placental function in maternal obesity. *Clin. Sci (Lond)., 134*(8), 961-984.

109. Acosta, O., et al. (2015). Increased glucose and placental GLUT-1 in large infants of obese nondiabetic mothers. *Am. J. Obstet. Gynecol*., 212(2), *227*, e1–7.

110. Gaither, K., Quraishi, A.N., & Illsley, N.P. (1999). Diabetes alters the expression and activity of the human placental GLUT1 glucose transporter. *J. Clin. Endocrinol. Metab*., *84*(2), 695–701.

111. HAPO Study Cooperative Research Group, et al. (2008). Hyperglycemia and adverse pregnancy outcomes. *N. Engl. J. Med*., *358*(19), 1991–2002.

112. Barbour, L.A. (2019). Metabolic Culprits in Obese Pregnancies and Gestational Diabetes Mellitus: Big Babies, Big Twists, Big Picture : The 2018 Norbert Freinkel Award Lecture. *Diabetes care*, *42*(5), 718–726.

113. Perazzolo, S., et al. (2017). The influence of placental metabolism on fatty acid transfer to the fetus. *J. Lipid. Res., 58*, 443–454.

114. Heerwagen, M.J.R., et al. (2018). Placental lipoprotein lipase activity is positively associated with newborn adiposity. *Placenta, 64*, 53–60.

115. Dube, E., et al. (2012). Modulation of fatty acid transport and metabolism by maternal obesity in the human full-term placenta. *Biol. Reprod., 87*, 11–14.

116. Sinha, N., & Dabla, P.K. (2015). Oxidative stress and antioxidants in hypertension-a current review. *Curr. Hypertens. Rev.,11*, 132-142.

117. Chiarello, D.I., et al. (2020). Oxidative stress: Normal pregnancy versus preeclampsia. *Biochimica et Biophysica Acta (BBA) - Molecular Basis of Disease*, *1866*(2), 165354.

118. Mueller, A., et al. (2005). Placental defense is considered sufficient to control lipid peroxidation in pregnancy. *Med. Hypotheses, 64*(3), 553e7.
119. Al-Gubory, K.H., Fowler, P.A., & Garrel, C. (2010). The roles of cellular reactive oxygen species, oxidative stress and antioxidants in pregnancy outcomes. *Int. J. Biochem. Cell Biol., 42*(10), 1634–1650.
120. Malti, N., et al. (2014). "Oxidative Stress and Maternal Obesity: Feto-Placental Unit Interaction." *Placenta (Eastbourne)*, *35* (6), 411–16..
121. Santos-Rosendo, C., et al. (2020). Placental adaptive changes to protect function and decrease oxidative damage in metabolically healthy maternal obesity. *Antioxidants*, *9*, 794.
122. Myatt, L., & Cui, X. (2004). Oxidative stress in the placenta. *Histochem. Cell Biol., 122*(4), 369–382.
123. Kelly, A., et al. (2023). Maternal obesity alters the placental transcriptome in a fetal sex-dependent manner. *Frontiers in Cell and Developmental Biology*, *11.*
124. Borengasser, S.J., et al. (2014). In utero exposure to prepregnancy maternal obesity and postweaning high-fat diet impair regulators of mitochondrial dynamics in rat placenta and offspring. *Physiological Genomics*, *46*(23), 841–850.
125. Mele, J., et al. (2014). Impaired mitochondrial function in human placenta with increased maternal adiposity. *American Journal of Physiology-Endocrinology and Metabolism*, *307*(5).
126. Hastie, R., & Lappas, M. (2014). The effect of pre-existing maternal obesity and diabetes on placental mitochondrial content and electron transport chain activity. *Placenta*, *35*(9), 673–683.
127. Calabuig-Navarro, V., et al. (2017). Effect of Maternal Obesity on Placental Lipid Metabolism. *Endocrinology*, 158(8), 2543–55.
128. Dennery, P.A. (2007). Effects of oxidative stress on embryonic development. *Birth Defects Res C Embryo Today, 81*(3), 155e62.

129. Qanungo, S., & Mukherjea, M. (2000). Ontogenic profile of some antioxidants and lipid peroxidation in human placental and fetal tissues. *Mol Cell Biochem*, 215, 11e9.

130. Katsyuba, E., et al. (2020). “NAD + Homeostasis in Health and Disease.” *Nature Metabolism*, *2*(1), 9–31.

131. Covarrubias, A.J., et al. (2021). NAD^+ metabolism and its roles in cellular processes during ageing. *Nat. Rev. Mol. Cell Biol., 22*(2), 119-141.

132. Imai, S.I., et al. (2000). Transcriptional silencing and longevity protein Sir2 is an NAD-dependent histone deacetylase. *Nature*, *403*, 795–800.

133. De Flora, A., et al. (2004). Autocrine and paracrine calcium signaling by the CD38/NAD^+/cyclic ADP-ribose system. *Ann. N. Y. Acad. Sci., 1028*, 176–191.

134. Bai, P., & Cantó, C. (2012). The role of PARP-1 and PARP-2 enzymes in metabolic regulation and disease. *Cell Metab., 16*, 290–295.

135. Bai, P., et al. (2011). PARP-1 inhibition increases mitochondrial metabolism through SIRT1 activation. *Cell Metab., 13*, 461–468.

136. Imai, S.I., & Guarente, L. (2014). NAD^+ and sirtuins in aging and disease. *Trends Cell Biol., 24*, 464–471.

137. Liu, L., et al. (2018). Quantitative Analysis of NAD Synthesis-Breakdown Fluxes. *Cell metabolism*, *27*(5), 1067–1080.e5.

138. Frye, R. A. (2000). Phylogenetic classification of prokaryotic and eukaryotic Sir2-like proteins. *Biochem. Biophys. Res. Commun., 273*, 793–798.

139. Bell, N. A. W., & Molloy, J.E. (2023). Single-molecule force spectroscopy reveals binding and bridging dynamics of PARP1 and PARP2 at DNA double-strand breaks. *Proceedings of the National Academy of Sciences*, *120*(22).

140. Vyas, S., et al. (2014). Family-wide analysis of poly(ADP-ribose) polymerase activity. *Nat. Commun*., 5, 4426.

141. Caron, M.C., et al. (2019). Poly(ADP-ribose) polymerase-1 antagonizes DNA resection at double-strand breaks. *Nat Commun.,* 10, 2954.

142. Attia, S.M., & Al-Enazi, K.A. (2014). PARP Enzymes are Potential Targets for Cancer Chemotherapy.

143. Mouchiroud, L. et al. (2013). The NAD+/sirtuin pathway modulates longevity through activation of mitochondrial UPR and FOXO signaling. *Cell, 154*, 430–441.

144. Braidy, N., et al. (2011). Age related changes in NAD+ metabolism oxidative stress and Sirt1 activity in wistar rats. *PLoS One, 6*, e19194.

145. Berger, N.A. (1985). Poly(ADP-ribose) in the cellular response to DNA damage. *Radiat. Res., 101*, 4–15.

146. Kam, T. I., et al. (2018). Poly (ADP-ribose) drives pathologic α-synuclein neurodegeneration in Parkinson's disease. *Science (New York, N.Y.)*, *362*(6414), eaat8407.

147. Mao, K., et al. (2020). Poly (ADP-ribose) polymerase 1 inhibition prevents neurodegeneration and promotes α-synuclein degradation via transcription factor EB-dependent autophagy in mutant α-synucleinA53T model of Parkinson's disease. *Aging cell*, *19*(6), e13163.

148. Hageman, G.J., et al. (2003). Systemic poly (ADP-ribose) polymerase-1 activation, chronic inflammation, and oxidative stress in COPD patients. *Free Radic. Biol. Med.*, *35*, 140–8.

149. Hwang, J.W., et al. (2010). Cigarette smoke-induced autophagy is regulated by SIRT1-PARP-1-dependent mechanism: implication in pathogenesis of COPD. *Arch. Biochem. Biophys.*, *500*, 203–9.

150. Moonen, H.J., et al. (2005). Theophylline prevents NAD+ depletion via PARP-1 inhibition in human pulmonary epithelial cells. *Biochemical and biophysical research communications*, *338*(4), 1805–1810.

151. Lee, M.H., et al. (2024). Bi-directional regulation of AIMP2 and its splice variant on PARP-1-dependent neuronal cell death; Therapeutic implication for Parkinson's disease. *acta. neuropathol. commun., 12*, 5.

152. Kovács, D., et al. (2021). Olaparib: A Clinically Applied PARP Inhibitor Protects from Experimental Crohn's Disease and Maintains Barrier Integrity by Improving Bioenergetics through Rescuing Glycolysis in Colonic Epithelial Cells. *Oxidative medicine and cellular longevity*, 7308897.

153. Bogan, K.L., & Brenner, C. (2008). Nicotinic acid, nicotinamide, and nicotinamide riboside: A molecular evaluation of NAD+ precursor vitamins in human nutrition. *Annu. Rev. Nutr., 28*, 115–130.

154. Martens, C.R., et al. (2018). Chronic nicotinamide riboside supplementation is well-tolerated and elevates NAD+ in healthy middle-aged and older adults. *Nat. Commun., 9*, 1268.

155. Mills, E., et al. (2003). The safety of over-the-counter niacin. A randomized placebo-controlled trial. *BMC Clin. Pharmacol.*, *3*(4).

156. Dollerup, O.L, et al. (2018). A randomized placebo-controlled clinical trial of nicotinamide riboside in obese men: Safety, insulin-sensitivity, and lipid-mobilizing effects. *Am. J. Clin. Nutr., 108*(2), 343–353.

157. Dollerup, O.L., et al. (2020). Nicotinamide riboside does not alter mitochondrial respiration, content or morphology in skeletal muscle from obese and insulin-resistant men. *J. Physiol.*, *598*(4), 731–754.

158. Yaku, K., & Takashi, N. (2023). "NAD + Precursors in Human Health and Disease: Current Status and Future Prospects." *Antioxidants & Redox Signaling*, *39*(16–18), 1133–49.

159. Remie, C.M.E., et al. (2020). Nicotinamide riboside supplementation alters body composition and skeletal muscle acetylcarnitine concentrations in healthy obese humans. *The American journal of clinical nutrition*, *112*(2), 413–426.

160. Lapatto, H.A.K., et al. (2023). Nicotinamide riboside improves muscle mitochondrial biogenesis, satellite cell differentiation, and gut microbiota in a twin study. *Science advances*, *9*(2), eadd5163.

161. Yang, Q., et al. (2021). NAD+ repletion attenuates obesity-induced oocyte mitochondrial dysfunction and offspring metabolic abnormalities via a SIRT3-dependent pathway. *Clinical and translational medicine*, *11*(12), e628.

162. Wang, H., et al. (2021). NAMPT reduction-induced NAD+insufficiency contributes to the compromised oocyte quality from obese mice. *Aging cell*, *20*(11), e13496.

163. Jahan, F., et al. (2023). NAD+ Depletion and Altered Mitochondrial Function Are Key to the Establishment of Placental Dysfunction in an

Inflammatory-Driven Subclass of Preeclampsia. *BioRxiv: The preprint server for Biology.*

164. Cantó, C. et al. (2012). The NAD+ precursor nicotinamide riboside enhances oxidative metabolism and protects against high-fat diet-induced obesity. *Cell Metab., 15*, 838–847.

165. Yoshino, J., et al. (2011). Nicotinamide mononucleotide, a key NAD(+) intermediate, treats the pathophysiology of diet- and age-induced diabetes in mice. *Cell Metab., 14*, 528–536.

166. Dellinger, R.W., et al. (2017). Repeat dose NRPT (nicotinamide riboside and pterostilbene) increases NAD^+ levels in humans safely and sustainably: a randomized, double-blind, placebo-controlled study. *NPJ aging and mechanisms of disease*, *3*, 17.

167. Stromsdorfer, K.L. et al. (2016). NAMPT-mediated NAD+ biosynthesis in adipocytes regulates adipose tissue function and multi-organ insulin sensitivity in mice. *Cell Rep., 16*, 1851–1860.

168. Rajman, L., Chwalek, K., & Sinclair, D.A. (2018). Therapeutic Potential of NAD-Boosting Molecules: The In Vivo Evidence. *Cell metabolism*, *27*(3), 529–547.

169. Chen, C., et al. (2023). NAD+Metabolism and Immune Regulation: New Approaches to Inflammatory Bowel Disease Therapies. *Antioxidants (Basel, Switzerland)*, *12*(6), 1230.

170. Dunwoodie, S.L., et al. (2023). Nicotinamide adenine dinucleotide deficiency and its impact on mammalian development. *Antioxidants & Redox Signaling*, *39*(16–18), 1108–1132.

171. Cuny, H., et al. (2020). NAD deficiency due to environmental factors or gene-environment interactions causes congenital malformations and miscarriage in mice. *Proceedings of the National Academy of Sciences of the United States of America*, *117*(7), 3738–3747.

172. Mandò, C., et al. (2018). Impact of Obesity and Hyperglycemia on Placental Mitochondria. *Oxidative medicine and cellular longevity*, 2378189.

173. D'Amours, D., et al. (1999). Poly(ADP-ribosyl)ation reactions in the regulation of nuclear functions. *Biochem. J., 342*(2), 249–68.
174. Weaver, A.N., & Yang, E.S. (2013). Beyond DNA Repair: Additional Functions of PARP-1 in Cancer. *Front. Oncol., 3*, 290.
175. Kanai, M., et al. (2007). Inhibition of Crm1-p53 interaction and nuclear export of p53 by poly(ADP-ribosyl)ation. *Nat. Cell Biol., 9*, 1175–1183.
176. Fischbach, A., et al. (2018). The C-terminal domain of p53 orchestrates the interplay between non-covalent and covalent poly(ADP-ribosyl)ation of p53 by PARP1. *Nucleic Acids Res., 46*, 804–822.
177. Zerfaoui, M., et al. (2010). Poly(ADP-ribose) polymerase-1 is a determining factor in Crm1-mediated nuclear export and retention of p65 NF-kappa B upon TLR4 stimulation. *J. Immunol., 185*, 1894–1902.
178. Yang, H., et al. (2007). Nutrient-sensitive mitochondrial NAD^+ levels dictate cell survival. *Cell, 130*, 1095–1107.
179. Gomes, A.P., et al. (2013). Declining NAD^+ induces a pseudohypoxic state disrupting nuclear-mitochondrial communication during aging. *Cell*, *155*, 1624–1638.
180. Bankhead, P., et al. (2017). QuPath: Open source software for digital pathology image analysis. *Sci. Rep.,* 7, 16878.
181. Mayor, R.S., et al. (2015). Maternal high-fat diet is associated with impaired fetal lung development. *American Journal of Physiology-Lung Cellular and Molecular Physiology*, *309*(4).
182. Ke, Y., et al. (2019). The Role of PARPs in Inflammation-and Metabolic-Related Diseases: Molecular Mechanisms and Beyond. *Cells*, *8*(9), 1047.
183. Ahmed, M., Praneet Ng, A., & L'Abbe, M.R. (2021). Nutrient intakes of Canadian adults: results from the Canadian Community Health Survey (CCHS)-2015 Public Use Microdata File. *The American journal of clinical nutrition, 114*(3), 1131–1140.
184. Speakman, J.R. (2019). Use of high-fat diets to study rodent obesity as a model of human obesity. *Int. J. Obes., 43*, 1491–1492.

185. Hall, K.D, & Jordan, P.N. (2008). Modeling weight-loss maintenance to help prevent body weight regain. *Am. J. Clin. Nutr.*, *88*(6), 1495.

186. Katan, M.B., & Ludwig, D.S. (2010). “Extra Calories Cause Weight Gain—But How Much?” *JAMA : The Journal of the American Medical Association*, *303*(1), 65–66.

187. Wyatt, S., et al. (2015). Fully-automated, high-throughput micro-computed tomography analysis of body composition enables therapeutic efficacy monitoring in preclinical models. *Int. J. Obes., 39*, 1630–1637.

188. Wu, H., et al. (2018). Normal diet Vs High fat diet—A comparative study: Behavioral and neuroimmunological changes in adolescente male mice. *Metab. Brain Dis.*

189. Kim, D.H., et al. (2017). Dual function of *Lactobacillus kefiri* DH5 in preventing high-fat-diet-induced obesity: direct reduction of cholesterol and upregulation of PPAR-α in adipose tissue. *Mol. Nutr. Food. Res.*

190. Dutta, S., & Sengupta, P. (2016). Men and mice: Relating their ages. *Life Sciences*, *152*, 244–248.

191. World Health Organization (2015). Guideline: Sugars Intake for Adults and Children. *57*.

192. Wang, Y.F., et al. (2020). Canadian Adults with Moderate Intakes of Total Sugars have Greater Intakes of Fibre and Key Micronutrients: Results from the Canadian Community Health Survey 2015 Public Use Microdata File. *Nutrients*, *12*(4), 1124.

193. Wartella, E.A., et al. (2010). Front-of-Package Nutrition Rating Systems and Symbols: Phase I Report. *National Academies Press (US)*, *4*.

194. US Department of Health and Human Services. (2015). 2015–2020 Dietary Guidelines for Americans. *8*.

195. Kibblewhite, R., et al. (2017). Estimating free and added sugar intakes in New Zealand. *Nutrients, 9*, 1292.

196. Stanhope, K.L., et al. (2009). Consuming fructose-sweetened, not glucose-sweetened, beverages increases visceral adiposity and lipids and

decreases insulin sensitivity in overweight/obese humans. *J. Clin. Invest., 119*, 1322–1334.

197. Hinkle, S.N., Sharma, A.J., & Dietz, P.M. (2010). Gestational weight gain in obese mothers and associations with fetal growth. *Am. J. Clin. Nutr., 92*(3), 644-651.

198. Fowden, A.L., Camm, E.J., & Sferruzzi-Perri, A.N. (2020). Effects of maternal obesity on placental phenotype. *Curr. Vasc. Pharmacol., 19*(2), 113–131.

199. Kiel, D.W., et al. (2007). Gestational weight gain and pregnancy outcomes in obese women: how much is enough? *Obstet. Gynecol., 110*(4), 752–758.

200. Catalano, P.M. (2007). Increasing maternal obesity and weight gain during pregnancy: the obstetric problems of plentitude. *Obstet. Gynecol., 110*(4), 743–744.

201. Park, S., et al. (2011). Assessment of the Institute of Medicine recommendations for weight gain during pregnancy: Florida, 2004–2007. *Matern. Child. Health. J., 15*(3), 289–301.

202. Liu, C., et al. (2024). High-fat and high-sucrose diet impairs female reproduction by altering ovarian transcriptomic and metabolic signatures. *J. Transl. Med., 22*, 145.

203. Gao, X., et al. (2021). Obesity induces morphological and functional changes in female reproductive system through increases in NF-κB and MAPK signaling in mice. *Reprod. Biol. Endocrinol*., *19*, 148.

204. Muhammad, T., et al. (2023). Maternal obesity: A potential disruptor of female fertility and current interventions to reduce associated risks. *Obesity reviews : an official journal of the International Association for the Study of Obesity*, *24*(10), e13603.

205. Marinelli, S., et al. (2022). Female obesity and infertility: outcomes and regulatory guidance. *Acta bio-medica : Atenei Parmensis*, *93*(4), e2022278.

206. Sanches, A., et al. (2022). Obesity phenotype induced by high-fat diet leads to maternal-fetal constraint, placental inefficiency, and fetal growth restriction in mice. *The Journal of nutritional biochemistry*, *104*, 108977.

207. Simino, L., et al. (2020). Maternal resistance to diet-induced obesity partially protects newborn and post-weaning male mice offspring from metabolic disturbances. *J. Dev. Orig. Health. Dis*., *1-11*.

208. Lewandowska, M. (2021). Maternal Obesity and Risk of Low Birth Weight, Fetal Growth Restriction, and Macrosomia: Multiple Analyses. *Nutrients*, *13*, 1213.

209. Murphy, V.E., & Smith, R. (2006). Endocrine regulation of human fetal growth: The role of the mother, placenta, and fetus. *Endocr. Rev., 27*, 141–169.

210. Beaten, J.M., & Bukusi, E.A. (2001). Pregnancy complications and outcomes among overweight and obese nulliparous women. *Am. J. Public. Health., 91*, 436–440.

211. KC, K., Shakya, S., & Zhang, H. (2015). Gestational Diabetes Mellitus and Macrosomia: A Literature Review. *Annals of Nutrition & Metabolism*, *66*, 14–20.

212. Drever, H.J., et al. (2023). Factors associated with higher risk of small-for-gestational-age infants in women treated for gestational diabetes. *Australian and New Zealand Journal of Obstetrics and Gynaecology*, *63*(5), 714–720.

213. Langer, O., et al. (1989). Glycemic control in gestational diabetes mellitus-how tight is tight enough: Small for gestational age versus large for gestational age? *Am. J. Obstet. Gynecol., 161*(3), 646–653.

214. Radulescu, L., et al. (2013). The implications and consequences of maternal obesity on fetal intrauterine growth restriction. *Journal of medicine and life*, *6*(3), 292–298.

215. Cotechini, T. et al. (2014). Inflammation in rat pregnancy inhibits spiral artery remodeling leading to fetal growth restriction and features of preeclampsia. *J. Exp. Med., 211*, 165–179.

216. Tosun, M. et al. (2010). Maternal and umbilical serum levels of interleukin-6, interleukin-8, and tumor necrosis factor-alpha in normal pregnancies and in pregnancies complicated by preeclampsia. *J. Matern. Fetal Neonatal Med., 23*, 880–886.

217. Amarilyo, G. et al. (2011). Increased cord serum inflammatory markers in small-for-gestational-age neonates. *J. Perinatol., 31*, 30–32.

218. Wilson, M.E., & Ford, S.P. (2001). Comparative aspects of placental efficiency. *Reprod. Suppl., 58*, 223–232.
219. Hayward, C. E., et al. (2016). Placental Adaptation: What Can We Learn from Birth Weight:Placental Weight Ratio? *Frontiers in physiology, 7*, 28.
220. Wang, M., et al. (2022). Diallyl Trisulfide Promotes Placental Angiogenesis by Regulating Lipid Metabolism and Alleviating Inflammatory Responses in Obese Pregnant Mice. *Nutrients*, *14*(11), 2230.
221. Kingdom, J., et al. (2000). Development of the placental villous tree and its consequences for fetal growth. *Eur. J. Obstet. Gynecol. Reprod. Biol., 92*(1), 35–43.
222. Mifsud, W., & Sebire, N.J. (2014). Placental pathology in early-onset and late-onset fetal growth restriction. *Fetal Diagn. Ther., 36*(2), 117–128.
223. Morley, L.C., et al. (2021). Placental blood flow sensing and regulation in fetal growth restriction. *Placenta*, *113*, 23–28.
224. Shim, K., et al. (2020). Complement activation in obesity, insulin resistance, and type 2 diabetes mellitus. *World journal of diabetes*, *11*(1), 1–12.
225. Spradley, F.T., Palei, A.C., & Granger, J.P. (2015). Immune Mechanisms Linking Obesity and Preeclampsia. *Biomolecules, 5*, 3142–3176.
226. Balneger, N., et al. (2021). Generation of αcd11b-CPG antibody conjugates for the targeted stimulation of myeloid cells. *Journal of Controlled Release*, *332*, 148–159.
227. Zhu, M.J., et al. (2010). Maternal obesity up-regulates inflammatory signaling pathways and enhances cytokine expression in the mid-gestation sheep placenta, *Placenta, 31*, 387e391.
228. Frias, A.E., et al. (2011). Maternal high-fat diet disturbs uteroplacental hemodynamics and increases the frequency of stillbirth in a nonhuman primate model of excess nutrition. *Endocrinology, 152*, 2456e2464.
229. Kretschmer, T., et al. (2020). Effect of Maternal Obesity in Mice on IL-6 Levels and Placental Endothelial Cell Homeostasis. *Nutrients*, *12*(2), 296.

230. Thompson, J.A., et al. (2015). “The Contribution of Toll-like Receptors to Placental Inflammation in Diet-Induced Maternal Obesity.” *Placenta (Eastbourne)*, *36*(10), 1204–06.

231. Oliva, K., et al. (2012). The effect of pre-existing maternal obesity on the placental proteome: two-dimensional difference gel electrophoresis coupled with mass spectrometry. *J. Mol. Endocrinol., 48*(2), 139–149.

232. Varastehpour, A., et al. (2006). Activation of phospholipase A2 is associated with generation of placental lipid signals and fetal obesity. *J. Clin. Endocrinol. Metab., 91*(1), 248–255.

233. Saben, J., et al. (2014). Maternal obesity is associated with a lipotoxic placental environment. *Placenta, 35*(3), 171–177.

234. Christian, L.M., & Porter, K. (2014). Longitudinal changes in serum proinflammatory markers across pregnancy and postpartum: Effects of maternal body mass index. *Cytokine.*

235. Friis, C.M., et al. (2013). Adiposity-related inflammation: effects of pregnancy. *Obesity (Silver Spring), 21*(1), E124–E130.

236. Ernst, L.M., et al. (2021). Chronic villitis of unknown etiology: Investigations into viral pathogenesis. *Placenta*, *107*, 24–30.

237. Leon-Garcia, S.M., et al. (2016). “Maternal Obesity and Sex-Specific Differences in Placental Pathology.” *Placenta (Eastbourne)*, *38*, 33–40.

238. Loardi, C., et al. (2016). Placental morphology in pregnancies associated with pregravid obesity. *The Journal of Maternal-Fetal & Neonatal Medicine*, *29*(16), 2611–2616.

239. Redline, R.W. (2007). Villitis of unknown etiology: noninfectious chronic villitis in the placenta. *Hum. Pathol., 38*(10), 1439–46.

240. Becroft, D.M., Thompson, J.M., & Mitchell, E.A. (2005). Placental villitis of unknown origin: epidemiologic associations, *Am. J. Obstet. Gynecol., 192*(1), 264–71.

241. Feeley, L., & Mooney, E.E. (2010). Villitis of unknown aetiology: correlation of recurrence with clinical outcome, *J. Obstet. Gynaecol., 30*(5), 476–9.

242. Leon, R. L., et al. (2022). Placental vascular malperfusion lesions in fetal congenital heart disease. *American Journal of Obstetrics and Gynecology*, *227*(4).

243. Visser, L., et al. (2021). Maternal vascular malperfusion in spontaneous preterm birth placentas related to clinical outcome of subsequent pregnancy. *The journal of maternal-fetal & neonatal medicine*, *34*(17), 2759–2764.

244. Pugnaloni, F., et al. (2023). Gender differences in congenital heart defects: a narrative review. *Translational pediatrics*, *12*(9), 1753–1764.

245. Peelen, M.J.C.S., et al. (2016). Impact of fetal gender on the risk of preterm birth, a national cohort study. *Acta Obstetricia et Gynecologica Scandinavica*, *95*(9), 1034–1041.

246. Liu, C., et al. (2017). The role of poly ADP-ribosylation in the first wave of DNA damage response. *Nucleic Acids Res., 45*, 8129–8141.

247. Schuhwerk, H., et al. (2016). PARPing for balance in the homeostasis of poly(ADP-ribosyl)ation. *Semin Cell Dev. Biol., 63*, 81–91.

248. Wei, H., & Yu, X. (2016). Functions of PARylation in DNA Damage Repair Pathways. *Genomics Proteomics Bioinformatics, 3*,131-139.

249. Luo, X., & Kraus, W.L. (2012). On PAR with PARP: Cellular stress signaling through poly (ADP-ribose) and PARP-1. *Genes Dev., 26*, 417–432.

250. Alemasova, E.E., & Lavrik, O.I. (2019). Poly (ADP-ribosyl) ation by PARP1: Reaction mechanism and regulatory proteins. *Nucleic Acids Res., 47*, 3811–3827.

251. Hassa, P.O., et al. (2005). Acetylation of poly(ADP-ribose) polymerase-1 by p300/CREB-binding protein regulates coactivation of NF-kappaB-dependent transcription. *J. Biol. Chem., 280*, 40450–40464.

252. Mota, R.A., et al. (2005). Inhibition of poly(ADP-ribose) polymerase attenuates the severity of acute pancreatitis and associated lung injury. *Lab. Investig., 85*, 1250–1262.

253. Kamboj, A., et al. (2013). Poly(ADP-ribose) polymerase 2 contributes to neuroinflammation and neurological dysfunction in mouse experimental autoimmune encephalomyelitis. *J. Neuroinflamm., 10*, 49.

254. Gariani, K., et al. (2017). Inhibiting poly ADP-ribosylation increases fatty acid oxidation and protects against fatty liver disease. *J. Hepatol*., *66*(1), 132-141.

255. Mukhopadhyay, P., et al. (2017). PARP inhibition protects against alcoholic and non-alcoholic steatohepatitis. *J. Hepatol., 66*(3), 589-600.

256. Pacher, P., & Szabó, C. (2005). Role of poly(ADP-ribose) polymerase-1 activation in the pathogenesis of diabetic complications: endothelial dysfunction, as a common underlying theme. *Antioxid. Redox Signal.*, *7*(11-12), 1568-80.

257. Goodman, R.P., Calvo, S.E., & Mootha, V.K. (2018). Spatiotemporal compartmentalization of hepatic NADH and NADPH metabolism. *J. Biol. Chem., 293*(20), 7508-7516.

258. Turunen, R., et al. (2024). Maternal Diabetes and Overweight and Congenital Heart Defects in Offspring. *JAMA Netw. Open., 7*(1), e2350579.

259. Iessa, N., & Bérard, A. (2015). Update on Prepregnancy Maternal Obesity: Birth Defects and Childhood Outcomes. *J. Pediatr. Genet., 4*(2), 71-83.

260. Capaldi, R.A., et al. (1994). Coupling between catalytic sites and the proton channel in F1F0-type ATPases. *Trends Biochem. Sci., 19*, 284–289.

261. Nijtmans, L.G., et al. (1995). Assembly of mitochondrial ATP synthase in cultured human cells: implications for mitochondrial diseases. *Biochim. Biophys. Acta. 1272*, 190–198.

262. De Meirleir, L., et al. (2004). Respiratory chain complex V deficiency due to a mutation in the assembly gene ATP12. *J. Med. Genet*., *41*, 120–124.

263. Jonckheere, A.I., Smeitink, J.A., & Rodenburg, R.J. (2012). Mitochondrial ATP synthase: architecture, function and pathology. *Journal of inherited metabolic disease, 35*(2), 211–225.

264. Moosavi, E.A. et al. (2019). The assembly of succinate dehydrogenase: A key enzyme in bioenergetics. *Cell. Mol. Life Sci., 76*, 4023–4042.

265. Baines, K.J., & West, R.C. (2023). Sex differences in innate and adaptive immunity impact fetal, placental, and maternal health, *Biology of Reproduction*, *109*(3), 256–270.

266. Eriksson, J.G., et al. (2010). Boys live dangerously in the womb. *Am. J. Hum. Biol., 22*(3), 330-5.

267. Choy, L.N., et al. (1992). Adipsin and an endogenous pathway of complement from adipose cells. *J. Biol. Chem., 267*, 12736–12741.

268. Nilsson, B., et al. (2014). C3 and C4 are strongly related to adipose tissue variables and cardiovascular risk factors. *Eur. J. Clin. Invest., 44*, 587–596.

269. Lynch, A.M., et al. (2012). Prepregnancy obesity and complement system activation in early pregnancy and the subsequent development of preeclampsia. *Am. J. Obstet. Gynecol., 206*, 428, e1–428.e8.

270. Lynch, A.M., et al. (2012). Alternative complement pathway activation fragment Bb in early pregnancy as a predictor of preeclampsia. *Am. J. Obstet. Gynecol., 198*, 385, e1–385.e9.

271. Fu, Y., et al. (2021). USP12 promotes CD4+ T cell responses through deubiquitinating and stabilizing BCL10. *Cell Death Differ., 28*, 2857–70.

272. Lu, P., et al. (2021). De-ubiquitination of p300 by USP12 critically enhances METTL3 expression and Ang II-induced cardiac hypertrophy. *Experimental Cell Research*, *406*(1), 112761.

273. Lehmann, M., et al. (2014). Artd1-induced poly-ADP-ribose formation enhances PPARΓ ligand binding and co-factor exchange. *Nucleic Acids Research*, *43*(1), 129–142.

274. Cuzzocrea, S., & Wang, Z.Q. (2005). Role of poly (ADP-ribose) glycohydrolase (PARG) in shock, ischemia and reperfusion. *Pharmacol. Res., 52*, 100–108.

275. Oliver, F.J., et al. (1999). Resistance to endotoxic shock as a consequence of defective NF-κB activation in poly (ADP-ribose) polymerase-1 deficient mice. *Embo. J., 18*, 4446–4454.

276. Bai P., et al. (2007). Poly(ADP-ribose) polymerase-2 [corrected] controls adipocyte differentiation and adipose tissue function through the regulation of the activity of the retinoid X receptor/peroxisome proliferator-activated receptor-gamma heterodimer. *J. Biol. Chem*., *282*, 37738–37746.

277. Uddin, G. M., et al. (2020). Administration of nicotinamide mononucleotide (NMN) reduces metabolic impairment in male mouse offspring from obese mothers. *Cells*, *9*(4), 791.

278. Youngson, N.A., et al. (2019). Impacts of obesity, maternal obesity and nicotinamide mononucleotide supplementation on sperm quality in mice. *Reproduction*, *158*(2), 171–181.

279. Uddin, G.M., et al. (2015). Effects of high fat diet induced obesity on mitochondrial biogenesis and function – impact of exercise or nicotinamide mononucleotide (NMN). *The FASEB Journal*, *29*(S1).

280. Fukamizu, Y., et al. (2022). Safety evaluation of β-nicotinamide mononucleotide oral administration in healthy adult men and women. *Scientific reports*, *12*(1), 14442.

281. Bieganowski, P., & Brenner, C. (2004). Discoveries of nicotinamide riboside as a nutrient and conserved NRKgenes establish a Preiss-Handler independent route to NAD+ in fungi and humans. *Cell, 117*, 495–502.

282. Belenky, P., et al. (2007). Nicotinamide riboside promotes Sir2 silencing and extends lifespan via Nrk and Urh1/Pnp1/Meu1 pathways to NAD+. *Cell, 129*, 473–484.

283. Revollo, J.R., Grimm, A.A., & Imai, S. (2004). The NAD+ biosynthesis pathway mediated by nicotinamide phosphoribosyltransferase regulates Sir2 activity in mammalian cells. *J. Biol. Chem., 279*, 50754–50763.

284. Mehmel, M., Jovanović, N., & Spitz, U. (2020). Nicotinamide Riboside-The Current State of Research and Therapeutic Uses. *Nutrients*, *12*(6), 1616.

285. Shats, I., et al. (2020). Bacteria boost mammalian host NAD metabolism by engaging the deamidated biosynthesis pathway. *Cell Metab., 31*, 564–579.e7.

286. Gariani, K., et al. (2017). Inhibiting poly ADP-ribosylation increases fatty acid oxidation and protects against fatty liver disease. *J. Hepatol., 66*, 132–141.

287. Lehwald, N., et al. (2012). β-Catenin regulates hepatic mitochondrial function and energy balance in mice. *Gastroenterology, 143*, 754–764.

288. Eriksson, S., et al. (2015). Dietary methionine can sustain cytosolic redox homeostasis in the mouse liver. *Nat. Commun., 6*, 64792015.

289. Tummala, K.S., et al. (2014). Inhibition of de novo NAD(+) synthesis by oncogenic URI causes liver tumorigenesis through DNA damage. *Cancer Cell*, *26*, 826–839.

290. Berger, F., et al. (2005). Subcellular compartmentation and differential catalytic properties of the three human nicotinamide mononucleotide adenylyltransferase isoforms. *Journal of Biological Chemistry*, *280*, 36334–36341.

291. Nikiforov, A., et al. (2011). Pathways and subcellular compartmentation of NAD biosynthesis in human cells: From entry of extracellular precursors to mitochondrial NAD generation. *Journal of Biological Chemistry*, *286*, 21767–21778.

292. VanLinden, M.R., et al. (2015). Subcellular distribution of NAD+ between cytosol and mitochondria determines the metabolic profile of human cells. *Journal of Biological Chemistry*, *290*, 27644–27659.

293. Gulshan, M., et al. (2018). Overexpression of NMNAT3 efficiently increases nad and ngd levels and ameliorates age-associated insulin resistance. *Aging Cell*, *17*(4).

294. Bowlby, S.C., et al. (2012). Nicotinamide phosphoribosyl transferase (Nampt) is required for de novo lipogenesis in tumor cells. *PLoS One*, *7*(6), e40195.

295. Wei, Z., et al. (2020). Nampt-mediated spindle sizing secures a post-anaphase increase in spindle speed required for extreme asymmetry. *Nature Communications*, *11*(1), 3393.

296. Von Schönfels, W., et al. (2015). Metabolomic tissue signature in human non-alcoholic fatty liver disease identifies protective candidate metabolites. *Liver Int., 35*, 207–214.

297. Musso, G., et al. (2003). Dietary habits and their relations to insulin resistance and postprandial lipemia in nonalcoholic steatohepatitis. *Hepatology, 37*, 909–916.

298. Sookoian, S., et al. (2008). Should nonalcoholic fatty liver disease be included in the definition of metabolic syndrome? A cross-sectional comparison with adult treatment panel III criteria in nonobese nondiabetic subjects: Response to Musso. *Diabetes Care, 31*, e42.

299. Gariani, K., et al. (2016). Eliciting the mitochondrial unfolded protein response by nicotinamide adenine dinucleotide repletion reverses fatty liver disease in mice. *Hepatology, 63*, 1190–204.

300. Yamaguchi, S., & Yoshino, J. (2017). Adipose tissue NAD+ biology in obesity and insulin resistance: From mechanism to therapy. *BioEssays : news and reviews in molecular, cellular and developmental biology*, *39*(5).

301. Poljsak, B., & Milisav, I. (2018). Vitamin B3 forms as precursors to NAD+: Are they safe? *Trends in Food Science & Technology*, *79*, 198–203.

302. Snaidr, V.A., Damian, D.L., & Halliday, G.M. (2019). Nicotinamide for photoprotection and skin cancer chemoprevention: A review of efficacy and safety. Experimental *Dermatology, 28*, 15–22.

303. Bertoldo, M.J., et al. (2020). NAD^+ Repletion Rescues Female Fertility during Reproductive Aging. *Cell reports*, *30*(6), 1670–1681.e7.

304. Lappas, M., & Permezel, M. (2011). The anti-inflammatory and antioxidative effects of nicotinamide, a vitamin B3 derivative, are elicited by FoxO3 in human gestational tissues: Implications for preterm birth. *The Journal of Nutritional Biochemistry*, *22*(12), 1195–1201.

Appendix

Protocol Detail Report

Printed By: Josefina, Yusmaris
2024-05-10 7:50:16 AM

Report Comments

Protocol Information

Version # 5

Reference Number	3937		
Protocol Number	CMMe-3937-R1		
Protocol Title	Role of poly (ADP-ribose) polymerases in placental and fetal development during maternal obesity		
Protocol Type:	Renewal		
Principal Investigator:	Bainbridge, Shannon	**Approval Date:**	2023-11-22
Submittal Date:	2023-10-31	**Effective Date:**	2023-11-22
Author:	Bainbridge, Shannon	**Renewal Date:**	2024-09-30
Status:	Active Approved Protocols	**Next Review Date:**	2024-08-20
Inactive Date:		**Expiration Date:**	2026-09-30

Renewal 1

PERSONNEL UPDATES 1.1

Please use this renewal as an opportunity to review the personnel listed in the OVERVIEW section under PROTOCOl ASSOCIATES. Personnel no longer working in your lab should be removed.

Renewal Type 1.2

Renewal Type

- ☐ Annual Renewal
- ☑ Annual Renewal/Amendment

Annual Renewal 1.2.1

Annual Renewal/Amendment 1.2.2

Amendment Type 1.2.2.1

Select all that apply.

- ☑ Personnel
- ☐ Animals
- ☑ Procedures

Personnel 1.2.2.1.1

Animals 1.2.2.1.2

Procedures 1.2.2.1.3

Explanation for Amendment of Procedures 1.2.2.1.3.1

Provide justification and amend the relevant section(s) within the existing protocol below.

An additional blood pressure measurement will be performed at the 9 month age mark. We want to include this addition to the procedures, as we have measured blood pressure at both the 3 month and 6 month marks for mice that were born to obese (high-fat high-sugar diet) mothers and healthy diet mothers, and have noted differences in blood pressure. At 3 months, there was a trend where female and male offspring born to obese moms were trending towards higher systolic and diastolic blood pressures. At 6 months, these differences became significant in males with those born to obese mothers having higher systolic and diastolic blood pressures than those born to healthy mothers. So we are interested to see if this difference will become even more significant at 9 months of age, thus demonstrating adverse developmental programming effects of maternal obesity on offspring cardiometabolic health. This will be performed via tail cuff method as previously approved. As such, the euthanization of all offspring will be moved to 38 weeks of age (2 weeks after completion of the third set of blood pressure measurements).

Progress Report - Experimental Aims 1.3

Describe any progress made within the last approval period towards fulfilling the specific aims of this work, specifically pertaining to the animal subjects.

For all wild type mice (Wild-type (WT)-Chow-Saline-maternal euthanized at E19 (n=5), WT-Chow-NR-maternal sacrifice at E19 (n=5), WT-HFHS-Saline-maternal euthanized at E19 (n=5), WT-HFHS-NR-maternal euthanized at E19 (n=5), Wild-type (WT)-Chow-Saline-offspring (n=5), WT-Chow-NR-fetal offspring (n=5), WT-HFHS-Saline-offspring (n=5), and WT-HFHS-NR-offspring (n=5)) they have completed their 12 week diet administration. Echo-MRI, fasting glucose testing, and blood collection after 12 weeks of diet was completed. All trio mating was completed. The NR/Saline administration via oral gavage over the course of pregnancy (E0.5-19) was completed. All euthanizations for wild type mouse mothers were completed ((Wild-type (WT)-Chow-Saline-maternal euthanized at E19 (n=5), WT-Chow-NR-maternal sacrifice at E19 (n=5), WT-HFHS-Saline-maternal euthanized at E19 (n=5), and WT-HFHS-NR-maternal euthanized at E19 (n=5)) and maternal organs, placenta and fetuses were collected.
For the groups Wild-type (WT)-Chow-Saline-offspring (n=5), WT-Chow-NR-fetal offspring (n=5), WT-HFHS-Saline-offspring (n=5), and WT-HFHS-NR-offspring (n=5), all mothers delivered their offspring, and all offspring have been weaned. Litter culling has been completed, with 2 male and 2 female offspring per litter. At 12 weeks Echo-MRI was complete as well as fasted glucose testing. OGTT was completed at 18 weeks of age. CLAMS was completed at 20 weeks of age. Blood pressure measurements at 12 weeks and 24 weeks of age has been completed, and blood pressure measurements at 36 weeks of age has yet to be done (will be completed at the 36 weeks of age mark). Offspring euthanizations at 38 weeks of age has yet to be performed.
All experiments for NAD+ content/activity, PARP content/activity and mitochondrial health/function using n=10 animals/group: high performance liquid chromatography (HPLC), qPCR, RNA-seq, western blot, seahorse assay, and oxygraph using tissue homogenates are beginning to be performed. Placental histology, morphology, and proliferation (Ki-67) staining have been completed. The ultrasound pilot was also completed successfully.

Progress Report - Animal Use 1.4

Please indicate the number of animals used in the past year, and the number of animals you expect to use in the year to come, with a justification.

Cohort 1: 40 female mice + 20 male mice; 40 female mice were comprised of 4 groups of 10 mice each: Control-Water (n=10), Control-Nicotinamide Riboside (NR; n=10), High-Fat High-Sugar (HFHS) Water (n=10), HFHS-NR (n=10). As the project is assessing maternal obesity, n=20 male mice were used to trio mate with the 40 female mice (1 male mouse to 2 female mice) as the project was assessing the effects of obesity during pregnancy. All of these mice have now been euthanized. From 7 of these female mice, 28 offspring were kept (14 female offspring and 14 male offspring) which are being kept for ongoing analysis.
Cohort 2: 40 female mice + 20 male mice; given that some female mice were lost from the first cohort and I didn't have enough for analysis, we ordered another cohort of mice to pull up the number of samples. Again these 40 female mice were separated into the same four groups of n=10 mice each. The male mice were used to trio mate with the female mice. All of these mice have now been euthanized.
a total of 3 female mice: 1 was lost due to experimental purposes (when I was gavaging this mouse, she moved on me and I think I hurt her lung so she had to be euthanized). 2 were lost due to health concerns: 1 had a large facial mass, and the other one was just found dead in its cage (I'm unsure what the cause was).
Although we didn't lose as many mice as I thought, we did have to do a second cohort because in addition to the 3 female mouse deaths, 9 of our female mice never got pregnant, which is essential to studying our subject of interest: maternal obesity and subsequent effects on the placenta. So given that in total, we didn't get to use 12 (9 not pregnant + 3 deaths) of our mice for the study, we decided to order in a second cohort.
No more mice have since been ordered for this protocol. The animals we expect to us in the year to come are the 28 offspring (14 female and 14 male) from cohort 1 which are being kept for ongoing analysis.

Progress Report - Three Rs 1.5

Describe any progress made with respect to the Three Rs of replacement, reduction and refinement of animal use. Reviewing the CCAC website when considering the 3Rs may be helpful.

Replacement: A cell culture model representing maternal obesity was tried being used to partially replace using as many animals for this project, but it could not accurately replicate what we wanted to observe. Results from this model were not reliable or replicable. In this case, our study had to turn to fully using an animal model to assess the impacts of maternal obesity on placental health and fetal outcomes, as to get more reliable and replicable results.
Reduction: We used trio mating instead of pair mating to reduce the number of male mice used for this study. In this sense we reduced the number of male mice used by half (20 male mice instead of 40 to mate with 40 female mice). Also the offspring generated from obese and control wildtype mothers are going to be used for another project in our lab that studies developmental effects of maternal obesity on cardiometabolic programming, instead of generating more offspring for their experiments, which reduces the amount of mice used.
Refinement: The female mice used in my study exhibited an excess of grinding behaviour with the high fat high sugar diet. To minimize stress and grinding behaviour, nylon bones, wood blocks, and extra nesting were placed into respective cages with grinders. This high fat high sugar diet was also topped up more frequently (every 1-2 days) with smaller quantities of food so that there was less food ground on the bottom of the cage, causing stress to the mice. These cages were also changed more frequently (weekly) rather than every 2 weeks.
Another thing to minimize stress is animals were trained for procedures. For the animals undergoing blood pressure testing, they were subjected to 1 week of acclimatization before 1 week of measurements, to get them used to the procedure. Animals were also handled regularly by the same person (Hannah Poisson) who weighed them weekly, prior to starting other tests including: oral gavage, glucose tests, etc.
Animals were humanely euthanized via cervical dislocation. All lab members who performed cervical dislocation for this study (Hannah Poisson and Yusmaris Cariaco) were properly trained by ACVS to ensure no animal distress or suffering.

Problems/Adverse Events 1.6

Using lay terms, describe any complications encountered relative to animal use (unpredicted outcomes, and any animal pain, distress or mortality). Indicate the cause(s) if known and how these events were resolved.

No abnormal animal pain, distress, or mortality occurred.

Refinement of Animal Endpoints 1.7

Describe how the experimental and humane endpoints for this work helped to prevent animal pain and distress. Were the endpoints appropriate in practice? If not, what modifications will be made moving forward?

This thesis work involved studying the effects of maternal obesity on placental mitochondrial health. Cervical dislocation without prior anesthesia was used as endpoint. We must use a physical method without prior anesthetic as anesthetic can disrupt the integrity of the mitochondria. As the mitochondria is an essential part of our study to assess NAD+ content/activity, and furthermore its role in placental disruption and fetal programming, its integrity must be maintained. 20-Sept-22 --> Live cervical dislocation was performed by Hannah Poisson, Alex Green or Yusmaris Josefina Cariaco, proper training has been completed with Courtney Reeks for this procedure. This endpoint was appropriate and worked well for our study, and we will continue to use the same endpoints going forward.

Publications 1.8

Identify any publications in the past year (including theses) related to this work.

Abstract/Poster Presentation, Published in Placenta Journal https://doi.org/10.1016/j.placenta.2023.07.229

Overview 2

Introduction 2.1

Thank you for completing the following animal use protocol form for all studies involving vertebrate animals or cephalopods. Complete, clear answers to the questions simplify approval by the Animal Care Committee, which approves animal use on behalf of the university and the wider community. uOttawa has formal agreements with funders, is certified by the Canadian Council on Animal Care (CCAC), has licenses under the Ontario Animals for Research Act and an Animal Welfare Assurance by the US Public Health Service, and must meet Canadian, Ontarian and international animal care and use standards on an ongoing basis.

Please note that *Cell*, *Nature* and many other journals have adopted the ARRIVE (Animal Research: Reporting of In Vivo Experiments) guidelines. These guidelines are intended to improve the reporting of research using animals − maximizing information published and minimizing unnecessary animal studies. We encourage you to use the ARRIVE checklist when preparing your animal experiments and protocols to facilitate publication of your results.

Protocol Detail Report

Printed By: Josefina, Yusmaris
2024-05-10 7:50:16 AM

Reference Number **2.2**

This is a system generated number.
3937

Principal Investigator **2.3**

The principal investigator must be selected from a system defined list. If you are not the investigator, please choose the appropriate PI.

Bainbridge, Shannon	sbainbri@uOttawa.ca	562-5800 ext 8569

Protocol Number **2.4**

Protocol Number
CMMe-3937-R1

Title **2.5**

This field can contain a maximum of 255 characters, please be concise.
Role of poly (ADP-ribose) polymerases in placental and fetal development during maternal obesity

Protocol Associates **2.6**

Identify all personnel who will perform work with animals or who are associated with this study using the green orb button.

You may also:

· Check the 'Co-Investigator' box if you want the individual to be able to alter this protocol on your behalf.

· Check the 'Key Associate' box if you want the individual to receive an email notification when the protocol status changes.

· Check the 'Authorized to Order Animals' box if you want to grant permission to an individual to place animal requests.

Note: New personnel are manually added to the Topaz database once they have registered with ACVS for training. If the proposed person has registered online and does not appear in the list, please ensure you are searching beyond Page 1 (the search function will only search the active page).

Bainbridge, Shannon			
Responsibilities	Supervision of project		
Comments			
☐ Co-Investigator	☑ Key Associate	☑ Authorized To Order	
Menzies, Keir J.			
Responsibilities	Supervision of project		
Comments			
☐ Co-Investigator	☑ Key Associate	☑ Authorized To Order	
Josefina, Yusmaris			
Responsibilities	Postdoc that will help with animal procedures, breeding, diet administration and euthanasia		
Comments			
☐ Co-Investigator	☑ Key Associate	☑ Authorized To Order	
Poisson, Hannah			
Responsibilities	Primary student responsible for experimental procedures and welfare of the animals, breeding, diet administration, genotyping and euthanasia		
Comments			
☑ Co-Investigator	☑ Key Associate	☑ Authorized To Order	
Larionov, Nikita			
Responsibilities	Lab technician that will help in experimental protocols and be responsible for animal welfare		
Comments			
☐ Co-Investigator	☑ Key Associate	☑ Authorized To Order	

Green, Alexander			
Responsibilities	Postdoc that will help in experimental protocols, breeding, diet administration and genotyping		
Comments			
☐ Co-Investigator	☑ Key Associate	☑ Authorized To Order	
Jahan, Fahmida			
Responsibilities	PhD student that will provide assistance with NR treatment and experimental procedures		
Comments			
☐ Co-Investigator	☑ Key Associate	☑ Authorized To Order	
Gamelin Kao, Jade			
Responsibilities	Over the summer, Jade will be working alongside Hannah and Yusmaris, helping with setting up timed matings, checking plugs, sub-cutaneous injections, sacrifice and tissue dissections. In Sept, Jade will begin her MSc with me, at which point she will take on a more independent role with these same tasks.		
Comments			
☐ Co-Investigator	☐ Key Associate	☐ Authorized To Order	

Author **2.7**

If you would like to permit another individual to access and edit this protocol in its unsubmitted state, please identify them here using the 'Select Staff' button to the left of the current name.
This person can also initiate an amendment or renewal.

Bainbridge, Shannon

Created By **2.8**

This is a system generated field.

Josefina, Yusmaris

External Collaborators **2.9**

Will any external collaborators be actively involved in the animal work proposed in this protocol?

- ☐ Yes
- ☑ No

Yes	**2.9.1**
No	**2.9.2**

Submission Type **2.10**

Select the appropriate submission type.

- [x] New protocol
- [ ] Protocol that has had 3 renewals and work is ongoing

New protocol **2.10.1**

Protocol that has had 3 renewals and work is ongoing **2.10.2**

Protocol Purpose **2.11**

Please identify the purpose of this protocol.

- [x] Research
- [ ] Teaching

Research **2.11.1**

Peer Review **2.11.1.1**

Has the work supported by this protocol been reviewed for scientific merit, as outlined in the ACC policy on Ensuring Scientific Merit of Animal-Based Research?

- [x] Yes - outside agency (e.g. granting agency)
- [ ] Yes - within university
- [ ] No

Yes - outside agency (e.g. granting agency) **2.11.1.1.1**

Specify Reviewing Agency **2.11.1.1.1.1**

Specify the reviewing agency.

CIHR

Date of Outside Agency Review **2.11.1.1.1.2**

Provide the date of review.

2016-03-01

Yes - within university **2.11.1.1.2**

No **2.11.1.1.3**

Funding Type **2.11.1.2**

Select all that apply.

- [x] Grant
- [ ] Contract
- [ ] Other

Grant **2.11.1.2.1**

Grant Details **2.11.1.2.1.1**

Click on the green orb button to complete the following table.

This information is essential for the release of grant funds.

Funding Source	RE Form Number	Grant Number	Grant Title	Date	Duration
CIHR	147217	153055	NAD+ depletion as a cause of placental dysfunction in preeclampsia	2016-10 to 2023	7 years

'Other' Funding Source **2.11.1.2.1.2**

If you have specified 'Other funding source' in the table above, please provide the name of the funding source here.

N/A

Contract **2.11.1.2.2**

Other **2.11.1.2.3**

Teaching **2.11.2**

Billing Information **2.12**

Will the project costs be recovered using uOttawa accounts?

- [x] Yes, uOttawa FOAP(s) applicable
- [ ] No

Yes, uOttawa FOAP(s) applicable **2.12.1**

FOAP Authorization 2.12.1.1

Attachments: Authorization Form - Cost Centre.pdf

Financial information must be provided in order to proceed with work under this protocol. Download the attached form and submit to the ACVS.
This information is confidential, for business purposes only, and required to receive animal care services.

No 2.12.2

Emergency Contact Information 3

Study Type 3.1

Will you be working with wild animals in the field?

- ☐ Yes
- ☑ No

Yes 3.1.1

No 3.1.2

Emergency Response 3.1.2.1

If contacts cannot be reached in the event of an emergency or humane endpoint, the decision of the ACVS veterinarian concerning the management and disposition of the animal, including euthanasia, is final.

Emergency Contacts 3.1.2.2

Identify a minimum of two contacts named on the protocol using the green orb button. These contacts must be empowered to make a final decision regarding the disposition of the animal.

If an office or lab is listed as the Daytime Phone #, you must provide a different number at which the contact can be reached out of hours.

Name	Daytime Phone #	Out of Hours Phone #	Email Address
Yusmaris Cariaco			
Nikita Larionov			
Hannah Poisson			

Classes of Animal Use 4

CCAC Purposes of Animal Use 4.1

Choose the relevant CCAC Purpose of Animal Use using the green orb button.

Fundamental Studies - CCAC 1 4.1.1

Lay Summary 5

Lay Summary 5.1

In simple, clear, non-technical language, briefly describe the research this protocol supports and summarize your study objectives. This section should be suitable for release to the public and the media. Please do not copy your grant proposal summary. See the help menu for additional information.

With the recent rise in the obesity epidemic, there are increasingly more mothers who are pregnant and obese. According to developmental origins of health and disease (DOHaD) paradigms, the inflammation inflicted by obesity has been shown to trigger placental dysfunction. In turn, these placental abnormalities program fetuses to be at a higher risk of developing metabolic impairments, chronic diseases, and comorbidities including: gestational diabetes, hypertension and large for gestational age (LGA) deliveries.
In particular, obesogenic diets have been shown to affect the activity of NAD+, a cofactor responsible for multiple key cellular energy reactions. NAD+ contents depend on the balance between enzymes that consume it and those that synthesize it. However stressful conditions, such as obesity, can disrupt this balance. Namely, stress caused by inflammation increases parylation, a post-translational reversible protein modification produced by enzymes called PARPs and counteracted by another enzyme called PARG. Under normal conditions, parylation is a signal to other proteins to trigger DNA repair or gene expression regulation while not lowering NAD+ levels. But in stressful conditions, PARPs consume significant amounts of NAD+, which can increase to 90% NAD+ consumption in times of extreme stress. In essence, the overactivity of PARP proteins lowers NAD+ levels, diminishing its availability for important cellular functions, thus leading to energetic stress and cell death. In fact, overactive PARP activity has been previously linked to pregnancy complications such as preeclampsia. While it is known that obesity perpetuates inflammation in pregnant mothers, and that inflammation can overstimulate parylation, the roles of specific PARP proteins (i.e. PARP-1, PARP-2) in obesity induced inflammation in the placenta and its effects on fetal programming are unknown. Thus, this protocol will apply a high-fat high-sugar (HFHS) diet to new mouse models (i.e. PARP-1 knockout, PARP-2 knockout, PARP-½ knockout, PARG knockout) to understand obesity's effects on inflammation, and this inflammation's subsequent effects on parylation activity. Moreover, we will assess how decreased or increased parylation activity affects placental and fetal health. Last, we will verify if NAD+ boosting with NR (nicotinamide riboside) treatment could improve fetal and placental development in this context.

Experimental Design 6

Type of Animal Use 6.1

How will animals be used? Select all that apply.

- ☑ Research
- ☐ Teaching

Research 6.1.1

Replacement, Reduction & Refinement of Animal Use 6.1.1.1

CCAC guidelines and policies require you to consider alternatives to the use of animals.

More information on these guidelines can be found at the CCAC3Rs Microsite.

Replacement: The Animal Care Committee needs to understand why animals must be used for your work, instead of using replacement alternatives.

We encourage you to search for alternatives relevant to your work on sites such as the CCAC 3Rs Microsite for Teaching & Training or ALTWEB: Alternatives to Animal Testing.

Alternatives to Using Live Animals 6.1.1.2

1) Explain and justify why animals must be used within the larger context of your research program.

2) Indicate any replacement alternatives that you currently employ (see examples in the help menu).

Ethical and logistical obstacles hinder the study of molecular mechanisms during maternal obesity in humans. Likewise, trophoblast cell culture models do not fully reproduce the interactions that occur in a living organism or the complex microenvironment of the cells that populate the placenta. Because of this, it is necessary to use animals in this study. Nevertheless, in parallel to the use of experimental animals, we intend to verify whether NAD+ increase improves trophoblast functionality using a fatty acid overload cell culture model.

Experimental Design **6.1.1.3**

Attachments: Example of Flowchart and Timeline.docx,Experimental Timeline Oct 31 2023.pptx,Procedural Timeline October 31 2023.docx

Explain your overall experimental design within the context of your research goals, with an overview of the procedures to be performed. Identify the number of animals to be used per experiment.

Do not include the specifics of the procedures here (step by step methods, doses, etc.) as they will be requested in subsequent sections.

Please include a visual representation as it is most helpful to the Animal Care Committee, in particular for any more complex work. See the attachment below for an example flowchart (for overall study design) and procedural timeline (for individual experimental arms) .

Taken from the breeding protocol for this project: Initial cross-breeding of mice will take a minimum of 22 to 33 weeks to produce mice that are Parp1-LoxP+/+, Parp2-LoxP+/+ and Tg(CYP19A1-Cre)+/-; Parp1-LoxP and Tg(CYP19A1-Cre)+/-; Parp2-LoxP and Tg(CYP19A1-Cre)+/-; and Parg-LoxP and Tg(CYP19A1-Cre)+/-. Additionally we will have group of wild-type C57BL/6 mice we will have ordered in.
We will then be separating mice into: 24 groups of mice: Wild-type (WT)-Chow-Saline-maternal euthanized at E19 (n=10), WT-Chow-NR-maternal sacrifice at E19 (n=10), WT-HFHS-Saline-maternal euthanized at E19 (n=20), WT-HFHS-NR-maternal euthanized at E19 (n=20), Wild-type (WT)-Chow-Saline-offspring euthanized week 38 (n=5), WT-Chow-NR-fetal offspring at week 38 (n=5), WT-HFHS-Saline-offspring euthanized at week 38 (n=5), WT-HFHS-NR-offspring euthanized at week 38 (n=5), PARP-1 KO-Chow-Saline (n=10), PARP-1 KO-Chow-NR (n=10), PARP-1 KO-HFHS-Saline (n=10), PARP-1 KO-HFHS-NR (n=10), PARP-2 KO-Chow-Saline (n=10), PARP-2 KO-Chow-NR (=10), PARP-2 KO-HFHS-Saline (n=10), PARP-2 KO-HFHS-NR (n=10), PARP-1/2 KO-Chow-Saline (n=10), PARP-1/2 KO-Chow-NR (n=10), PARP-1/2 KO-HFHS-Saline (n=10), PARP-1/2 KO-HFHS-NR (n=10), PARG KO-Chow-Saline (n=10), PARG KO-Chow-NR (n=10), PARG KO-HFHS-Saline (n=10), and PARG KO-HFHS-NR (n=10). All knockout mothers will be euthanized at E19 with no surviving fetal offspring.
Experimental diets will be administered starting at 5 weeks of age to female mice, while all male mice will be fed with regular chow diet throughout experiments. Females diet will be administered for 12 weeks (until 17 weeks of age).
Following diet administration, EchoMRI will be used prior to inducing pregnancy on all female mice to quantify fat mass and lean mass percentages. This tool will be useful to detect fat accumulation/deposits in mice and confirm a state of obesity in the high-fat high-sugar diet fed mice.
At 17 weeks of age (week 12/13 of the project), food restriction will be set up for 6 h in order to take a fasting glucose sampling from all our female mice. Blood collection for this fasting glucose testing will be performed via a tail nick (at 17 weeks of age; week 12/13 of the project)-this collection will only be performed once. This collection will be performed using a minimal restraint via tail restriction to induce a lateral tail nick to minimize mouse distress, with no needle sampling required. 50 µL of blood will be collected.
This will be followed by mating mice (trio mating: 2 females to 1 male) to induce pregnancy. Vaginal plug detection and an awake ultrasound will be used as a method to confirm pregnancy. Once mice are pregnant (E0), administration of our treatment (NR or saline (control) will commence. NR/saline will be administered to all female mice via oral gavage at a dose of 400 mg/kg/day according to previously approved protocol from our lab. Reasoning for gavage - In a prior pregnancy study within our lab that studied the effects of inflammation on pregnant rats, we had a small window (19 days) to see a beneficial effect of NR. Our lab thought that administering NR in the diet would not ensure the exact amount of daily NR intake needed to see a preventative effect of NR in a severe model like preeclampsia. Additionally, using the oral gavage administrative method of delivering NR helped reduce the number of animals used and cut the cost of NR. Diet administration will continue throughout the
course of pregnancy. For the mothers being euthanized, blood collection for resting glucose testing will take place following euthanasia (week 15/16 of the project) This will be performed via a cardiac puncture technique which will aim to get as much blood as possible (app. 200 uL of blood). This will be done once. We will euthanize all of the mice from the knockout groups and half of the mice from the wild-type groups. Mice will be euthanized via a physical method without prior sedation (E19). Pups from euthanized mothers will be euthanized by cervical dislocation. For the mothers that are not being euthanized, they will also undergo resting glucose testing (at week 15/16 of the project) but via the tail nick method as was described previously. This will be done once.
Maternal and fetal organs will be harvested and weights recorded from euthanized mothers. Namely we will collect: the placenta, kidneys, liver, white adipose tissue, brown adipose tissue, and record number of fetal offspring. The placentas will be cut in half: half will be flash frozen with liquid nitrogen and the other half stored in 4% paraformaldehyde for histological and immunohistochemistry analyzes.
From the 4 wild-type mouse groups (Chow, Chow-NR, HFHS, and HFHS-NR), we will be euthanizing some dams at E19 as previously mentioned (n=10 from Chow groups and n=20 from HFHS groups, for a total of n=60 dams) and some dams to survive, complete their pregnancies, and give birth (n=5 from each group for a total of n=20 dams). Mothers will be maintained on their respective diets for the duration of lactation, and all offspring will be weaned at 21 days post birth. At the time of weaning, each litter will be culled to 2 male and 2 female offspring per litter. This will total 10 female and 10 male offspring per group (Chow=10 females, 10 males; Chow-NR=10 females, 10 males; HFHS=10 females, 10 males, HFHS-NR=10 females, 10 males. At 12 weeks of age (week 30 of the project) Echo-MRI will be performed (without anesthesia) followed by fasted glucose testing (6 hr food restriction) will be performed to measure glucose handling in all fetal offspring (n=4 offspring/mother; n=80 mice total (40 females and 40 males). Again, the blood collection for this fasted glucose testing will be performed via tail nick as previously described (at week 30 of the project). Blood pressure measurements using the

tail cuff system will be taken at 12 weeks (acclimatization) and 13 weeks (measurements) of age. An oral glucose tolerance test (OGTT) with 6 hour food restriction will be performed at age 18 weeks to measure glucose handling over time and metabolic CLAMS cage procedure at 20 weeks of age to measure energy expenditure. At 24 weeks of age and 36 weeks of age, mice will undergo blood pressure measurements again using the tail cuff method with 1 week of acclimatization and 1 week of measurements. This will help us to assess differences in blood pressure over time.
At 38 weeks of age, all offspring (n=80) will be sacrificed and the brain, heart, liver, muscle, adipose tissue, and kidneys collected, weighed, and fixed in 4% PFA for future histological analysis.
The following experiments will test for NAD+ content/activity, PARP content/activity and mitochondrial health/function using n=10 animals/group: high performance liquid chromatography (HPLC), qPCR, RNA-seq, western blot, seahorse assay, and oxygraph using tissue homogenates. Additionally, we will assess the ability of NR to repair metabolic impairments by applying it to HFHS cell culture, then testing PARP inhibitors, and PARP activity/expression. Also, we will assess placental histology, morphology, and proliferation (Ki-67). Again, all of these experiments will use n=10 animals per group.
As the initial cohort will be a pilot using ultrasound without anesthesia a small cohort size of 20 females will be set up for time mating's.

References **6.1.1.4**

Please attach or link any references you wish to provide.

Sanches, A., de Oliveira, J. L., Ferreira, M. S., Lima, B. S., Miyamoto, J. É., Simino, L., Torsoni, M. A., Torsoni, A. S., Milanski, M., & Ignácio-Souza, L. (2022). Obesity phenotype induced by high-fat diet leads to maternal-fetal constraint, placental inefficiency, and fetal growth restriction in mice. The Journal of nutritional biochemistry, 104, 108977. https://doi.org/10.1016/j.jnutbio.2022.108977
Simino, L., Panzarin, C., Torsoni, M., Ignácio-Souza, L., Milanski, M., & Torsoni, A. (2021). Maternal resistance to diet -induced obesity partially protects newborn and post-weaning male mice offspring from metabolic disturbances. Journal of Developmental Origins of Health and Disease, 12(4), 660-670. doi:10.1017/S204017442000094X

Teaching **6.1.2**

Multiple Procedures **6.2**

Will the same animals be undergoing multiple procedures?

- [x] Yes
- [ ] No

Yes **6.2.1**

Procedural Timeline **6.2.1.1**

Attachments: Example of Procedural Timeline.docx

Please provide one or more visual timelines that clearly outline all procedures the animals will undergo, and the frequency/time between all procedures, from the beginning of the study to the experimental endpoint(s). See the attachment for an example of a Procedural Timeline (bottom). If your timelines require further explanation, please describe below.

Please refer to the above section.

No **6.2.2**

Justification of Animal Numbers 6.3

Attachments: GPower.tif

Describe how animal numbers were calculated and provide a justification for the total number of animals to be used (based on your experimental design and number of animals per experimental group). The number of animals should be the minimum number required to obtain statistically/scientifically (or pedagogically, for teaching) valid results.

We aim to use 24 maternal experimental groups: Wildtype (WT)-Chow-Saline-maternal sacrifice at E19 (n=10), WT-Chow-NR-maternal sacrifice at E19 (n=10), WT-HFHS-Saline-maternal sacrifice at E19 (n=20), WT-HFHS-NR-maternal sacrifice at E19 (n=20), Wildtype (WT)-Chow-Saline-fetal sacrifice week 38 (n=5), WT-Chow-NR-fetal sacrifice at week 14 (n=5), WT-HFHS-Saline-fetal sacrifice at week 14 (n=5), WT-HFHS-NR-fetal sacrifice at week 14 (n=5), PARP-1 KO-Chow-Saline (n=10), PARP-1 KO-Chow-NR (n=10), PARP-1 KO-HFHS-Saline (n=10), PARP-1 KO-HFHS-NR (n=10), PARP-2 KO-Chow-Saline (n=10), PARP-2 KO-Chow-NR (=10), PARP-2 KO-HFHS-Saline (n=10), PARP-2 KO-HFHS-NR (n=10), PARP-1/2 KO-Chow-Saline (n=10), PARP-1/2 KO-Chow-NR (n=10), PARP-1/2 KO-HFHS-Saline (n=10), PARP-1/2 KO-HFHS-NR (n=10), PARG KO-Chow-Saline (n=10), PARG KO-Chow-NR (n=10), PARG KO-HFHS-Saline (n=10), and PARG KO-HFHS-NR (n=10).
We will additionally have 4 offspring groups (n=20 dams, 5/group) coming from mothers that were allowed to complete their pregnancies: WT-Chow-Saline (n=5 maternal dams; n=2 males and 2 females/dam = 10 males and 10 females =20 offspring total), WT-Chow-NR (n=5 maternal dams; n=2 males and 2 females/dam = 10 males and 10 females =20 offspring total), WT-HFHS-Saline (n=5 maternal dams; n=2 males and 2 females/dam = 10 males and 10 females =20 offspring total), WT-HFHS-NR (n=5 maternal dams; n=2 males and 2 females/dam = 10 males and 10 females =20 offspring total).
A power analysis using GPower 3.1 software suggest 10 samples per group are needed for 80% power at an alpha of 0.05 and effect size f =0.57 (See appended figure). In our animal studies, each pregnancy is considered an n=1. Therefore, we require 10 pregnant dams/group.

Types and Numbers of Animals 7

CHANGE TO NEW FORM 7.1

Please note that this new form allows you to enter all of your strain/stock/breeds under "Mouse #1", "Rat #1", "Fish #1" and so on for all animal types.
You are no longer required to have separate sections for each strain/stock/breed. Please read the Section 6 instructions carefully to ensure you are following the proper format of this new form.

Types of Animals 7.2

Select all types of animals to be used with the green orb button.

Click on the name in the subsequent list to enter additional information.

Mouse #1 7.2.1

Strain/Stock/Breed **7.2.1.1**

Using the green orb button, select all of the strains you intend to use. If your strain does not appear to be listed, please email to add a new strain to the master list.

This section will link your strains to the animal ordering and census modules.

If you intend to transfer animals between protocols, please ensure that you use the exact same strain name/nomenclature on all protocols, otherwise the transfer will not be possible.

C57BL/6N
Parg-loxP
Parg-LoxP; Tg(CYP19A1-cre)1Jri
Parp1-loxP
Parp1-LoxP; Parp2-LoxP
Parp1-LoxP; Parp2-LoxP; Tg(CYP19A1-cre)1Jri
Parp1-LoxP; Tg(CYP19A1-cre)1Jri
Parp2-LoxP
Parp2-LoxP; Tg(CYP19A1-cre)1Jri

Species Description **7.2.1.2**

Species Description

Details and Amounts 7.2.1.3

Complete the table below for each strain that you will be using (as listed above). Information regarding either age or weight or gestation is required.

· Additional information regarding abnormal phenotypes will be requested in the Monitoring and Endpoints section, please answer Y or N in this table.

· Indicate how these animals are to be used on this protocol in the 'Purpose of Use' field. For example: backcrossing, intercrossing, fostering, experimental use, etc. (indicate all that apply)

Rows may be added to the table using the green orb button.

Strain/Stock/Bred	Number To Be Used	Sex	Age (Units)	Weight (Units)	Gestation	Purpose of Use	Abnormal Phenotype? Y/N
C57BL/6N offspring from C57BL/6N females	40	F	4 weeks	-	-	Experimental	N
C57BL/6N offspring from C57BL/6N females	40	M	4 weeks	-	-	Experimental	N
Parp2-LoxP and Tg(CYP19A1-Cre)+/-	40	F	4 weeks	-	-	Experimental	Unknown
C57BL/6N	40	M	8 weeks	-	-	Mating	N
Parg-LoxP	20	M	8 weeks	-	-	Experimental	Unknown
Parp1-LoxP+/+, Parp2-LoxP+/+ and Tg(CYP19A1-Cre)+/-	40	F	4 weeks	-	-	Experimental	Unknown
Parp1-LoxP and Tg(CYP19A1-Cre)+/-	40	F	4 weeks	-	-	Experimental	Unknown
Parp2-LoxP	20	M	8 weeks	-	-	Experimental	Unknown
Parp1-LoxP	20	M	8 weeks	-	-	Experimental	Unknown
Parp1-LoxP+/+, Parp2-LoxP+/+	20	M	8 weeks	-	-	Experimental	Unknown
C57BL/6N	80	F	4 weeks	-	-	Experimental	N
Parg-LoxP and Tg(CYP19A1-Cre)+/-	40	F	4 weeks	-	-	Experimental	Unknown

Authorized Amounts 7.2.1.4

Indicate the maximum applicable category of invasiveness using the green orb button. Once you have done so, fill in the total number of this type of animal to be used in the 'Authorized' box. This number should include both animals to be ordered and those produced from breeding.

Pain Category	Authorized	Requested	On Order	Received	Adjustment	Available
CCAC Category C	440	0	0	46	0	394
Totals	440	0	0	46	0	394

Procedures 8

Study Type 8.1

Select all that apply.

- [x] Animals in Facilities
- [ ] Wild Animals in the Field

Animals in Facilities 8.1.1

Purpose-Built Animal Facilities 8.1.1.1

Select the purpose-built animal facility where you expect to work using the green orb button.

Roger Guindon Hall 8.1.1.1.1

Multiple Animal Facilities 8.1.1.2

Will you be using more than one animal facility, or did you select 'Other Location' in the above list?

- [ ] Yes
- [x] No

Yes 8.1.1.2.1

No 8.1.1.2.2

Procedure Location 8.1.1.3

Under normal circumstances, all animal procedures should be performed within purpose-built animal facilities.

Will any animal care and/or use, including terminal procedures or euthanasia, take place outside of the purpose-built facilities? (Eg. in your laboratory)

- [x] Yes
  Use of animals in any areas outside of purpose-built facilities (eg. laboratories, teaching areas) must be justified to and approved by the Animal Care Committee. The ACC or a delegate must visit and approve these areas for use and revisit them regularly to ensure compliance.
- [ ] No

Yes 8.1.1.3.1

Location & Justification 8.1.1.3.1.1

Identify where animal work will be performed and provide justification for the need to work outside of purpose -built animal facilities.

Experimental animals will be brought to lab 2108 for dissection purposes. This room is primarily used for necropsies and has all the necessary equipment including liquid nitrogen and a -80C freezer. Our harvesting experiments require rapid processing and storage therefore we must do it in our necropsy room.

Details 8.1.1.3.1.2

List which procedures will take place in laboratories or other areas and how long animals will be kept there.

Animals will be brought to the lab for euthanasia and dissection within a couple of hours depending on the number of animals. Animals are euthanized via live cervical dislocation as all methods of anesthesia/euthanasia will effect collection.

ACVS Authorization 8.1.1.3.1.3

If animals are to be kept for more than 12 hours outside of purpose-built animal facilities, please contact the ACVS to reach an agreement on how animals will be cared for and observed − this will be needed before the protocol is approved. Attach the ACVS agreement here.

No 8.1.1.3.2

Housing and Enrichment 8.1.1.4

Are there any restrictions and/or additions to the standard ACVS housing and enrichment?

- ☐ Yes
- ☑ No

Yes 8.1.1.4.1

No 8.1.1.4.2

Procedures **8.1.1.5**

Select all that apply.

For animals undergoing different procedures: all selected procedures should be apparent in the procedural timeline(s) appended in the Experimental Design section.

☑	Use of Animals for Tissue/Cell Collection
☐	Maintenance of a Breeding Colony
☑	Breeding/Timed Mating (for experimental use)
☐	Surgery
☑	Animal Identification
☑	Restraint
☑	Administration of Chemicals or Biologicals
☐	Osmotic Minipump
☑	Blood Withdrawal
☑	Imaging
☐	Radiation
☑	Deprivation/Restriction of Food or Water
☐	Paralytic Agents
☑	Other Procedures (e.g. behaviour tests)

Use of Animals for Tissue/Cell Collection	**8.1.1.5.1**
Maintenance of a Breeding Colony	**8.1.1.5.2**
Breeding/Timed Mating (for experimental use)	**8.1.1.5.3**

Timed Mating Details **8.1.1.5.3.1**

Provide the details of your timed matings and indicate the planned outcome for embryos or offspring.

We need to perform timed matings and visualization of copulatory plugs, in order to properly date pregnancies and initiate NR treatment on the appropriate days of gestation (as detailed in the procedural timeline). Our endpoint measurements take place following euthanasia of the mother on E19 (to prevent natural labor and birth). Only breeding from 4 experimental groups is taking place for the purposes of obtaining offspring: Wildtype (WT)-Chow-Saline-fetal euthanized week 14 (n=5), WT-Chow-NR-fetal euthanized at week 14 (n=5), WT-HFHS-Saline-fetal euthanized at week 14 (n=5), WT-HFHS-NR-fetal euthanized at week 14 (n=5). Mothers will be maintained on their respective diets throughout lactation, and offspring will be weaned at 21 days post birth, at which time the litters will be culled to 2-3 male offspring and 2-3 female offspring per dam (n=40 offspring total). At 12 weeks of age, fasted glucose and insulin testing (6 hr food restriction) will be performed to measure glucose handling in all fetal offspring (n=4 offspring/mother; n=40 mice total), and mice will undergo blood pressure and heart rate measurements daily over the course of two weeks (1 week acclimatization, 1 week of experimental measurements) using the tail cuff method. An oral glucose tolerance test (OGTT) with 6 hour food restriction will be performed at age 18 weeks to measure glucose handling over time and metabolic CLAMS cage procedure at 20 weeks of age to measure energy expenditure. At 24 weeks of age, mice will undergo blood pressure measurements again using the tail cuff method with 1 week of acclimatization and 1 week of measurements. This will help us to assess differences in blood pressure over time. At 36 weeks of age (9 months), mice will undergo tail cuff method again to assess further differences in blood pressure over time. At 38 weeks of age, all offspring (n=40) will be euthanized and the brain, heart, liver, muscle, adipose tissue, and kidneys collected, weighed, and fixed in 4% PFA for future histological analysis. All euthanizations will be via cervical dislocation without anesthesia, as we are assessing the mitochondria (using anesthesia could confound our results).

Surgery **8.1.1.5.4**

Animal Identification **8.1.1.5.5**

Identification Methods **8.1.1.5.5.1**

Describe all animal identification methods to be used for each species (eg. ear tags, notches, tattoo, cage cards).

Ear tags and cage cards.

Restraint **8.1.1.5.6**

Method of Restraint **8.1.1.5.6.1**

Describe how and for which procedures animals will be restrained.

For vaginal plug detection, mice will be restrained manually firmly holding the base of the tail.

For gavage treatment, the conscious mice will be firmly manually restrained by grasping a fold of neck skin behind the back and holding the base of the tail, immobilizing the animal's head in the process.

For blood sample collection, mice will be restrained for short period inside blood collection restrainer.

Animals will be manually restraint for the use of ultrasound as anesthesia can not be given due to experimentation

Prolonged Restraint **8.1.1.5.6.2**

Will prolonged restraint (over 30 minutes) be used in this study?

Please note: Animals must be monitored constantly while they are restrained.

- ☐ Yes
- ☑ No

Yes	**8.1.1.5.6.2.1**
No	**8.1.1.5.6.2.2**
Administration of Chemicals or Biologicals	**8.1.1.5.7**
Administration Guidelines	**8.1.1.5.7.1**

Will compounds be administered according to ACC-4 Good Practice Guide to the Administration of Substances?

- ☑ Yes
- ☐ No

Yes	**8.1.1.5.7.1.1**
No	**8.1.1.5.7.1.2**

Administration of Chemicals or Biologicals 8.1.1.5.7.2

Provide the information requested in the table below for substances other than anesthetics/analgesics (these will be provided in the Anesthesia, Pain and Distress section).

If the administration protocol is complex, you may attach a separate table detailing the drug administration schedule.

If you will be administering via minipump please fill out the Osmotic Minipump section instead of including the information in this table.

Rows may be added to the table using the green orb button.

Substance	Species	Route	Dose/Dose Range	Volume	Dosing Frequency	Total Number of Administrations	Clinical Effect(s
High fat, high sucrose diet	Mice	Oral	42% fat, 34.5% sucrose	Ad libitum access to pellet diet	Continuous, 3 months before mating and throughout pregnancy	3 months	Obesity, high blood glucose, insulin resistance, high blood pressure
Control diet (Standard Chow RM1 Diet)	Mice	Oral	7% simple sugars, 3% fat (wt/wt): 10.74 kJ/g	Ad libitum access to pellet diet	Continuous, 3 months before mating and throughout pregnancy	3 months	None
Nicotinamide riboside (NR)	Mice	Oral gavage ***NR has good bioavailability when administered orally. Also, this route is relevant to the translation of oral NR supplementation in pregnant women***	400mg/kg/day	200 uL	Daily, starting on E0.5	x18	None

Osmotic Minipump 8.1.1.5.8

Blood Withdrawal 8.1.1.5.9

Blood Collection Guidelines 8.1.1.5.9.1

Attachments: ACC-3 Blood Collection Guidelines_Nov 2019.pdf

Will blood sampling be performed according to the attached ACC Policy on blood collection guidelines?

- [x] Yes
- [ ] No

Yes 8.1.1.5.9.1.1

No	8.1.1.5.9.1.2

Blood Withdrawal 8.1.1.5.9.2

Complete the table below for all blood collection procedures.

For 'Technique' please indicate the needle gauge and any other pertinent details (eg. catheterization with a 22g butterfly needle).

Rows may be added to the table using the green orb button.

Species	Sampling Site	Technique	Volume	Frequency
Mice	Heart	Cardiac Puncture	Exsanguination	Once-at the time of euthanasia
Mice	Saphenous vein or tail nick	23-25g needle used We will perform only a minimal restraint via tail restriction to induce a lateral tail nick to minimize mouse distress. Only 2 µL of blood is required for blood glucose measurements so no needle sampling is required. Our previous experience is that this gives accurate blood glucose measurement while avoiding elevated blood glucose levels due to excessive stress and cortisol levels. Our experience is that we are also able to collect 50 µL of blood with gentle massage of the tail in a capillary tube for insulin measurements. Alternatively, for mice that appear particularly stressed we will use an acrylic mouse restrainer to make the initial superficial cut.	50uL	Once-before mating

Imaging	8.1.1.5.10

Types of Imaging 8.1.1.5.10.1

Select all that apply using the green orb button. Please ensure that you have included all of your planned imaging sessions of live animals on your procedural timelines in the Experimental Design section.

Echo-MRI	8.1.1.5.10.1.1
Ultrasound	8.1.1.5.10.1.2

Imaging Methods **8.1.1.5.10.2**

Indicate the species and describe how the imaging procedure(s) will be performed. You may attach and/or refer to relevant SOPs.

All female C57BL/6N mice will be imaged via EchoMRI including: Parp 1/2 Knockout (KO; Parp1-LoxP+/+, Parp2-LoxP+/+ and Tg(CYP19A1-Cre)+/-); Parp 1 KO (Parp1-LoxP and Tg(CYP19A1-Cre)+/-); Parp-2 KO (Parp2-LoxP and Tg(CYP19A1-Cre)+/-); and Parg KO (Parg-LoxP and Tg(CYP19A1-Cre)+/-), as well as wild type C57BL/6N mice-including both mice that were fed a standard chow diet and those that were fed a high-fat high-sugar diet. This tool will be useful to detect fat accumulation/deposits in mice and confirm a state of obesity in the high-fat high-sugar diet fed mice. In this process, fat tissues are characterized by peculiar contrast in magnetic resonance Imaging (MRI) that can distinguish between fat and water protons thanks to their different magnetic resonance properties (Marzola et al., 2016). Measurements performed by Echo-MRI have high precision and accuracy, and are carried out using NMR-MRI-based technology.
Essentially, this imaging procedure will be performed on all female mice before the induction of pregnancy following 12 weeks of diet administration to quantify fat mass and lean mass percentages-and thus to confirm states of obesity in mice fed a high-fat high-sugar diet. The procedure will be booked via the echo-MRI infinity system and performed by behaviour core staff at ACVS. Echo-MRI will not use any anesthesia as we are studying the mitochondria and using anesthesia could confound our results.
Echo-MRI will also be used on offspring (at age 12 weeks) born from all female C57BL.6N mice to quantify fat mass and lean mass percentages. This tool will be useful to detect fat accumulation/deposits in offspring and confirm fetal programming effects of maternal obesity. This is important given that our study will be determining the effects of maternal obesity on fetal programming, which may involve effects on lean and fat mass of offspring.
Ultrasound will be used as a method to confirm pregnancy in all C57BL/6N mothers. This is important to do as obese mice may have vaginal plugs but not gain too much weight. Thus, it is difficult to determine whether they are pregnant and have a few growth-restricted fetuses, or if they are not pregnant at all. Ultrasound will solve this problem and provide a more sure method of pregnancy confirmation. An awake ultrasound will be performed on all mice as a confirmation of pregnancy. No anesthesia must be used as our study assesses mitochondrial health, and anesthesia could confound these results. Instead of anesthesia, mice will become acclimatized to ultrasound via handling and restraint followed by treats (peanut butter and sweet liquid). First, mice will undergo 1 week of acclimatization to ultrasound prior to mating. On days 1-3 of week 1, mice will be offered a treat (peanut butter) followed by handling. On days 4-7 of week 1, mice will be offered a treat (peanut butter) followed by restraint. While in restraint, mice will be offered another treat (sweet liquid). At the end of the session, mice will be offered another treat (peanut butter). After week 1, mice will be mated. Mice will undergo ultrasound during the third trimester of pregnancy using the same treat delivery method.
Marzola, P., Boschi, F., Moneta, F., Sbarbati, A., & Zancanaro, C. (2016). Preclinical In vivo Imaging for Fat Tissue Identification, Quantification, and Functional Characterization. Frontiers in pharmacology, 7, 336. https://doi.org/10.3389/fphar.2016.00336

Radiation	**8.1.1.5.11**
Deprivation/Restriction of Food or Water	**8.1.1.5.12**

Food or Water Deprivation and/or Restriction Details 8.1.1.5.12.1

1) Explain the details of the deprivation/restriction request and why it is necessary.

2) Describe the methods to be employed for assessing the health and wellbeing of the animals.

1) We will be depriving all female mice of food in order to carry out fasting glucose sampling. This will be performed right before mating mice (approximately week 13; day 91-after acclimatization to diet) to gain an understanding of how they handle glucose at baseline. Collecting fasting glucose levels produces less variable results than fed glucose levels, and there are clearly established ranges which would be considered normal levels for glucose after fasting. Thus, this will help us to establish whether the administration of our HFHS diet has been successful at stimulating obesity, if indeed their fasting glucose levels are out of range. This is the only time throughout the study that we will fast the mice.

Although it is well established to fast mice 10-12 hours overnight, our fasting glucose sampling will be of shorter duration to avoid starving mice since their metabolic rates are higher than humans at night since they are nocturnal feeders. It has also been shown that the differences in glucose intolerance between high fat diet and chow diet fed animals is not evident after an overnight fast, but more evident following a shorter fast. Given that we are assessing glucose tolerance following a high fat high sugar diet, we will carry out a shorter 5-6 hour fast during photophase to comply with mouse feeding behaviour.

Our second glucose sampling will be a resting, fed sample performed on female mice prior to euthanasia. We will not fast them prior to euthanasia as this could disrupt our understanding of how obesogenic diets impact the pregnant mother, her placenta, and her fetal offspring.

2) To ensure proper mouse health and wellbeing, we will make sure the environment near the mouse cages is quiet, and will minimize disturbances including: noise, lightening vibration, and strong odors. We will also make sure that mice are acclimatized to being handled, by handling them at least once a week throughout diet administration, so as to not stress them out when handling them for glucose/insulin tests. We will also make sure the bedding is changed regularly as obesity diets may require more frequent bedding changes.

Additionally, the health and wellbeing of the animals will be assessed by monitoring body weight (in at least 48 hours intervals), body condition and hydration status. Those mice who present clinical signs will be reported to care staff. Significant weight loss (e.g. exceeding 15% of baseline body weight) at any time throughout the study, body condition score <2 or abnormal behavior (increased aggression, ruffled fur, recurrent episodes of self-harming) will be considered signs of intervention.

Policy on Deprivation and/or Restriction 8.1.1.5.12.2

Will you be following Policy ACC-14 Restriction and Manipulation of Diet and Fluid for Research?

- [x] Yes
- [ ] No

Yes 8.1.1.5.12.2.1

No 8.1.1.5.12.2.2

References **8.1.1.5.12.3**

Please provide references for the deprivation/restriction request.

Ayala, J.E., Bracy, D.P., McGuinness, O.P., Wasserman, D.H., 2006. Considerations in the design of hyperinsulinemic-euglycemic clamps in the conscious mouse. Diabetes 55, 390−397.

Ayala JE, Samuel VT, Morton GJ, et al. Standard operating procedures for describing and performing metabolic tests of glucose homeostasis in mice. Dis Model Mech. 2010;3(9−10):525−534.

Andrikopoulos S, Blair AR, Deluca N, Fam BC, Proietto J. Evaluating the glucose tolerance test in mice. Am J Physiol Endocrinol Metab. 2008;295(6):E1323−E1332.

Benedé-Ubieto, R., Estévez-Vázquez, O., Ramadori, P., Cubero, F. J., & Nevzorova, Y. A. (2020). Guidelines and Considerations for Metabolic Tolerance Tests in Mice. Diabetes, metabolic syndrome and obesity : targets and therapy, 13, 439−450.

Grasemann, C., Devlin, M.J., Rzeczkowska, P.A., Herrmann, R., Horsthemke, B., Hauffa, B.P., Grynpas, M., Alm, C., Bouxsein, M.L., Palmert, M.R., 2012. Parental Diabetes: The Akita Mouse as a Model of the Effects of Maternal and Paternal Hyperglycemia in Wildtype Offspring. PLOS ONE 7, e50210.

Rogers, I.T., Holder, D.J., McPherson, H.E., Acker, W.R., Brown, E.G., Washington, M.V., Motzel, S.L., Klein, H.J., 1999. Influence of Blood Collection Sites on Plasma Glucose and Insulin Concentration in Conscious C57BL/6 Mice. Contemp Top Lab Anim Sci 38, 25−28.

Jensen TL, Kiersgaard MK, Sorensen DB, Mikkelsen LF. Fasting of mice: a review. Lab Anim. 2013;47(4):225−240.

Ullman-Culleré, M. H., and Foltz, C. J. “Body condition scoring: a rapid and accurate method for assessing health status in mice”. Comparative Medicine, 49(3), pages 319-323: 1999.

Paralytic Agents	**8.1.1.5.13**
Other Procedures (e.g. behaviour tests)	**8.1.1.5.14**

Other Procedures **8.1.1.5.14.1**

Attachments: PHYS-2 CLAMS.doc

Describe any procedures to be performed that were not previously addressed in the Procedures list.

Fasting Blood Glucose: At 12 weeks of age, fasted glucose testing (6 hour food restriction) will be performed to measure glucose handling in all fetal offspring (n=4 offspring/mother; n=40 mice total), and mice will undergo blood pressure and heart rate measurements daily over the course of two weeks (1 week acclimatization, 1 week of experimental measurements) using the tail cuff method (see procedural timeline for more details).
Oral Glucose Tolerance Test (OGTT): This test explores glucose metabolism over time. Hyperglycemia is caused by oral administration of glucose; glucose is then measured in the blood over a three hours period. Oral administration produces a physiological glycemic shock that allows for an assessment of the contribution of gastrointestinal hormones to the secretion of insulin. The amount of glucose solution administered is calculated according to the body weight and diet of each animal: approximately ≤4g glucose / kg of the animal for testing GTT. The mouse is then placed in a restraining cage to make an incision on the tail vein at the side using a scalpel. A drop of blood (~2 microL) is taken to measure glucose concentration. Note the initial rate of glucose (T0). The wound is compressed for a few seconds. The glucose solution is administered orally. This step marks the beginning of timing. The mouse is then placed back in its cage.
After 15 minutes the mouse is again placed in the restraining cage to collect another drop of blood to measure blood glucose and ≤ 50 ul to determine insulin levels (only at this time point). Wherever possible, blood is collected from the same incision by removing the clot with a paper towel and massaging the tail if necessary to bleed again. Note the rate of glucose measured with the strip (T15) Similarly, blood glucose will be measured at T30, T45, T60, T90, T120, T150 and T180 if blood glucose has not returned to its basal levels (maximum total blood volume taken is 9 x ≤5 + 50 uL = 95 microL).
The mouse is placed in its home cage with food and water.
Metabolic CLAMS; to measure energy expenditure of animals by indirect calorimetry (see attached SOP) Measurement of energy expenditure of mice by indirect calorimetry (measuring oxygen consumption by CLAMS). The spontaneous locomotor activity and ingestion of food and water are simultaneously recorded. Immediately prior to the CLAMS procedure, the mice will undergo EchoMRI to establish body composition to allow normalization of CLAMS data. The CLAMS system consists of an open circuit for incoming and outgoing air in closed plastic cages (1 mouse per cage, 206.25 cm2 surface area, 12.7 cm height). Very precise detectors measure the O2 and CO2 from the air entering and leaving (the flow of air into the cages is constant) so that an assessment rate of oxygen consumed during a given period is obtained. Infrared detectors, at 2 and 8.5 cm from the bottom of the cage, allow recording of locomotor activity. Feeding behavior is measured automatically over several hours by evaluating the number of food pellets distributed and the number of licks from two bottles. Food distribution is controlled by a system with a photosensitive cell, which issues a new 20 mg pellet if the previous one was removed.

Calibrate before using the device (O2, CO2, food and water). Place each mouse individually in the appropriate plexiglass boxes. 12 animals can be examined at a time. The animals have access to food and water during the test. The animals are in the cages for 72 hours (48 hours to acclimatize to the single housing and 24hrs for measurements). At regular intervals, the camera makes automatic measurements of O2 and CO2 in and out of each box, and measures the intake of food and drink automatically. The spontaneous activity is also automatically measured throughout the test (24 hours). At the end of the test, animals are placed in their cage with food and water.
We will follow the attached SOP. The only exception would be the completion of the CLAMS at 28-30oC. We would like to extend the temperature range to include mild sub-thermoneutral temperatures as well (i.e. room temperature ~23oC and thus ~23-30oC) because of the importance of skeletal muscle in thermoregulation. Acute thermoregulation is primarily achieved via shivering or mild muscle contraction (https://journals.physiology.org/doi/full/10.1152/physrev.00015.2003 scetion V). The 23oC temperature would represent a mild thermal and metabolic stress to the animals. Furthermore, it likely reflects normal housing temperatures with bedding and multiple mice and human environmental stress as discussed in https://www.ncbi.nlm.nih.gov/pmc/articles/PMC3757658/ Additionally, our previous experiments have shown a gradual shift in fuel utilization to glucose over time in mice housed in the CLAMS at 28oC, which would be reflective of decreased thermogenesis from uncoupling mediated mechanisms (activated by fatty acids and primarily dependent upon fatty acid oxidation as their fuel).

Other Potential Stressors **8.1.1.6**

Will there be any other potential stressors that have not already been addressed? (use of noxious stimuli, environmental stress⋯)

- ☐ Yes
- ☑ No

Yes	**8.1.1.6.1**
No	**8.1.1.6.2**
Wild Animals in the Field	**8.1.2**
Surgery	**9**
Surgery	**9.1**

Will surgery be performed on animals in this study?

- ☐ Yes
- ☑ No

Yes	**9.1.1**
No	**9.1.2**
Anesthesia, Pain and Distress	**10**
Anesthesia, Analgesia, Antibiotics or Other Medications	**10.1**

Will animals in this study require the use of anesthesia, analgesia, antibiotics or other medications?

- ☐ Yes
- ☑ No

Yes	**10.1.1**
No	**10.1.2**
Monitoring and Endpoints	**11**
Study Type	**11.1**

Select all that apply.

- ☑ Animals in Facilities
- ☐ Wild Animals in the Field

Animals in Facilities	**11.1.1**

Impact of Procedures on Animal Health/Welfare 11.1.1.1

What are the likely impacts on animal health/welfare (pain, distress, discomfort) as a result of the procedures to be performed? Describe any anticipated adverse effects and the associated clinical signs (e.g., disease, pathology, weight change, behavioural change, disability, pain, distress, toxicity, mortality).

1) High-fat high-sugar diets are known to lead to obesity and related complications including: heart dysfunction, high blood pressure, high glucose levels, insulin resistance, and fatty liver disease.
2) Metabolic CLAM cage procedure to assess energy expenditure - the animal will not experience any pain but may experience low stress as a result of acclimatizing to a new cage environment and new food. The procedure will not exceed 96 hours.

3) Glucose tolerance test to explore glucose metabolism over time - the animal may briefly experience a small amount of stress during the oral gavage of glucose, and may experience low stress from being placed in a restraining cage every 15 minutes up to minute 180 (maximum total of 9 placements in cage for blood sampling, maximum 5 minutes/sampling)

Impact of Phenotype on Animal Health/Welfare 11.1.1.2

Will any of your strains display abnormal phenotypes that could impact on animal health/welfare?

- ☐ Yes
- ☑ No

Yes 11.1.1.2.1

No 11.1.1.2.2

Monitoring Details 11.1.1.3

How often will the animals' condition be monitored by the research team, in particular during any times when significant adverse effects on animals are likely? Include details for both animals affected by experimental procedures as well as for strains possessing abnormal phenotypes (if applicable).

Mice will be assessed daily during the experimental procedures.

Intervention Points and Endpoints 11.1.1.4

Intervention points and endpoints are meant to be applied to protect animal health and welfare. They are determined using both scientific goals and animal health considerations. Standard ACVS endpoints have been developed and are outlined in Policy ACC-2 Endpoints and Intervention for Laboratory Mammals Species. Relevant information can also be found within the CCAC guidelines on choosing an appropriate endpoint in experiments using animals for research, teaching and testing and ACVS veterinarians are available to assist you with this and any other questions.

Endpoints for Procedure Type 11.1.1.5

Will animals be undergoing invasive procedures?

- ☐ Yes
- ☑ No

Yes	11.1.1.5.1
No	11.1.1.5.2

Poor Condition/Ill/Injured Animals 11.1.1.6

Protocol associates will be informed by ACVS of animals that are in poor condition following experimental procedures, or that become ill or injured outside of experimentation − these animals will be treated/euthanized as appropriate under veterinary supervision, based on this protocol, on Policy ACC-2 Endpoints and Intervention for Laboratory Mammal Species, and on relevant standards of veterinary care for each type of animal.

- ☑ I do agree

I do agree	11.1.1.6.1
When Humane Endpoints Occur Out-of-hours	11.1.1.6.1.1

Provide carcass disposal instructions for ACVS.

Select all that apply.

- ☑ Refrigerate at 4°C
- ☑ Freeze at -20°C
- ☐ Tissue specimens in 10% buffered formalin
- ☐ Do not keep carcass
- ☐ Other

Refrigerate at 4°C	11.1.1.6.1.1.1
Freeze at -20°C	11.1.1.6.1.1.2
Tissue specimens in 10% buffered formalin	11.1.1.6.1.1.3
Do not keep carcass	11.1.1.6.1.1.4
Other	11.1.1.6.1.1.5
Wild Animals in the Field	11.1.2
Euthanasia	12

Euthanasia **12.1**

Will animals in this study require euthanasia?

- [x] Yes
- [ ] No

Yes **12.1.1**

Euthanasia Responsibility **12.1.1.1**

Please indicate who will be responsible for performing euthanasia.

- [ ] ACVS
- [x] Research staff

ACVS **12.1.1.1.1**

Research staff **12.1.1.1.2**

Guidelines on Euthanasia **12.1.1.1.2.1**

Guidelines for humane euthanasia are outlined in the CCAC guidelines on euthanasia of animals used in science as well as ACC Policy 7 - Euthanasia of Laboratory Animals.

The appropriate procedures for euthanasia of rodents are described in SOP EUTH-2 Standard Methods for RodentEuthanasia.

Species to be Euthanized **12.1.1.2**

Please indicate the species to be euthanized. Select all that apply.

- [x] Mice/Rats
- [ ] Rabbits/Other large mammals
- [ ] Guinea Pigs
- [ ] Fish/Amphibians
- [ ] Reptiles
- [ ] Wild Animals in the Field
- [ ] Other

Mice/Rats **12.1.1.2.1**

Method of Euthanasia for Mice/Rats 12.1.1.2.1.1

Indicate the proposed method of euthanasia that will be conducted according to ACC Policy 7 - Euthanasia of Laboratory Animals as well as SOP EUTH-2 Standard Methods for Rodent Euthanasia.

- ☐ Inhalation of carbon dioxide followed by a physical method to ensure death
- ☐ Anesthetic followed by a physical method to ensure death
- ☑ Physical method without prior anesthesia
- ☐ IP/IV injection of barbiturate
- ☐ Other method

Inhalation of carbon dioxide followed by a physical method to ensure death	12.1.1.2.1.1.1
Anesthetic followed by a physical method to ensure death	12.1.1.2.1.1.2
Physical method without prior anesthesia	12.1.1.2.1.1.3

Description & Justification of Physical Method 12.1.1.2.1.1.3.1

Please describe the method in detail and provide justification for its use without prior anesthesia. Indicate where this procedure is to be performed.

We will be performing a cervical dislocation followed by cardiac puncture to collect blood.

We must use a physical method without prior anesthetic as anesthetic can disrupt the integrity of the mitochondria. As the mitochondria is an essential part of our study to assess NAD+ content/activity, and furthermore its role in placental disruption and fetal programming, its integrity must be maintained. 20-Sept-22 --> Live cervical dislocation will be performed by Hannah Poisson, Alex Green or Yumaris Josefina, proper training has been completed with Courtney Reeks for this procedure.

IP/IV injection of barbiturate	12.1.1.2.1.1.4
Other method	12.1.1.2.1.1.5
Rabbits/Other large mammals	12.1.1.2.2
Guinea Pigs	12.1.1.2.3
Fish/Amphibians	12.1.1.2.4
Reptiles	12.1.1.2.5
Wild Animals in the Field	12.1.1.2.6
Other	12.1.1.2.7
No	12.1.2

Hazardous or Biological Agents 13

Use of Hazardous or Biological Agents 13.1

Will any radioisotopes, nanoparticles, biological agents/products (including cell lines, anti-serum, etc.), toxins, or hazardous chemicals or pharmaceuticals be used in this study?

- ☐ Yes
- ☑ No

Yes	13.1.1
No	13.1.2

Investigator Declaration and Certifications 14

Investigator Certifications 14.1

I certify that:

· All animals will be cared for in accordance with uOttawa policies and procedures, the Ontario Animals for Research Act, and CCAC standards

· All of the animal using members of my team will be provided with the final version of this protocol, will follow it and will be trained and competent to carry out the procedures

· I will submit an amendment to the Animal Care Committee and will obtain approval before initating any changes to the protocol

· I will renew this protocol annually through the Animal Care Committee if this work is ongoing

- An ACVS veterinarian will be promptly notified of any unanticipated animal pain or distress, morbidity or mortality

☑ I do certify.

I do certify.	14.1.1